

We received three sets of reviewer comments and three short comments, all of which suggested helpful improvements to the manuscript. Our responses below have been color coded and formatted as follows:

Reviewer/short comments are in gray and indented.

Our responses are in black and not indented.

“Changes to the text are in quotation marks, in dark blue and indented”

Hopefully this formatting is helpful and keeps things clear.

Authors' responses to comments from Reviewer 1:

This paper describes in detail 3 new model intercomparison projects, MISMIP+, ISOMIP+ and MISOMIP1 for marine ice sheet and regional ocean models. MISMIP+ is dedicated to the marine ice sheet models, ISOMIP+ to the ocean models incorporating an ice-shelf cavity and MISOMIP1 to the coupling of both type of models. This paper is well written, clear and it is an important contribution for the ice-sheet/ocean community. I have only one main concern regarding the diffusion of the setups through different canals (this paper and a web site) and few minor remarks listed below. I will mostly comment on the ice part of the experiments, being not an oceanographer.

Thank you for taking the time to review our manuscript. We are glad you found the paper to be clear and well written, and the experiments to be worthwhile for the community. We have endeavored to address your concerns as detailed below.

My main concern is the existence of more than one place to find the description of the experiments, which might be confusing and source of errors for the participants. It should be stated clearly with which document participants should be working, both on the GMD paper and on the CLIC webpages hosting the description of the MISOMIP experiments. This is also true for supplement material, part of it being attached as a supplement of this paper and an other part being located on the webpage. I suggest that if this GMD paper is the reference for these experiments that all the needed material (input files, examples of model description, etc) is provided as a supplement of this paper.

The GMD being the reference, it questions the way changes or updates (which might be necessary when participants will start running the experiments and find some ambiguities in the experiments description, because it is always difficult to think about all possible configurations in advance) will be provided to the community. The strategy for setup update after the GMD paper is accepted should be clearly stated in the GMD paper itself (a link to an update webpage on the MISOMIP website for example).

We agree that it is important not to have two versions of the experiments, one on the MISOMIP website and one in this manuscript. We plan to modify the MISOMIP website to make clearer that it is meant to provide a short summary of the experiments as well as some supporting material, and that the GMD manuscript is the definitive description of each MIP.

Since this manuscript has been granted an extended discussion period, this has allowed various groups to try out the MISMIP+, ISOMIP+ and MISOMIP1 experiments and to raise issues and concerns. We have attempted to address these concerns in the updated manuscript to the best of our abilities. We feel that it is important that the experiments be “finalized” so that researchers do not face a continually moving target. We realize that this will necessarily mean that the experiments remain imperfect. A web page with updates to the experiments could theoretically allow for further changes to the experiments over time but this would likely make it nearly impossible to know which version of the experiments each participant was performing and would make the results difficult to compare. For that reason, we will consider the experiments within

this manuscript to be the final version without allowing for a process for making further changes. In practice, it will still be possible to make further changes by consensus among participants, as long as these deviations from the standard protocol are documented along with each participant's submission.

The fact that the supplementary material is supplied in three ways (as a zip file through GMD, a DOI for the ISOMIP+ topography data sets, and links to example results on the MISOMIP website) is unfortunate but necessary. We wished to supply the small scripts and example MISIMP+ data in the simplest and most easily accessible form as a supplement to the manuscript itself. This was not possible for the ISOMIP+ topography data sets because they are too large. We did not feel that it was appropriate to give a DOI to the example results for ISOMIP+ and MISOMIP1. For one thing, the simulations had to be re-run based on recent changes made to the experiments, meaning the results were not available early enough for a DOI to be possible. In addition, that POP2x and POPSICLES results will be included in the ISOMIP+ and MISOMIP1 analyses, respectively, and that the results will be archived with a DOI in that process. For the time being, inclusion on the MISOMIP website seems more appropriate. A description of each code and data set is now included in a new section called Code and Data Availability (Sect. 5).

Other remarks

page 9865, line 13: performed simulations used offline . . . → performed offline coupled simulations . . . (?)

Changed as requested.

page 9869, first equations and all over in the paper. Some of the notations are not homogeneous through all the paper. For example, the bed (which is also the bathymetry) is written B here, z_b after Eq. (8) and (13). Then when a quantity is evaluated at the bed (in fact the bottom ice surface) it is noted b ($\tau_{nt}|_b$ in Eq. (6)). I would suggest to adopt the same notations as in the previous ISMIP and ISMIP3d experiments for the geometry: b for the bedrock (and bathymetry), z_s for the ice upper surface and z_b for the ice bottom surface, this latter being equal to b when the ice is grounded and describes the ice-ocean interface (ice draft for the ocean model) when ice is floating. The same apply for the coordinates which are sometime written using lowercase (ice part) and sometime uppercase (ocean part). Legend of figures will have to be updated accordingly.

Thank you for pointing out these discrepancies. As I'm sure you can appreciate, different communities have different conventions, and these were mixed more than they should have been in the previous draft.

The suggested notation (z_s , z_b and b) is not very intuitive from the ocean's perspective, where z_b would be the surface. We have opted for a somewhat more neutral notation throughout: z_s is the ice surface, z_d is the ice draft (lower surface of the ice/upper surface of the ocean) and z_b is the bed topography/bathymetry.

page 9869, line 20: the fact that either A and β^2 (or both) should be modified is repeated at different places, but I would suggest to write it as a preamble of how the steady state is obtained. This is an important point and the strategy of doing it this way should be explained. Also, it should be stated more clearly if A and β^2 should only be one single scalar for the whole domain (or the whole bedrock) or if participants are free to have space evolving A and/or β^2 .

We have removed the redundancy. We feel that the results will not be strongly sensitive to the precise method used to adjust A and β^2 , so we leave it up to participants to choose an optimization strategy that is appropriate for their model:

“We prescribe that the steady-state grounding line should cross the centerline of the trough at $x = 450 \pm 10$ km, ensuring that all models start from similar initial states. Participants should adjust the grounding line position by modifying first the values of A and, if necessary, the value of β^2 .

beginning with the suggested values given in Table 1. We have adopted this approach for model initialization to be more consistent with the methods used to initialize models for real-world problems: unknown parameters or fields are determined by search or inversion techniques so that initial conditions are consistent with observations. The precise method used to adjust A and/or β^2 and for finding the steady state is left up to the participant. Some participants will spin up their models for tens of thousands of years with different parameter values until the grounding line lies within the desired position. Others might construct a more formal optimization problem and solve it with variational methods.”

page 9870, line 1: The tangential component . . . → Where the ice is grounded, the tangential component . . .

We have made this change.

Eq. (7): I have two points here: the first is on how the Tsai friction law, and its dependency to water pressure, is written. The second is on the use of Tsai and others (2015) friction law instead of the C 1 Coulomb-type friction law proposed by Schoof (2005) and Gagliardini and others (2007).

First, I would suggest to really make the distinction between the friction law itself and the way the effective pressure entering the friction law is estimated. I would suggest to write the Tsai and others (2015) friction law as:

[see pdf] (1)

and then explain how the effective pressure is estimated: $N = -\sigma_{nn} - \rho_{sw} g z_b$ (assuming that sea level is 0). It should be stated clearly (more clearly than in the Tsai and others (2015) paper at least) that the water pressure is assumed over all the bed to be given by the ocean hydrostatic pressure, which can be seen as a zero order hydrology model assuming a perfect connection of all the bedrock interface to the ocean (which is certainly a good approximation in the close vicinity of the GL but might give too large water pressure far inland if bedrock elevation decrease again). Then you might want to explain that N can be expressed using the floatation thickness as $N = \rho_i g (h - h_f)$.

As you requested, we have separated out the effective pressure explicitly, making clear the assumption that N is determined with the assumption of connectivity to the ocean throughout the domain:

“We note that Eq. (8) is a zeroth-order hydrology model that assumes connectivity to the ocean throughout the domain and is likely only valid within a few tens of kilometers of the grounding line (Leguy et al. 2014). It is likely that simulations using more realistic topography would require a more sophisticated hydrology model to produce results consistent with observations inland of the grounding line.”

Second, I would suggest that the participants can choose between Tsai and others (2015) friction law and the most commonly used so far Coulomb-type friction proposed by Schoof (2005) and Gagliardini and others (2007):

[see pdf] (2)

which depends on the same number of parameter than the Tsai and others (2015) friction law. Moreover, if $C = f$ and $A_s = (\beta^2)^{-m}$, both law are very similar, but the latter is C1 and always bijective, whereas the former might conduct to numerical difficulties when the plateau is reached. I would suggest that at least the participants have the choice between both effective pressure dependent friction laws.

We agree that there is no reason not to also allow the Schoof (2005) basal traction parameterization (a limiting case of that of Gagliardini et al. 2007). We have added the option to use this parameterization of the basal traction in the current draft. We would point out, however, that the Schoof (2005) basal friction is *not* C1 continuous at the grounding line, though it is C1 continuous within the ice sheet. It is also not clear

in our experience that a C1 continuous basal traction has particular numerical advantages, whereas there are several studies (e.g. Gladstone et al. 2010, Leguy et al. 2014) point out the numerical advantages of C0 continuity in the basal traction at the grounding line.

Eqs. (6) and (7): u should be u_t (only the tangential part to the bed of the velocity vector) and one should define the norm of the tangential velocity (noted u_b above) instead of $|u|$.
page 9870, line 18: computing basal melt by balancing . . . \rightarrow computing basal melt bellow the ice-shelf by balancing . . .

We have adopted your suggested notation and made the suggested change (though we find it unlikely that modelers will expect basal melting under grounded ice in these experiments).

page 9871, line 2: u_* is the friction velocity . . . \rightarrow u_* is the ocean water friction velocity . . .

Changed as suggested.

the elevation of the bedrock is already defined before. thickness, and where $u_{*,0}$. . . \rightarrow thickness, and $u_{*,0}$. . .

Changed as suggested.

page 9872, line 14: in units definition, "yr" should be written "a" all over the manuscript.

We think this is a matter of taste and style, as the year is not an SI unit, but we have made this change.

page 9875, line 23: in a. pdf file . . . \rightarrow in a pdf file . . .

Changed as suggested.

page 9876, points 2 and 3: if A and/or β^2 are not uniform, how should they be given?

The experiments prescribe both A and β^2 as uniform constants. Some forms of the basal traction involve additional constants but they still involve β^2 as a constant. If participants did choose, for some reason, to use non-constant A and/or β^2 , we think it is clear that these should be described here as well. It would be up to the participant to decide how these are given.

page 9877, line 4: of ice, not water equivalent) . . . \rightarrow of ice (not water equivalent) . . .

Changed as suggested.

page 9877, line 9: what is expected here is the basal traction at the bottom interface, so using your notation it should be $\tau_{nt|zd}$, but adopting what I have suggested it should write $\tau_{nt|zb}$ (this should be corrected at many other places in the manuscript).

Changed to consistently use $\tau_{nt|zd}$ throughout the manuscript.

page 9879, line 15: Ocean2 has a fixed geometry?

Hopefully the following change clarifies this point: "...to accommodate the retreated ice-shelf topography used in Ocean2, which is also the most retreated state in Ocean3 and Ocean4."

page 9879, line 27: the web site address is given at different places in the manuscript. I would suggest to give it once at a judicious place where you should also explain which document is the reference document for the experiences and what can be found in the MISOMIP website (see my main comment).

In this particular point in the text, we now cite a DOI for the topography data used in ISOMIP+. In place of other references to the MISOMIP website, we now include a single reference in the new "Code and Data Availability" section, and refer to that section instead of the website in other parts of the manuscript. We make clear in this new section that this manuscript, not the website, is the definitive description of the experiments.

page 9880, line 12: why it is important should be stated more clearly? Also, are the ocean models supposed to account for the iceberg melting. I guess not, but it should be stated that when calved, iceberg are simply removed from the system and don't induce any fresh water flux to the ocean model.

We have added further clarification of why this is important:

"...include the effects of a cliff-like calving front so that participating ocean models will be required to demonstrate their ability to handle advance and retreat of this jump in topography. We feel that this

is important because ocean models will require this capability to handle real-world problems with dynamic calving fronts.”

We added the following text to address the second point:

“Calved ice is simply removed from the domain, and contributes no freshwater flux to the ocean. We feel this is justified partly because it keeps the problem as simple as possible and partly because an Antarctic iceberg would be transported out of the ISOMIP+ domain in a matter of months, meaning most meltwater would be deposited elsewhere in a real-world problem.”

page 9881, Eqs. (15) and (16): would suggest to replace = . . . by \approx . Coordinates are now in uppercase. Should keep this homogeneous through the manuscript.

We have removed the ellipsis (...) and made clear that this is the time-rate of change of T and S due only to restoring. We're not sure what you mean by coordinates being uppercase. T and S are always written with uppercase letters, and x and z are lowercase here.

page 9881, line 14: T_{bot} should be T_b (using my notation suggestion), but then in Eqs. (21)-(24), it should be T_{z_b} , S_{z_b} and p_{z_b} . . .

We agree that a consistent notation is helpful. However, T_{bot} is the temperature at $z=z_{b,\text{deep}}$, not a $z=z_b$, so we stick with the notation T_{bot} . It was never our intent that subscripts would necessarily indicate the z depth of a given quantity.

3.2 to 3.5: would suppress "experiment i": ISOMIP+ experiment 1 (Ocean1): . . . \rightarrow ISOMIP+ Ocean1: . . . and only refer to this experiment by Ocean1 (not experiment 1 of ISOMIP+). Same for 4.1 and 4.2 for the IceOcean experiments.

Changed as suggested.

In part 3.2, both Ocean1 and Ocean2 are in fact described.

We have created a new section 3.2 called “Experiments,” that includes Ocean0-4 as subsections. Text that applies to multiple experiments is now in the introduction to this section.

page 9893: for ISMIP+, a pdf file is asked. Should be the same? Also, I suggest to have also the required inputs in this file to be in a numbered list, as for ISMIP+.

Presumably this refers to MISMIP+? As you have realized later, we do describe a readme file that will include all these details. At your suggestion, we have made this readme a pdf file to allow for better formatting. We have add examples for the POP2x and POPSICLES results to the supplementary material.

page 9894, line 18: from Parallel Ocean Program version 2 extended (POP2x) . . . \rightarrow from POP2x . . .

Changed as suggested.

page 9897, lines 18-20: I would suggest to remove these two sentences, which are a bit contradictory?

We can see how these sentences were confusing but we don't see them as contradictory. However, they have been removed in the updated manuscript. While we feel that it will be important to compare results with various stress approximations, MISMIP+ rather than MISOMIP1 is the appropriate place to explore this. We no longer suggest a particular stress approximation in MISOMIP1.

page 9898, line 12: website address already given.

Changed as suggested.

Table 1: ρ_{fw} not given (but may be too obvious to be ambiguous?)

ρ_{fw} constant has been added to Table 4. It is incorporated into Ω but is not needed anywhere else in MISMIP+, so is not needed in Table 1.

Table 2, caption: A list . . . \rightarrow List . . .

Changed as suggested.

Figure 1: change notations if bedrock equations are modified

We maintain the functions B(x) and B(y) in constructing $z_b(x,y)$, so there is no need to change the notation in the figure or caption.

Figure 2: axes label are a bit small

The figure has been replotted with larger labels.

Figure 3: the color bar should be the same height than the plot itself.

Changed as suggested.

Figure 8: replace "expt i" by "Oceani" in the legend.

Changed as suggested.

Figure 13a: the colorbar legend is too small and I would suggest to avoid a colored background.

We have replaced this figure with one showing several cross-sections of T (four per experiment), which also show the evolution of the ice-shelf geometry, as suggested by reviewer 2.

Authors' responses to comments from Reviewer 2:

General comments

This article introduces the interrelated inter-comparison suites MISMIP+ (for marine ice sheets in contact with ocean), ISOMIP+ (for coastal ocean in contact with ice shelves) and MISOMIP+ (for interaction of marine ice sheet and ocean models). I support the idea to publish the needed steps to participate in a paper alongside the necessary web-page. Inter-comparison projects have become very popular during the last 10 years and in my opinion sometimes the threshold of launching new initiatives should be set to a higher level. Nevertheless, I think in view of the challenges in improving on the prognostic modeling approach to sea level rise this is a necessary and useful setup. I am quite sure that there will be issues in the yet unexplored effects introduced not only by the separate components (i.e., ice sheet and ocean circulation models) but mainly the to date largely unexplored coupling effects coming up and that this will not be the last MISOMIP (or however future projects will be named) activity. I think it is a good crystallization point for development of coupled ice sheet/ocean models and by this a welcome initiative. Restricting myself to my field of expertise, i.e., ice-sheet models, I can say that by previous work from Gudmundsson et al. (2012) the glaciological part of the inter-comparison experiments is a good choice. I have little to contribute on the ocean model side concerning this aspect. The article fulfills its major purpose, namely, to describe the setups of the experiments, the preliminary model requirements and the expected output. The outline is clear and structured and, by reading through the paper I - at least for the ice-sheet and coupling part - find the instructions to be generally clear (I elaborate on those parts which I think still need improvements). I have the main issues summarized in the following section. If these are addressed I would recommend the article to be published in GMD.

Thank you for reviewing our manuscript, and for your detailed response. We are glad that you find these MIPs to be worthwhile and, for the most part, well designed. We have done our best to address your remaining concerns, as detailed in what follows.

Main points of criticism

My first point of concern is the for me missing conclusive argumentation concerning the method to reach the spinup-state, also in connection with the choice of the ice-sheet model.

We have described the possible approaches for initializing models and tuning parameters (A and/or β^2) in more detail:

“Some participants will spin up their model for tens of thousands of years with different parameter values until the grounding line lies within the desired position. Others might construct a more formal optimization problem and solve it with variational methods”

As you correctly pointed out, the MISMIP3d exercises revealed a discrepancy between the steady state position of full-Stokes and higher order (from full-Stokes perspective: lower order) models. As you choose the latter to act as the reference, which, despite your later statement, has potential also to become the quasi benchmark,...

We found this remark somewhat alarming. We have attempted to emphasize throughout the text that the results presented here are *not* to be treated as benchmarks. We do not wish in any way to include results that will be treated in this way, nor do we claim to have models that would be appropriate as benchmarks. We have added the following text to Sec. 2.2 to try to further emphasize this point:

“We emphasize that the example results shown in this figure are *not* intended as a benchmark for other simulations, but simply to demonstrate generally what type of behavior might be expected in each experiment.”

In Sec 3.2, we added:

“We emphasize that we do *not* intend these results to be treated as a benchmark for other participants to try to match. Instead, the examples show that the simulations can be performed and that they achieve their intended purposes. They should give the participants a qualitative idea of what to expect. After all, the MIP is not to attempt to produce identical results with all models but rather to try to understand the differences that occur.”

...it actually would have been

nice to analyze how much the initial state varies between different SSA models and (if possible) a full-Stokes and a SSA model - I know that one full-Stokes model was used in the Gudmundsson et al. (2012) paper, which tells me that in principle initial MISMIP+ tests would have been possible.

We fully intend to compare a variety of models, including Stokes models in the paper describing the MISMIP+ results. This manuscript is not the place for performing such a comparison, and the danger of the example results being treated as a benchmark would only be increased by including results from a variety of models here. We feel strongly that this paper is not the place for intercomparing results except where it motivates the choice of parameterizations and parameters (e.g. basal traction and viscosity).

Connected to spinnup and model choice I have the following points that need clarification in this context:

- You refer to "realistic simulation", which I understand means realistic not in terms of physics but in terms of model approach (e.g., SSA). Do you basically render any Blatter-Pattyn or full-Stokes approach as unrealistic? If so, you should state more clearly that this is SSA-business, only (and not later add that "other models are welcome"). The clear preference of depth averaged models continues within the choice of the sliding law (page 9870), which assumes hydrostatic pressure distribution at the base and the not further specified calving front boundary condition.

These comments would seem to reveal at least two potential misunderstandings of the intent of these experiments, particularly the coupled experiments (MISOMIP1). We seem to have struck a nerve by inadvertently implying a preference for SSA models over other stress approximations. Our purpose in requesting results with a particular stress approximation was merely to allow us to control for stress approximation while allowing the other modeling choices to vary among models. Our feeling was that this would be more likely to allow us to understand the relative importance of differences in stress approximation compared to these other variations. Because SSA seems to be the stress approximation appropriate for this marine ice sheet/shelf that was available in the largest number of models, we wished to solicit results from as many models as possible with the SSA *in addition to* other stress approximations. However, we decided that it was adequate to analyze results with various stress approximations in MISMIP+, and that there was no need to specifically request results with any particular stress approximation in MISOMIP1. Therefore, no specific stress approximation is requested under MISOMIP1 in the current version of the manuscript.

By “realistic simulations” we refer to simulations with realistic forcing and topography. We feel that this term is well understood in the community, and does not refer to any modeling approach (e.g. SSA vs. Stokes vs. Blatter-Pattyn).

We have attempted to remove inadvertent biases toward vertically integrated models elsewhere in the manuscript. As requested by Reviewer 1, the effective pressure within the sliding laws is now expressed in

terms of σ_{nn} instead of the lithostatic pressure ($\rho_i g h$). We now state explicitly in Sec. 2.1, “As in the previous MISMIP experiments, MISMIP+ uses a symmetry boundary condition at the ice divide, ocean pressure (up to sea level) at the ice-ocean interface, and stress-free boundary conditions at the upper surface (see Pattyn et al. 2012, 2013 for details).” These boundary conditions should be appropriate for all stress approximations.

- You let modelers choose to freely change viscosity as well as basal sliding parameter and/or sliding law (but therein restricted to Tsai and power law – why not the law proposed by Schoof/Gagliardini (Gagliardini et al. 2007)?) to achieve the initial spinup geometry.

Reviewer 1 also felt that the Schoof/Gagliardini basal friction laws should be allowed. We have added the option to use this parameterization of the basal traction in the current version of the manuscript.

I do not claim that this is

a bad choice, but I have the suspicion that even for each single model this is not unique, i.e., you can have a multitude of parameter combinations that produce you initial conditions with grounding lines intersecting a certain single point, but showing different volume fluxes.

We have attempted to allay this concern by stating a preference for adjusting A first and β^2 only if necessary in Sec. 2.1:

“Participants should adjust the grounding line position by modifying first the values of A and, if necessary, the value of β^2 beginning with the suggested values given in Table 1. The precise method used to adjust A and/or β^2 is left up to the participant.”

It is likely true that one could arrive at the same grounding-line position with different choices of A and β^2 within the same model. However, the same grounding-line position implies (nearly) the same catchment and therefore, in steady state, the same volume flux. Even so, the point is well taken that the different choices of A and β^2 could affect the resulting dynamics. This is likely inevitable, and consistent with the variation and uncertainty that we introduce when we initialize models with realistic topography and forcing.

I would expect

a justification, e.g. some proof of (non)-sensitivity of the spinup-state to variations of the freely chosen parameters within the chosen sliding law and rate-factor from Tab. 1. Could it be that this in some aspect might already exist either in form of a journal article or in form of the (page 9868) two models from MISMIP3d that were applied to the spinup state? For the latter, could you please elaborate which physics (approximation to Stokes) and which sliding/viscosity parameters these two models had in order to increase or relate the information to the reader/future MISMIP+ Participant?

We have added a new figure (Fig. 5) that indicates the sensitivity of the grounded area in the Ice1r experiment to the three friction laws that we allow. We include results with both SSA and SSA* approximations (which were shown to bound Stokes results in MISMIP3D). The figure shows little difference between these two stress approximations and little difference between Tsai and Schoof/Gagliardini friction laws. We do see significant sensitivity to the use of the Weertman sliding law, even if the value of A is tuned to match the steady state grounding-line position. We have added the following text describing the sensitivity results:

“Figure 5 shows the sensitivity of the BISICLES Ice1r results to various choices of basal traction, stress approximation, and values of A . Results are nearly insensitive to the differences between the basal-traction parameterizations of Tsai et al. (2015) and Schoof (2005), and also to differences between two stress approximations, SSA and SSA* (Schoof and Hindmarsh, 2010). However, the simulations with the basal traction of Weertman (1974) show a significant difference in both the initial grounded area and the rate of retreat compared with the other parameterizations.

Furthermore, even when A is adjusted so that the initial grounding-line position (and therefore the grounded area) is in agreement with the other configurations, the rate of retreat remains significantly slower than for the other parameterizations.”

Secondly, – and that was mentioned already in my first point – I could not find any hint on two boundary conditions for the ice sheet model within the text: What I am missing is the free-surface accumulation pattern (or rather constant value) needed to grow the ice-sheet into a steady state, neither if one has to apply accumulation/ablation on the free surface during the experiments. Even if this is trivial (as I conclude from Tab. 1), I think you should to provide that information in the text – from earlier experience with MISMIP3d I also can recommend to double-check its value before people start doing simulations. Also the dynamic condition at the artificial calving front is missing. For depth-averaged (SSA-ish) models it is one and the same, but for full-Stokes you have to specify whether you apply sea water pressure (up to sea level) or a cryostatic pressure distribution over the full thickness (mimicking an infinite long ice shelf).

Regarding the surface mass balance, we now state, “A constant accumulation rate a , with the value given in Table 1, is applied over the entire ice surface.” As mentioned earlier, we added in Sec. 2.1, “As in the previous MISMIP experiments, MISMIP+ uses a symmetry boundary condition at the ice divide, ocean pressure (up to sea level) at the ice-ocean interface, and stress-free boundary conditions at the upper surface (see Pattyn et al. 2012, 2013 for details).” This should make clear that the Stokes boundary conditions are to apply ocean pressure up to sea level, as opposed to an constant cryostatic pressure.

Thirdly, could you please elaborate on how the output of the grounding line should work. In particular, models based on SSA often apply sub-grid schemes for grounding line dynamics and hence a clearer rule on whether you demand output of properties on such an interpolated line (leading hence to interpolated values) or at the last grounded/first floating mesh-point would be at place (NB: with a full-Stokes model this would not be an issue).

We feel that it is up to the participant to determine where the grounding line is located in their model. Variations based on different methods for locating the grounding line are expected to be negligible compared to differences in the grounding-line location between models. We added the following text to section 2.3:

“It will be left to each participant to decide how to determine location of the grounding-line points (e.g. taking cell edges between grounded and floating regions or performing sub-grid-scale interpolation).”

Finally, I think section 4.5 on the results of the coupled simulation in my opinion is a little bit thin. I have the feeling that you could do better on displaying the IceOcean1 result (rather perhaps stick to 2D cuts, where one actually can see something). Also some figures displayed on MISMIP+ and ISOMIP+ results reveal their information only beyond a zoom-factor of 200% (which is not acceptable on the printouts); I elaborate this case-by-case in the next section where I think that there would be space for improvements.

We have taken your suggestion for the IceOcean1 (and IceOcean2) results, and have displayed temperature snapshots at various points in time. We have adopted this approach for the ISOMIP+ experiments as well. These new figures have larger axes, so they should be more readable.

Good luck with this inter-comparison!

Technicalities (sorted by their occurrence)

Line numbers refer to the printer-friendly version of the document that is to be found under <http://www.geosci-model-dev-discuss.net/8/9859/2015/gmdd-8-9859-2015-print.pdf>. I further include here also manifestation of the main points of critics of the previous section:

* page 9862, line 2: "At the first MISOMIP workshop held at New York University, Abu Dhabi in October 2014, participants decided that inter-comparisons of ice sheet-ocean dynamics in realistic configurations would be more credible if it was preceded by a more idealized intercomparison and evaluation process for the standalone components and coupled models Involved."

Is there some official document or maintained URL available on this workshop, where one could see what type of workshop (invited or open) that was and who of the community participated? This is interesting if the author list is a sub-set of the participation list, simply, because expressions like "we decided" occur frequently in this paper.

We have added a footnote with the location, dates and URL for the workshop. We have changed "we decided..." to "the participants decided...", as the coauthors of the paper and the workshop's participants are distinct groups.

* page 9863, line 6: "The second marine ice-sheet MIP, MISOMIP3d (Pattyn et al., 2013), aimed at exploring grounding-line dynamics on centennial timescales in a configuration that varied in two horizontal dimensions (2HD)."

This is just a suggestion, but as there are multiple non-marine ice sheet MIPs, it might be a good idea to be explicit on that.

We now introduce three other previous MIPs:

"A number of previous MIPs not specifically focused on marine ice sheets have explored model physics (EISMINT: Payne et al. 2000), provided benchmarks (ISMIP-HOM: Pattyn et al. 2008) and demonstrated modes of internal variability (ISMIP-HEINO: Calov et al. 2010), improving our understanding of ice-sheet models."

* page 9863, line 20: "topoography →topography"

This has been fixed.

* page 9868, line 8: "First, it started from a steady state that was invariant in the cross-flow direction – that is, 1HD – and did not involve significant lateral stresses."

Minor issue, but, if you refer to the initial state, the fact that it was effectively 1HD tells us that the initial state involved no lateral stresses. Else, add an "... during the applied perturbations" at the end of the sentence.

We have changed "and did not..." to "meaning it did not.."

* page 9869, line 19: "A suggested value for A is given in Table 1, but participants should modify this value (and/or the coefficient β^2 that appears in the basal traction below) so that the steady state grounding line crosses the center of the trough at $x = 450 \pm 10$ km."

That is in particular the sentence I referred to in the previous section. I would say that as a minimum you have to provide a good argument why you think that this is {a good enough, the best of all, the only possible choice} to obtain comparable spinup. At the best, you demonstrate the

non-sensitivity of both, the spinup as well as the perturbation phase with simulations obtained by one or (preferred) multiple model(s) with respect to variation of A , β^2 as well as the chosen sliding law.

We now give a more detailed description of the thinking behind adjusting an unknown parameter value (in this case A) to match an “observed” grounding-line position:

“We prescribe that the steady-state grounding line should cross the centerline of the trough at $x = 450 \pm 10$ km, ensuring that all models start from similar initial states. Participants should adjust the grounding line position by modifying first the values of A and, if necessary, the value of β^2 beginning with the suggested values given in Table 1. We have adopted this approach for model initialization to be more consistent with the methods used to initialize models for real-world problems: unknown parameters or fields are determined by search or inversion techniques so that initial conditions are consistent with observations. The precise method used to adjust A and/or β^2 finding the steady state is left up to the participant. Some participants will spin up their models for tens of thousands of years with different parameter values until the grounding line lies within the desired position. Others might construct a more formal optimization problem and solve it with variational methods”

Also, as previously noted, we have added a new Fig. 5 that explores the sensitivity of the results to three different choices of the basal-friction law, two different values of A and two different stress approximations (SSA and SSA*, which have been shown to produce significantly different steady-state grounding-line positions in MISMIP3d). This figure suggests that the choice of basal friction law is likely to affect the dynamics more than the the choice of A (which moves the initial grounding line position, but appears to have relatively little impact on the amount of retreat) or the stress approximation.

We feel that a more detailed demonstration of the sensitivity (or lack thereof) to various parameters and in various models lies more in the scope of the analysis of MISMIP+ than in its description.

* page 9870, line 1 - 17: That paragraph links to the question why – if allowing for choices in the type of the sliding law – you confine it to (6) and (7)? First of all, I think (6) is not a good choice, as it is not bounded, secondly, the sliding law introduced in detail by Gagliardini et. al. (2007) would at least be an equally good alternative to (7). The free choice between two sliding laws introducing further model variety should be justified. Explain also what a model that does not include the assumption of a hydrostatic pressure distribution should do with (7) - I guess the answer will be, effective pressure at the base.

As noted in our response to Reviewer 1, we now allow the Schoof/Gagliardini friction law. Figure 5 now shows that the example results are nearly indistinguishable from those with the Tsai law.

We have found that there are strong feelings in the community about which friction law was the “right” one to use, and the decision made at a splinter meeting before the IGS symposium in Cambridge last year was that multiple friction models should be allowed. Initially, we felt that the results would be simpler to analyze with just two choices, but we have found in our own tests (again see Fig. 5) that there is little difference between Tsai and Schoof/Gagliardini, so there seems little down side to allowing both.

Following Reviewer 1’s suggestion, we have changed (7) to use the effective pressure N . We no longer assume the ice-sheet model uses the lithostatic approximation.

* page 9871, equations (10)-(13): This is just a suggestion, but I think a simple 2D flow-line sketch instead or in addition to the 3D pictures showing all the relevant geometrical parameters, such as z_d , z_0 and H_c would be

good for readers not being that familiar with marine ice sheet setups.
A panel has been added to Fig. 3 with a sketch of the geometry, as you suggest.

* page 9872, equation (14): I am aware that you explain your cut-off value before, but, the statement that (14) is a result of (10)-(13) with a lumped coefficient does not apply, as $|z_d - z_0|$ and $\max(z_0 - z_d, 0)$ simply are not the same. My suggestion would be to either rewrite (12) or postpone the explanation of this cut-off to after (14).

We have corrected this problem by changing the notation in what is now (15) (previously (12)) to also use $\max(z_0 - z_d, 0)$.

* page 9872, line 14: "The coefficient Ω has been given a value of 0.2 yr^{-1} , corresponding to a maximum ambient ocean temperature $\sim 1.0^\circ\text{C}$, which leads to a melt rate with a maximum value of $m_i \approx 75 \text{ m yr}^{-1}$ near the grounding line (see Fig. 2)."

First of all, is m_i ice or water equivalent? Secondly, I guess the 75 m yr^{-1} correspond to the steady state spun-up configuration of BISICLES in your setup. If so, then please explicitly mention this.

This has been fixed as suggested. We now show both m_i in m/a of ice and m_w in water equivalent in (12) ((9) in the previous draft) to highlight the distinction.

* page 9875, line 4: "xGL(nPointGL,nTime), yGL(nPointGL,nTime) [m].
The x and y coordinates of a given point on the grounding line."
As mentioned in my general comments, this would need more detailed rules for models using sub-grid representation of the grounding line.

Again, we feel that the way that participants choose to locate points on the grounding line is up to them and cannot usefully be prescribed.

* page 9875, line 23: ". . . , in a pdf file, . . . "
There is an orphan dot in this line.

This has been fixed.

* page 9876, line 1: "2. Englacial stresses: the stress model and coefficients (e.g. SSA, $A = 2.0 \times 10^{-17} \text{ Pa}^{-3} \text{ yr}^{-1}$)."
I would rather call it stress approximation model.

We have changed "stress model" to "stress approximation".

* page 9876, line 13: Conventional models should simply carry out a convergence study of experiment Ice1r and Ice1ra, showing that the grounding line shape and positions at the start and end of Ice1r and the volume-above-flotation curves throughout the experiments converge with mesh refinement and differ by a fraction at the finer resolutions.

Conventional = SSA? Please explain what you mean by conventional.

Conventional certainly was not intended to mean SSA. "Conventional models should" has been changed to "Typically, models should..." This is the typical way of demonstrating sufficient resolution, though we are open to other methods.

* page 9879, line 11: ". . . of most Antarctic ice shelves. . . "

This has been fixed.

* page 9879, line 18: "We prescribe an f plane configuration . . . "

Like there was a reference for the SSA in the part prescribing the MIS-MIP+ experiments, I think – in order to keep symmetry between the level of explaining typical approximations in glaciology and oceanography – it would also be appropriate to introduce the standard literature for glaciologists that want to invest into reading about the nature and consequences of such approximations in ocean models.

We have added references to Gill (1982) and Pond and Pickard (1983), which are good general oceanography references. We specifically reference a chapter in each about the the f-plane (which assumes that the Coriolis parameter f does not vary with space).

* page 9880, line 17: "Ice thinner than $H_{\text{calve}} = 100$ m (equivalent to an ice draft above ~ -90 m) is considered to have calved and the ice draft is set to zero."

It is clear from the text why you want to have a calving front within the ocean model domain. But could you provide some motivation (if there is) why exactly at 100 m and not another number? For instance, something along the line that there are no shelf thicknesses below that threshold observed in Amundsen sea area, or 100 m gave a nice ratio between shelf-covered and open ocean in the model setup.

We have added the following justification for this choice:

"This threshold was chosen to eliminate the thinnest ice on eastern and western flanks of the ice tongue while maintaining the tongue itself. A thicker threshold, more consistent with typical Antarctic ice shelves, would eliminate large portions of the ice shelf during retreat and making analysis of the evolving melt-rate field more challenging."

* page 9887, line 26: " The WARM profiles was chosen to . . . "
Either profile was or (more likely) profiles were.

This has been fixed.

* page 9888, line 25: ". . . retreat from Ice1r."

This is just my personal view, so, leave or change it: If referring to other experiments from other sub-MIPs, you could put the corresponding MIP identifier in front, such as MIS-MIP+ Ice1r – easiest would have just been to use MIS-MIP+/ISOMIP+/MISOMIP in the experiment names (this is also just a personal opinion), but you might not want to change this at this stage.

We went through several iterations of naming conventions before settling on these names for the experiments. The numbering and punctuation already included in the MIP names made it impractical to use them as prefixes for the experiment names (e.g. MIS-MIP+1ra vs. MISOMIP1.1 was confusing). We have changed "Ice1r" here to "MIS-MIP+ Ice1r" and have done the same for the first mention of an experiment from another MIP in the other MIPs' sections. We feel it is too cumbersome to prefix the experiment name with the corresponding MIP each time.

* page 9893, line 26: "- A link to the repository where the model can be downloaded (if public) and specific tag, branch or revision (if available)."
Why such a demand is confined to the ocean models – should similar information not have been demanded from the ice-sheet model in MIS-MIP+ and MISOMIP suite?

This has been added to the ice-sheet model description as well.

* page 9896, line 6: "This should greatly reduce melting within a decade,

similarly to Ocean2, and allow ice to re-advance for the remaining 100 years of simulation."

Minor detail: If there is a retarded signal in lowering the melting from the ocean side that lasts a decade, there are no remaining 100 years for re-advance.

True. This has been changed to:

"The simulation evolves for another 100 years, during the first decade of which the ocean should cool and the melt rate should be greatly reduced, similarly to Ocean2. The reduced melting should allow ice to re-advance for the remainder of the simulation."

* page 9896, line 22: "Whereas the MISMIP+ experiments do not include a dynamic calving front, IceOcean2 prescribes the same simple calving criterion used in ISOMIP+: ice thinner than H calve = 100 m (equivalent to an ice draft above ~ -90 m) or beyond x calve = 640 km should be calved \rightarrow removed and the ice thickness set to zero." Two issues here: First, as stated already in a comment to section 3.1.2, you should provide motivation (either by physics or model setup) why you chose these values.

In this case, the threshold was chosen simply for consistency with ISOMIP+, as we now state.

Secondly, you did not mention the x calve -criterion in connection to ISOMIP+ section 3.1.2. This should be explicitly mentioned also there, if it was applied.

The ice draft (and ice surface elevation and floating mask) is already zero beyond $x = 640$ km in the topography data set supplied to the participants, so we do not feel it is necessary to mention this explicitly under ISOMIP+. We now mention the dynamic calving criterion and the fixed-front calving condition separately, so that it is clear that only the dynamic condition is adopted directly from ISOMIP+.

Minor detail: I would replace "calved" with "removed", as the first one suggests that this is according to a physical calving criterion.

This has been changed as you suggest.

* page 9897, line 9 + page 9898 1st paragraph: "Coupled ice sheet-ocean models are not well enough established to have typical resolutions and parameters. Therefore, we invite participants to submit several sets of results with parameter choices at their discretion in addition to the COM run and ensure these are well documented in the readme file.

The coupling interval for the model is left to each participant to decide. We recommend based on experience with the POPSICLES (coupled POP2x and BISICLES) model that participants use a coupling interval of six months or less if they are able, as results with yearly coupling diverged significantly from those with more frequent coupling. We ask participants who are able to do so to provide multiple sets of results using different coupling intervals."

Here in particular I would have liked to see a slightly more in-depth analysis of POPCYCLES results on IceOcean1 included in this article. You often use the terms "conventional" and "typical" within the text, so I think the participants of this inter-comparison would benefit from obtaining more information on the settings of a "typical" coupled setup, such as POPCYCLES. What, for instance, was the range of coupling timestep-sizes, what were the timestep-sizes in the sub-models, what computational load and wall-clock-times did those runs produce? From the next paragraph on page 9888 I conclude that you actually have more infor-

mation from variation of coupling intervals.

We appreciate your interest in seeing more results and analysis from the POPSICLES results. However, we feel strongly that this is not the right context for deeper analysis, including parameter studies. Other papers are in the works that will explore POPSICLES specifically, and the MISOMIP1 analysis paper will include POPSICLES results as well (possibly including several coupling intervals). We feel that the more emphasis that is placed on the POPSICLES results here, the more likely they will be to be treated as a benchmark for other results, which we adamantly wish to avoid.

To avoid confusion, we have removed the two uses of “conventional” from the paper (one referring to methods for determining convergence with resolution, one referring to basal-traction parameterizations) and use the word “typical” only to describe model configurations (as distinguished from the “common” configuration that prescribes more parameters and parameterizations). We do not refer to “typical” models. We do not feel that there are enough coupled ice sheet-ocean models in existence yet to have “typical” models, and do not wish to claim that POPSICLES is one.

In my personal opinion – if the results seem to be just around the corner – it would have been better to wait to have also IceOcean2 achieved before pushing the paper to publication, to have a complete set of simulations.

We now include IceOcean2 results in the revised manuscript. We think they are actually quite a bit more interesting than IceOcean1 because even a simple calving criterion such as we have here can produce rather dynamic results and appears to have a more pronounced effect on buttressing. To accommodate these extra results as well as those from the new Ocean0 experiment, we have had to remove some other figures and do not have room to add any more, but we provide extensive output including animations through the MISOMIP website.

Something completely different: I have the feeling that there is something strange with hyphenations (but that might be more a typesetting issue from Copernicus). I found two hyphenations that in my view are not correct and marked those in red - please check (in case with the GMD typesetter).

These are both correct hyphenations (strange as they may seem) according to a website dedicated to this topic:

<https://www.hyphenation24.com/word/recommend/>

<https://www.hyphenation24.com/word/coupling/>

In any case, the hyphenation rules that Copernicus chooses to use are really up to them and not something we are interested attempting to change.

* page 9889, section 4.5: As mentioned in the previous item and the main points of criticism, I think that you should reveal more information within this section.

We have added a paragraph each of analysis of the example results from IceOcean1 and IceOcean2. We feel that more is not appropriate for this manuscript. The text quoted below may not be terribly useful without the associated figures to refer to.

“The blue curves in Fig. 12 shows the mean melt rate and the grounded area and from an IceOcean1 simulation using the POPSICLES model (coupled POP2x and BISICLES). The top row of Fig. 13 shows the evolution of the ice draft and ocean temperature over the course of the simulation. The mean melt rate is initially relatively small, increasing by several orders of magnitude over the first decade as warm water reaches the cavity and initiating grounding-line retreat. Because of the ocean temperature profile, the melt rate is a strong function of the depth of the ice-ocean

interface. As the ice shelf thins, melting becomes concentrated over a steep region within the channel near the grounding line. As the grounding line retreats, the area of the cavity increases (no calving occurs except beyond $x=640$ km) while the total melt flux remains nearly constant, meaning that the mean melt rate gradually decreases. Between year 100 and about year 130, the melt rate decays by several orders of magnitude, reaching a nearly steady value for the remainder of the simulation as the ice shelf thickens and grounding line begin to re-advance.”

Later on, describing the IceOcean2 results:

“Mean melt rates and grounded area from an example POPSICLES IceOcean2 simulation are shown in the green curves in Fig. 12, and the evolution of the ice draft and ocean temperature are shown in the bottom row of Fig. 13. The beginning of the retreat phase of IceOcean2 proceeds similarly to IceOcean1, with small differences resulting from the smaller, thinner ice shelf that results from the calving criterion. Starting at around year 30, dynamic calving removes significant portions of the ice shelf. Although the melt flux remains relatively steady, the mean melt rate increases as the ice-shelf area decreases. Just after year 60, a large iceberg breaks off from the ice shelf, leading to an abrupt increase in the mean melt rate. For the remainder of the retreat phase, the ice shelf exists only as a small remnant of its initial size close to the grounding line. The re-advance phase begins at year 100 when the far-field restoring is switched to the COLD profiles. As the ocean cools, the melt rate decreases by several orders of magnitude. The ice-shelf area remains much smaller than in IceOcean1ra while melt fluxes are similar, meaning that the mean melt rate is nearly an order of magnitude higher.”

* page 9990, line 3: "The Supplement related to this article is available online at doi:10.5194/gmdd-8-9859-2015-supplement. "

This is useful.

References

From the ice-sheet point of view I have no complaints. One point I would like to have cleared and I think that also links to the editorial comment given in <http://www.geosci-model-dev-discuss.net/8/C3046/2015/gmdd-8-C3046-2015.pdf>: Is the link given in

Hunter, J. R.: Specification for test models of ice shelf cavities, Tech. Rep. June, Antarctic Climate and Ecosystems Cooperative Research Centre, available at: http://staff.acecrc.org.au/johunter/isomip/test_cavities.pdf (last access: 7 November 2015), 2006. certainly available for a longer period – or would it be better to choose a certainly permanent URL to provide this data?

While we understand the concern about the persistence of the description and example results from the original ISOMIP experiment, it is not necessarily within the purview of this work of the MISOMIP target activity to take over the archival of ISOMIP.

Figures

* page 9912, Fig 1: "Figure 1. The bedrock topography for the three MIPs as defined by Eqs. (1)–(4). (a) $B_x(x)$, the variability of the bedrock topography \rightarrow topography in the x direction. The topography through the central trough is shown in blue and on the side walls is shown in red. (b) $B_y(y)$, the bedrock topography in the y direction \rightarrow direction relative to that at the center of the trough. (c) The topography in 3-D at 1 km resolution. Sea level is shown in translucent blue. "

These typos have been fixed.

(b) shows a cross section that to me seems only to be valid over the region of the trough (where threshold of $-B_{max}$ does not apply); here one could

get the impression that it applies to the whole region.

$B_y(y)$ is not a cross section of the topography. Like $B_x(x)$, shown in blue in (a), it is a function that is used to define the bedrock topography. Over most of the domain, cross sections of the bedrock topography do look like (b) with a vertical offset. We are uncertain how to better clarify this. We assume that participants will graph the topography for themselves and become acquainted with it.

* page 9913, Fig. 2: This figure is way to small, in particular in terms of annotated text. I think a plot of the corresponding velocities also would be interesting.

The figure has been simplified and the size of the annotations has been increased. We felt that an additional figure with velocities, while potentially interesting, would be too much.

* page 9916 + 9917, Fig. 5+6 : This is just my personal opinion, but I think that the boundaries of the ocean model are trivially clear (its a box outside the shelf) and leaving out the dark-blue side-walls would lower the complexity and improve the visualization of the essential information.

We appreciate the comment. We tried various versions of these figures both with and without the box, and it was unclear both where sea level was and exactly how the topography related to flat surfaces (the top and bottom edges of the box) without having the box itself. What may seem look like unnecessary clutter actually appeared to provided useful context. However, to make room for other figures that have been added, we have decided to remove these figures entirely from the paper.

* page 9920 - 9822, Fig. 9-11 : Again, too small if read in 1:1 size. Why do all the stream-functions extend beyond the ocean region? I guess they are derived quantities and take zero values there, but could you, for convenience, mask the areas where there is grounded ice? If using ParaView, the Threshold-filter might come handy. Same applies to Fig. 12 on page 9923.

These figures have been replaced by time series of temperature only. Animations of the time evolution of all the fields in the standard output are available on the MISOMIP website but fields other than temperature are not included in the manuscript. We have endeavored to make the fonts bigger in the figure. In the output that we provide on the MISOMIP website, we now mask the overturning and barotropic streamfunctions based on where there is ocean and where not. Masking streamfunctions is a slightly non-trivial operation because their computation involves both an integral over the domain and in our case two different transformations to staggered grids, so typically we don't bother. But it is true that the data is easier to interpret with the appropriate masking.

* page 9924, Fig. 13: Too small, again. Upper picture does not really convey a lot of information. You could think of using cross-sections to show the change in shape of the ice shelf as well as display the temperature distribution in the ocean.

We have replaced the figure as you suggested -- showing four cross sections of temperature at different times for each of the ISOMIP+ and MISOMIP1 experiments. The new figure should be a more acceptable size. The previous figure made for a better movie than a still image.

Authors' responses to comments from Dan Goldberg:

I think this intercomparison is a great idea and I applaud the authors' efforts. I agree with the philosophy of the experiments and think it is the right way forward. I have no high-level objections with any part.

Dan, we are very happy to have your support on these MIPs.

I would only like to make a few comments about Section 3, the ocean experiments.

Section 3.1.1: If an ocean model is using a lat-long grid (rectangular in the lat-lon space), it might be tricky to conform to the cartesian dimensions you state.

Xylar says: I do not think this should be very difficult. I have done this with POP2x in the past. I don't want to detail this in the paper because I feel like it isn't really the point, but the following python snippet should produce lon/lat points that have the appropriate spacing and the correct latitude at the center:

```
import numpy
import matplotlib.pyplot as plt

rEarth = 6.371e3

(X,Y) = numpy.meshgrid(numpy.linspace(320., 800., 241),
                       numpy.linspace(0., 80., 41))

x0 = 0.
y0 = 40.

lat0 = -75.*numpy.pi/180.
lon0 = 0.

# Y - y0 = rEarth*(Lat - lat0)
Lat = (Y - y0)/rEarth + lat0

# X - x0 = -rEarth*sin(Lat)*(Lon-lon0)
Lon = -(X - x0)/(rEarth*numpy.sin(Lat)) + lon0
```

The grid cells you get this way aren't equally spaced in longitude, as you might be used to from ISOMIP but the ocean model should be perfectly happy with this.

Section 3.1.2: I think some mention could be given to what is "allowed" for any model which attempts synchronous coupling, i.e. evolution of ice thickness at the ocean time step). An instantaneous removal of 100 m of ice over a grid cell may wreak havoc in the ocean. MITgcm, for instance, will need to interpolate in time from an ice-covered to ice-free state. I don't know if GFDL is participating but from offline conversation with Alon Stern it sounds as if their ocean model needs to do something similar to move around large icebergs.

Yep, that's a reasonable concern. There are bound to be things like this that we haven't thought of and that may be more specific to a given model. In general, I would think participants will need to figure out how to best handle these situations, as they presumably have done for the previous ISOMIP and any other test cases they may have run (e.g. the experiments from your 2012 papers). Here is what we have added to address this particular issue:

“Models that do not support a sheer calving face or which update the ice topography at each time step will likely need to smooth the calving face over several horizontal grid cells and/or to relax to the new geometry gradually over time. In such cases, it is suggested that participants interpolate the

geometry in time, then apply the calving criterion, and finally apply whatever smoothing or relaxation is required. This way, the (smoothed) calving front is expected to move relatively continuously in the horizontal, rather than abruptly jumping to the new location each year as the ice between the old and new calving fronts thins to zero.”

Also, MITgcm (without a rigid lid) and possibly other models specify surface pressure to control the elevation of the ice-ocean interface – would these models be allowed to specify ice mass per unit area instead (with a standard ice density)?

Good call. We added the following:

“Some participating ocean models require a surface pressure rather than the ice draft as the upper boundary condition. These models are free to compute the ice thickness from the ice surface elevation and ice draft provided in the input geometry, and multiply these by $\rho_i g$ to get a pressure. Equivalently, the pressure can be derived from the ice draft as $p_{zd} = -\rho_{sw} g z_d$. The elevation of the ice-ocean interface in the model will differ slightly from the prescribed z_d because of the dynamic pressure and difference between the reference density of seawater and the local ocean density, but these differences are expected to contribute negligibly to the differences between model results.”

Section 3.1.4: any mechanical bdry conditions on ice shelf front or other vertical parts of the ice shelf?

We added the following text that we hope will address this comment:

“Also we prescribe no melting or drag from vertical ice faces (e.g. the calving front) both for simplicity and because many models do not support melting on vertical faces.”

Immediately after this, we state (as before), “Participants that use other boundary conditions should note this when they submit their results”, which we hope makes clear that participants could use models with melting at vertical faces, as long as this is documented. Given that the area of the sloped ice draft is likely to be many orders of magnitude higher than the area of vertical faces, it may be that melting on vertical faces is negligible for this particular set of experiments. However, it would be interesting to show this with a model capable of doing so. POP2x, which we used for the example simulations, does not currently support melting at vertical faces.

Section 3.1.5: i think "digging" needs some explanation

We have removed the reference to “digging”. The text now states:

“Models with other vertical coordinates may be less restricted, but some modification of the topography may be required to maintain a minimum ocean-column thickness. In locations where the ocean column is too thin, participants will need to decide for themselves whether it is more practical to modify the topography (ice draft, bathymetry or both) or to remove the column from the ocean (i.e. mark it as “land”).”

Eq (3.1) – i really like this idea

Xylar says: Ironically, I tried this and it didn't quite work out, so I've updated the suggested procedure based on what worked for me in MPAS-Ocean (see response to Nicolas below). The essence of the original method is still there.

Section 3.1.8: i found the boundary layer a bit confusing, and there are quite a lot of cans of worms hidden here. for one thing, you refer to a boundary layer, which at first i thought meant the viscous sublayer, but later on i thought meant the layer over which the eddy size scales with distance from the wall (i don't know what this is called, but p9885 line 11) but later surmised you were referring to the mixed layer (eg p9885 l19), which is a bit larger and involves buoyancy and rotational effects.

The text that you found confusing has been significantly modified or removed. We now use the new Ocean0 experiment (see Yoshi's comment below) to calibrate the GammaT and GammaS coefficients, rather than relying on vague theoretical notions about how they should vary. We think the new approach will be less confusing and more consistent with how uncertain model coefficients are typically computed by inversion or "tuned" based on observations:

"Because of differences in vertical resolution, vertical mixing and the method for computing u_w , T_w and S_w , appropriate values of the heat- and salt-transfer coefficients, GammaT and GammaS, are likely to vary significantly between models. In Sect. 3.2.1, we prescribe a procedure for tuning these coefficients to achieve a desired mean melt rate. With the exception of GammaT and GammaS, we prescribe values for the coefficients in these equations in Table 4."

In this section there is mention of interpolating values (u,v,T,S) to 20m away from the interface. Should doing this not follow some prespecified theoretical boundary layer profile, as opposed to linear interpolation? My understanding is that this would be logarithmic in velocity, at least close to the wall ($< 2m?$); but I am not familiar enough with the theory to know what the "outer" parts of the profile are meant to be, nor do I know much about the theoretical T/S profiles.

This subsection is much less prescriptive in the current draft:

"Methods for computing the 'far-field' potential temperature, salinity and velocity (T_w , S_w and u_w) differ across models. Some models sample these fields at a fixed distance below the ice draft (e.g. Kimura et al. 2013) while others average the fields over a prescribed thickness (e.g. Losch 2008). Participants are asked to describe how T_w , S_w and u_w are computed in the pdf included with their results."

Furthermore I am of the opinion that for a synchronous approach with a dynamic grounding line (which ocean.3 and ocean.4 essentially are, from the view of the ocean) there should not be such a large minimum depth as 20m – but for column thicknesses below this range I would not imagine there are significant melt rates. How about rather than a minimum depth, it can be agreed that melting is shut off when column thickness is below this value?

Xylar says: The 20-m boundary layer is no longer prescribed, I think that will take care of your concern. I have found that it works fine to average over some fixed boundary-layer distance or the full ocean column, whichever is thinner. I don't think there is any need to explicitly shut off melting near the grounding line. This will tend to happen in some models because the flow is restricted and mixing is suppressed but there are no solid observational or theoretical reasons to require this. At this point, I think it's fine to let modelers do what they do.

Authors' responses to short comment from A. Kerkweg:

In my role as Executive editor of GMD, I would like to bring to your attention our Editorial version 1.1:

<http://www.geosci-model-dev.net/8/3487/2015/gmd-8-3487-2015.html>

This highlights some requirements of papers published in GMD, which is also available on the GMD website in the 'Manuscript Types' section:

http://www.geoscientific-model-development.net/submission/manuscript_types.html

In particular, please note that for your paper, the following requirements have not been met in the Discussions paper:

- "The main paper must give the model name and version number (or other unique identifier) in the title."
- "All papers must include a section, at the end of the paper, entitled 'Code availability'. Here, either instructions for obtaining the code, or the reasons why the code is not available should be clearly stated. It is preferred for the code to be uploaded as a supplement or to be made available at a data repository with an associated DOI (digital object identifier) for the exact model version described in the paper. Alternatively, for established models, there may be an existing means of accessing the code through a particular system. In this case, there must exist a means of permanently accessing the precise model version described in the paper. In some cases, authors may prefer to put models on their own website, or to act as a point of contact for obtaining the code. Given the impermanence of websites and email addresses, this is not encouraged, and authors should consider improving the availability with a more permanent arrangement. After the paper is accepted the model archive should be updated to include a link to the GMD paper."

With respect to MIPs the Editorial v1.1 explicitly states: "For model experiment description papers, similar version control criteria apply as to model description papers: the experiment protocol should be given a version number; boundary conditions should be given a version number and uploaded or made otherwise available; a data availability paragraph must be included in the manuscript; and links to the GMD paper should be included on the experiment website. Papers describing data sets designed for the support and evaluation of model simulations are within scope. These data sets may be syntheses of data which have been published elsewhere. The data sets must also be made available, and any code used to create the syntheses should also be made available. "

Therefore I ask you to change the title in your revised submission to GMD naming the three MIP experiments explicitly including a version number.

We have revised the title to now include the names and version numbers of each of the 3 MIPs. The title is very cumbersome, which we had sought to avoid, but should meet GMD's requirements:

"Experimental design for three interrelated Marine Ice-Sheet and Ocean Model Intercomparison Projects: MISMIP v. 3 (MISMIP+), ISOMIP v. 2 (ISOMIP+) and MISOMIP v. 1 (MISOMIP1)"

Additionally, please add a

"Code and/or Data Availability" Section comprising access information to all data and code named in your article.

A section called "Code and Data Availability" has been added. There, we provide information for accessing the BISICLES code, the topography data required for the ISOMIP+ experiments and the example results.

We state that source code for POP2x and POPSICLES is not currently available to the public. Negotiating the public release of these codes is outside the scope of this work.

Authors' responses to short comment from Y. Nakayama:

Authors summarize the experiments very well and descriptions of model experiments are easy to follow. I have one comment, which may make it easier for ocean modelers to compare their results without running experiments for 10-20 years.

+ I suggest adding 1-year ISOMIP experiments with warm initial condition and warm restoring. This way, at least in my setup, model melt rate converges within 4-6 months. I believe this makes it much easier for other ocean modelers to debug and test their code.

Yoshi, thank you for the suggestion. We have added a new Ocean0 experiment which we now use to specify a process for calibrating the coefficients Γ_T and Γ_S to achieve a desired melt rate. We agree that a shorter experiment that reaches quasi-equilibrium in a shorter time will be more practical for troubleshooting during model development (which is not to suggest that the example results should be used as a benchmark for model development!) and will also provide a fruitful starting point for parameter experiments in the future.

Authors' responses to short comment from N. Jourdain:

Thank you for your suggestions.

I would just like to add a few minor comments that could improve the clarity of the manuscript:

- Equation (20) : mention that T is potential temperature. Printer-friendly Version
- It would be convenient to use the same value and notation for ρ_{ref} (Eq. 20) and ρ_{sw} (Eq. 21,23). Values are very close (1027.51 and 1028 kg m⁻³ respectively).

Hmm, we agree that this would have been convenient but at this point it seems like it isn't worth changing. It's convenient to have a relatively round number for ρ_{sw} since it's also used for flotation in MISMIP+. On the other hand, ρ_{ref} comes from a linearization of the equation of state (using TEOS10) with round values for T and S, which results in ρ_{ref} not being a very round number. We don't feel that the convenience (for participants) of having these two values be the same is worth the inconvenience (for us) of modifying and rerunning the experiments, given that the differences are likely not to be significant. We added the following text to further address the issue:

[“Any model that requires \$\rho_{ref}\$ to be equal to \$\rho_{sw}\$ should use \$\rho_{ref}\$ for both values, and should note this difference along with their output.”](#)

- Equation (26) and (29) : T_f should probably be T_b as in equation (21).

This has been changed.

- About the artificial evaporative flux used to remove freshwater in models using volume fluxes : (i) this can be done on every time step, why using a 30-day characteristic time? (ii) it should be mentioned that this is evaporation with no associated latent heat (otherwise this will cool the surface).

The proposed scheme for maintaining sea level been modified significantly (see below). (We agree that freshwater could be removed at each time step to exactly counterbalance the melt flux, but this amounts to a global reduction at each time step that models might prefer to avoid. The original scheme was intended to remove excess mass based on only local quantities and without shocking the system too severely. None of this is particularly relevant, as the new scheme does not involve a characteristic time scale.) We now state:

[“Models using volume or mass fluxes will need a strategy for removing mass in the open ocean to compensate for the volume of melt water that enters the domain. Because of the small size of the](#)

domain, without such a strategy, sea level would likely rise by hundreds of meters in simulations with large melt rates (Ocean1 and Ocean3). One possible approach is to impose an artificial evaporative flux in the restoring region ($x > 790$ km). Corresponding salt and heat fluxes will be needed to prevent the top cells from becoming cooler and saltier as mass leaves the cell:

$$F_e = -\rho_{sw} \langle m_w \rangle \frac{A_{shelf}}{A_{res}},$$

$$F_{H,e} = c_w T_0 F_e,$$

$$F_{S,e} = S_0 F_e,$$

where F_e , $F_{H,e}$ and $F_{S,e}$ are the evaporative mass, heat and salt flux, respectively, A_{res} is the area of the restoring region, T_0 and S_0 are the prescribed temperature and salinity at the ocean surface in the restoring profile, and $\langle m_w \rangle$ is the melt rate averaged over the area of the ice shelf A_{shelf} and over a suitable period of time (perhaps one month). Participants are welcome to use alternative strategies. They are asked to document whichever approach (if any) they use for removing excess mass in their description pdf.”

- About u tidal (RMS velocity associated with tides): is it also used in the formulation of the bottom ocean drag?

No, it is only used in computing u^* to be used in the melt formulation. We assume that it is largely irrelevant, at least to the types of problems that these MIPs explore, if there is additional drag due to tidal motion at very low velocities, since the velocity is small to begin with. As with any modeling choices, participants may choose to deviate from this prescription as long as they document this. We now state:

“The computation of top and bottom drag do not incorporate u_{tidal} .”

Experimental design for three interrelated Marine Ice-Sheet and Ocean Model Intercomparison Projects: [MISMIP v. 3](#) [\(MISMIP+\)](#), [ISOMIP v. 2 \(ISOMIP+\)](#) and [MISOMIP v. 1 \(MISOMIP1\)](#)

**X. S. Asay-Davis¹, S. L. Cornford², G. Durand^{3,4}, B. K. Galton-Fenzi^{5,6},
R. M. Gladstone^{6,7}, G. H. Gudmundsson⁸, T. Hattermann^{9,10}, D. M. Holland¹¹,
D. Holland¹², P. R. Holland⁸, D. F. Martin¹³, P. Mathiot^{8,14}, F. Pattyn¹⁵, and
H. Seroussi¹⁶**

¹Earth System Analysis, Potsdam Institute for Climate Impact Research, Potsdam, Germany

²Centre for Polar Observation and Modelling, University of Bristol, Bristol, UK

³CNRS, LGGE, 38041 Grenoble, France

⁴Univ. Grenoble Alpes, LGGE, 38041 Grenoble, France

⁵Australian Antarctic Division, Kingston, Tasmania, Australia

⁶Antarctic Climate and Ecosystems Cooperative Research Centre, Hobart,
Tasmania, Australia

⁷Versuchsanstalt für Wasserbau, Hydrologie und Glaziologie (VAW), ETH Zurich, Switzerland

⁸British Antarctic Survey, Cambridge, UK

⁹Akvaplan-niva, Tromsø, Norway

¹⁰Alfred Wegener Institute, Helmholtz Centre for Polar and Marine Research,
Bremerhaven, Germany

- ¹¹Courant Institute of Mathematical Sciences, New York University, New York, NY, USA
¹²Center for Global Sea Level Change, New York University Abu Dhabi, Abu Dhabi, UAE
¹³Lawrence Berkeley National Laboratory, Berkeley, CA, USA
¹⁴Met Office, Exeter, UK
¹⁵Laboratoire de Glaciologie, Université Libre de Bruxelles, Brussels, Belgium
¹⁶Jet Propulsion Laboratory, California Institute of Technology, Pasadena, CA, USA

Correspondence to: X. S. Asay-Davis (xylar.asay-davis@pik-potsdam.de)

Abstract

Coupled ice sheet-ocean models capable of simulating moving grounding lines are just becoming available. Such models have a broad range of potential applications in studying the dynamics of marine ice sheets and tidewater glaciers, from process studies to future projections of ice mass loss and sea level rise. The Marine Ice Sheet-Ocean Model Intercomparison Project (MISOMIP) is a community effort aimed at designing and coordinating a series of model intercomparison projects (MIPs) for model evaluation in idealized setups, model verification based on observations, and future projections for key regions ~~in~~ of the West Antarctic Ice Sheet (WAIS).

Here we describe computational experiments constituting three interrelated MIPs for marine ice sheet models and regional ocean circulation models incorporating ice shelf cavities. These consist of ice sheet experiments under the Marine Ice Sheet MIP third phase (MISMIP+), ocean experiments under the ice shelf-ocean MIP second phase (ISOMIP+) and coupled ice sheet-ocean experiments under the MISOMIP first phase (MISOMIP1). All three MIPs use a shared domain with idealized bedrock topography and forcing, allowing the coupled simulations (MISOMIP1) to be compared directly to the individual component simulations (MISMIP+ and ISOMIP+). The experiments, which have qualitative similarities to Pine Island Glacier Ice Shelf and the adjacent region of the Amundsen Sea, are designed to explore the effects of changes in ocean conditions, specifically the temperature at depth, on basal melting and ice dynamics. In future work, differences between model results will form the basis for evaluation of the participating models.

1 Introduction

The Marine Ice Sheet-Ocean Model Intercomparison Project (MISOMIP) is a targeted activity of the World Climate Research Programme's Climate and Cryosphere (CliC) project. MISOMIP is a community effort aimed at better quantifying sea-level change induced by increased mass loss from the West Antarctic Ice Sheet (WAIS), particularly the Amund-

sen Sea region. At the first MISOMIP workshop ~~held at New York University, Abu Dhabi in October 2014~~¹, participants decided that intercomparisons of ice sheet-ocean dynamics in realistic configurations would be more credible if it was preceded by a more idealized intercomparison and evaluation process for the standalone components and coupled models involved. While MISOMIP's longer-term goal is to investigate WAIS, ~~we~~ participants in the workshop felt that the idealized MIPs would be applicable to a wide variety of models used to investigate a number of processes related to ice sheet and glacier interactions with the ocean. In addition to model evaluation, these idealized MIPs should be designed as a framework for exploring and comparing emergent properties of the coupled system.

1.1 Marine Ice Sheet Model Intercomparison Projects (MISMIPs)

At the time of the workshop, two previous Model Intercomparison Projects (MIPs) focused on verifying and evaluating standalone ice-sheet models for marine ice sheets had taken place and a third was under development. The first MISMIP (Pattyn et al., 2012) compared the grounding-line dynamics between 14 models with a total of 27 unique configurations, and with a semi-analytic solution (Schoof, 2007a, b). The MISMIP experiments were designed for flowline models in which topography and other model fields varied in only one horizontal dimension (1HD). Within each experiment, a parameter (the ice softness) was varied through a series of discrete values, leading to advance and subsequent retreat of the grounding line. At each stage of the advance and retreat cycle, the model was allowed to reach steady state, typically over timescales of thousands to tens of thousands of years. The results showed that steady-state grounding-line positions could differ markedly depending on the resolution, type of stress approximation, and discretization methods employed. Comparison between the semi-analytic solution and high-resolution models with adaptive grids allowed the community to assess which model configurations gave accurate results and which configurations were likely not appropriate for marine ice-sheet studies. An im-

¹Rising Coastal Seas on a Warming Earth, New York University Abu Dhabi, Abu Dhabi, UAE, October 27-29, 2014, <http://nyuad.nyu.edu/en/news-events/abu-dhabi-events/2014/10/rising-coastal-seas-on-a-warming-earth.html>

portant finding of MISMIP related studies (Durand et al., 2009; Gladstone et al., 2010; Cornford et al., 2013) was that models with fixed grids (as opposed to those that track the grounding line in time) and without sub-grid-scale parameterizations of the grounding line require grounding-line resolution on the order of hundreds of meters to accurately reproduce grounding-line dynamics.

The second ice-sheet MIP, MISMIP3d (Pattyn et al., 2013), aimed at exploring grounding-line dynamics on centennial timescales in a configuration that varied in two horizontal dimensions (2HD). ~~Dynamics~~ Dynamic changes were induced through a perturbation in the basal slipperiness in the center of the domain near the grounding line. MISMIP3d also tested the reversibility of the grounding-line position once the perturbation was removed. Results from 16 models with a total of 33 unique configurations showed that initial steady states as well as the reversibility of the dynamics differed significantly depending on the stress approximation and horizontal resolution.

Both MISMIP and MISMIP3d provided a basis for a number of follow-up studies focused on both improvements in numerical methods (e.g. Drouet et al., 2013; Leguy et al., 2014; Feldmann et al., 2014; Seroussi et al., 2014b) and exploring changes in the model topography and physics parameterizations (e.g. Leguy et al., 2014; Feldmann and Levermann, 2015; Tsai et al., 2015).

The third marine ice-sheet MIP (MISMIP+), described in Sect. 2, examines marine ice-sheet dynamics in 2HD with strong buttressing. An idealized bedrock ~~topography~~ topography, based on the work of Gudmundsson et al. (2012) and Gudmundsson (2013), was designed to produce a steady state featuring a grounding line lying partly on a retrograde slope in the absence of ice shelf melt. The three major MISMIP+ experiments prescribe melt rates varying from no melt in a control experiment, to strong melt rates concentrated either close to or far from the grounding line that are expected to drive rapid grounding-line retreat (up to ~ 50 km per century), followed by re-advance when the melt rates are restored to zero.

1.2 Ice Shelf-Ocean Model Intercomparison Projects (ISOMIPs)

ISOMIP was designed in an effort to identify systematic differences between ocean models with sub-shelf cavities. The specifications for the first ISOMIP (Holland et al., 2003; Hunter, 2006) included three idealized experiments with sub-ice-shelf cavities based on Grosfeld et al. (1997). In the first experiment, the entire domain was covered by an ice shelf while the second and third experiments included a sharp calving front and a region of open ocean with ~~simplified~~ simplified atmospheric/sea ice forcing in the form of surface restoring of temperature and salinity. The restoring was constant in time for the second experiment and varied seasonally in the third. Each experiment was prescribed to run for 30 years, at which point the ocean was expected to be close to steady state.

Unfortunately, ISOMIP results were never collected and compared in a formal publication. The few ISOMIP results that have been published or made publicly available (Hunter, 2003; Losch, 2008; Galton-Fenzi, 2009) suggest that melt rates as well as barotropic and overturning circulations varied between models depending on the vertical discretization and resolution of the model.

In Sect. 3, we describe the design for a second ocean MIP with ice-shelf cavities, ISOMIP+, which aims to improve upon the original ISOMIP in several ways. Bedrock and ice-shelf topographies, based on MISMIP+ results, are more like those of realistic ice shelves in that the water-column thickness goes to zero at the grounding line and the topography varies in 2HD, rather than 1HD. The melt parameterization and parameter choices for horizontal ~~and vertical~~ mixing are closer to those used in realistic applications. ~~The use of As opposed to forcing only at the ocean surface, ISOMIP+ uses far-field restoring, following the approach of throughout the water column following~~ Holland et al. (2008) and Goldberg et al. (2012a, b), ~~is an approach~~ more similar to ~~approaches those~~ commonly used in forced regional climate experiments. Importantly, preliminary results show that ~~the restoring restoring with a relatively warm far-field temperature profile~~ leads to a quasi-steady state within ~~about a decade one to two year~~, whereas the ~~30-30-year~~ ISOMIP experiments approached, but did not reach, a steady state in which the ocean was at the freezing point everywhere. Whereas

ISOMIP used static ice-shelf topography, two ISOMIP+ experiments prescribe dynamic topography, allowing models to test their ability to handle moving boundaries and to see the effects that moving topography has on ocean dynamics.

ISOMIP+ will also improve upon ISOMIP in terms of organised community involvement as well as scientific developments. ISOMIP+ is expected to benefit from the organisation and active community of MISOMIP, as well as the close relationship of ISOMIP+ to both MISOMIP+ and MISOMIP1 (through the shared experimental design and development towards coupled ice–ocean models). These factors are likely to lead a larger number of ISOMIP+ participants and formal publication of the analysis, both of which were lacking in ISOMIP.

1.3 Coupled ice sheet-ocean modeling

While no previous MIP has been performed with coupled ice sheet-ocean models, a number of studies have used coupled ice sheet-ocean models, most in idealized configurations. Grosfeld and Sandhäger (2004) performed ~~simulations used offline (file-based) coupling~~ offline-coupled simulations of a 3-D ocean and 2-D ice-sheet model including dynamic calving of tabular icebergs using idealized ~~geometry-topography~~ based on the Filchner-Ronne Ice Shelf. Walker and Holland (2007) and Walker et al. (2008, 2009) used idealized, coupled modeling in 2-D (one horizontal and one vertical dimension) to show that warm ocean conditions and variations in ice basal sliding affected grounding-line motion and ice-shelf topography on decadal timescales. Thoma et al. (2010) coupled 3-D ice-sheet and ocean models to study the dynamics of a sub-glacial lake. Determann et al. (2012) used the same models to perform ice-sheet simulations driven by melt rates computed in the ocean model, showing hysteresis following a melt perturbation applied to idealized ice-sheet ~~geometry-topography~~. Goldberg et al. (2012a, b) showed results from idealized, coupled experiments spanning 250 years using four different profiles for the ambient water temperature. They showed that feedbacks between the ocean and ice-sheet components led to steepening of the ice draft near the grounding line and strong melting in a channel on the western flank of the ice shelf. Gladish et al. (2012) performed coupled simulations of an idealized ice shelf based on Petermann Glacier with the plume ocean model

in 2HD of Holland and Feltham (2006), showing the influence of channelization on total melt fluxes and melt distribution. Sergienko (2013) used the same plume model to further explore melt channels in idealized configurations. Sergienko et al. (2013) used a plume ocean model in 1HD (Jenkins, 1991) to show that ice-shelf topography is controlled by a balance between ice advection and either ice deformation or ocean melting, depending on the temperature of the ambient ocean water. Walker et al. (2013) used coupled 1-D flow-line models to explore the effects of different melt parameterizations on coupled dynamics. A study by De Rydt and Gudmundsson (2016) used a coupled ice sheet-ocean model in an idealized configuration similar to Pine Island Glacier to show the effect a seabed ridge can have on grounding-line stability. They also concluded that coupled ice-ocean modeling was required in their problem because commonly used parameterizations of ice-shelf basal melting differed from those produced by their ocean model by more than 40%. While these individual studies have advanced our understanding of ice sheet-ocean processes, a MIP involving coupled ice sheet-ocean models is likely to improve our confidence in the models through greater understanding of the variability and the causes of differences in model results.

In Sect. 4, we describe the first Marine Ice Sheet-Ocean Model Intercomparison Project (MISOMIP1), which combines elements from MISMIP+ and ISOMIP+. In some ways, the MISOMIP1 setup is similar to that of Goldberg et al. (2012a, b) in that it includes a narrow channel with strong ice-shelf buttressing and strong far-field restoring in the ocean. MISOMIP1 differs from this previous work in having (1) steeper channel walls, meaning a stronger change in buttressing as the ice-shelf thickness changes, (2) a larger region of open ocean allowing for ocean dynamics both inside and outside the cavity, and (3) **making use of** a bedrock topography with an upward-sloping region in the ice-flow direction, allowing us to investigate the possibility that thinning or other changes in the state of the ice sheet could trigger a marine ice-sheet instability (MISI, e.g. Weertman, 1974).

1.4 Goals of the three new MIPs

The MIPs were designed with three main goals in mind. As in their predecessors (ISOMIP, MISMIP and MISMIP3d), the first goal of the MIPs is to provide a controlled forum for researchers to compare their model results with those from other models during model development. Furthermore, it is hoped that researchers will publish their MIP results and/or submit them to the relevant MIP database when they introduce new ice sheet models, ocean models with ice-shelf cavities or coupled ice sheet-ocean models. Differences between models should be investigated, understood and explained. We have endeavored to keep the MIP setups relatively simple to make them relevant and accessible to the largest possible number of potential contributors and to make them easy to duplicate, while still capturing physical processes relevant to ice sheet-ocean dynamics.

The second goal is **that for** the three MIPs **should to** provide a path for testing components in the process of developing a coupled ice sheet-ocean model. Within ISOMIP+, the experiments progress from static to dynamic (but prescribed) ice **geometry topography** with the same goal in mind. Meeting this goal has required that all three MIPs be designed simultaneously, ensuring that they use the same bedrock topography (bathymetry) and compatible domains. Grounding-line dynamics in MISMIP+ are controlled by a melt profile that adapts to the ice **geometry topography** and qualitatively mimics example results from ISOMIP+. Ice **geometry topography** (both static and dynamic) for ISOMIP+ comes from example **results from** MISMIP+ **results**. In addition, two ISOMIP+ experiments have been designed to produce large changes in melting over a short period of time (less than a decade), mimicking the abrupt changes in melt rate applied in MISMIP+. All three MIPs include an experiment with 100 **years** of ice retreat followed by 100 **years** of re-advance, allowing evaluation of standalone and coupled simulations of essentially the same problem.

Our third goal is that each MIP should provide a basic setup from which a large variety of parameter and process studies can usefully be performed. Each MIP setup uses idealized topography and simplifies or ignores known physics. These simplifications leave opportunities for others to study the effects of adding missing processes (e.g. a more realis-

tic calving law, a basal hydrology model, sub-glacial melt water runoff across the grounding line, wind stresses, sea-ice formation and export, tides, time-varying far-field ocean forcing). Results may be affected by parameterizations (e.g. ice sliding law, melt parameterization, mixing schemes in the ocean, equation of state, etc.) and other choices (e.g. horizontal and vertical resolution, coupling interval, ice rheology, etc.) that the community may choose to explore in more detail.

2 MISMIP+ design

A number of previous MIPs not specifically focused on marine ice sheets have explored model physics (EISMINT: Payne et al., 2000), provided benchmarks (ISMIP-HOM: Pattyn et al., 2008) and demonstrated modes of internal variability (ISMIP-HEINO: Calov et al., 2010), improving our understanding of ice-sheet models. The previous Marine Ice Sheet ~~Model-Intercomparison-Projects~~MIPs, MISMIP and MISMIP3d, tested the capabilities of ice sheet models to simulate advance and retreat cycles under changes in ice softness and basal sliding, respectively, each teaching the community a great deal about the numerical behavior of ice-sheet models of various types. Nonetheless, it was clear in discussions of a follow-up intercomparison exercise that the MISMIP3d experimental design had three shortcomings as a test of 2HD marine ice sheet models. First, it started from a steady state that was invariant in the cross-flow direction – that is, 1HD – and meaning it did not involve significant lateral stresses. Second, the initial grounding lines of the shallow-shelf approximation (SSA) (MacAyeal et al., 1996) models were around 80 km downstream from the Stokes models, but the grounding line only moved about 20 km in the perturbation experiment. That left an obvious question entirely unanswered: in a realistic simulation with the model parameters chosen to match geometry and velocity derived from observations, and thus with prescribed initial conditions, does the SSA provide a good approximation to the Stokes model? Third, grounding line migration was driven by changes to the basal traction field, rather than the ice shelf melting that is

thought to be the dominant driver of present-day grounding-line retreat in West Antarctica (Joughin et al., 2014; Favier et al., 2014; Seroussi et al., 2014a).

MISMIP+ has been designed to address each of ~~the shortcomings above these shortcomings~~. Regarding the first, the chosen geometry, based on Gudmundsson et al. (2012), results in strong lateral stresses that buttress the ice stream, ~~and, given particular parameter choices, results~~. The particular parameters chosen for MISMIP+ result in a stable grounding line crossing a retrograde slope, a configuration not possible in 1HD. Regarding the second, modelers are free to choose certain model parameters so that their initial grounding line is close to that at the center of the domain is within a tolerance of a ~~reference model~~, ~~and in preliminary tests two models that bracketed the high resolution prescribed location~~. Preliminary simulations with the BISICLES ice sheet model (Cornford et al., 2013) with two stress approximations that showed large differences in grounding-line position in the MISMIP3d results experiments have been found to have grounding lines within a few kilometers of one another in the MISMIP+ steady state. Finally, extensive grounding line retreat is driven by sub-shelf melt rates.

2.1 Experimental setup

The MISMIP+ domain is a box bounded by $0 \leq x \leq 640$ km and $0 \leq y \leq 80$ km.² The bedrock topography, shown in Fig. 1, is a smaller version of that given in Gudmundsson et al. (2012) and Gudmundsson (2013):

$$Bz_b(x, y) = \max \left[B_x(x) + B_y(y), -B_{\max} z_{b, \text{deep}} \right] \quad (1)$$

$$B_x(x) = B_0 + B_2 \tilde{x}^2 + B_4 \tilde{x}^4 + B_6 \tilde{x}^6, \quad (2)$$

$$\tilde{x} = x / \bar{x} \quad (3)$$

²The standalone ice sheet experiments place a calving front at $x_{\text{calve}} = 640$ km. The same is true of the standalone ocean experiments and the coupled experiments, but the ocean domain extends to $x = 800$ km.

$$B_y(y) = \frac{d_c}{1 + e^{-2(y-L_y/2-w_c)/f_c}} \frac{d_c}{1 + e^{-2(y-L_y/2-w_c)/f_c}} + \frac{d_c}{1 + e^{2(y-L_y/2+w_c)/f_c}} \frac{d_c}{1 + e^{2(y-L_y/2+w_c)/f_c}} \quad (4)$$

where the parameter values used in these equations, along with several others related to the MISMP+ experiment, are given in Table 1. As in Gudmundsson et al. (2012), there is a no-slip boundary condition at $x = 0$ and free-slip boundaries at $y = 0$ and 80 km. Ice is removed from the domain beyond $x_{\text{calve}} = 640$ km but no other calving criterion is specified.

Englacial deviatoric stresses τ_{ij} are related to strain-rates D_{ij} through Glen's flow law. As in previous MISMP exercises,

$$\tau_{ij} = A^{-1/n} D_e^{1/n-1} D_{ij} \quad (5)$$

where $n = 3$. D_e is the second scalar invariant of the strain-rate, given by $2D_e^2 = D_{ij}D_{ji}$, with the usual summation convention. The ice is isothermal, with a constant rate factor A . ~~A suggested value for A is given in Table 1, but participants should modify this value (and/or the coefficient β^2 that appears in the basal traction below) so that the steady state grounding line crosses the center of the trough at $x = 450 \pm 10$ km. independent of space, with a value determined by the participant as discussed below.~~

~~The~~ As in the previous MISMP experiments, MISMP+ uses a symmetry boundary condition at the ice divide, ocean pressure (up to sea level) at the ice-ocean interface, and stress-free boundary conditions at the upper surface (see Pattyn et al., 2012, 2013, for details). Where the ice is grounded, the tangential component of the basal traction $\tau_{nt}|_b = \tau_{nt}|_{z_b}$ is given by any of three relationships: a power law, ~~or by the a~~ modified power law relation introduced by Tsai et al. (2015), or a second modified power law relation introduced by Schoof (2005) and explored by Gagliardini et al. (2007) and Leguy et al. (2014). Participants are free to choose ~~either or both~~ any or all of these.

The power law is

$$\tau_{nt}|_{z_b} = \beta^2 u_b^{1/m-1} \mathbf{u}_t \quad (6)$$

where \mathbf{u}_t is the tangential component of the velocity with magnitude u_b , $m = 3$ and a suggested value for the constant, and β^2 is a friction coefficient, which is invariant in space and with a suggested value given in Table 1, but, like A , can be altered so that the steady state grounding line crosses the center of the trough at $x = 450 \pm 10$ km. The value of β^2 may be modified by the participant (see below).

The first modified law differs from the power law by preventing the basal traction from exceeding the value given by a Coulomb law, that is, a fraction of the effective pressure: Assuming the effective pressure at the bed to be approximately hydrostatic: N :

$$\tau_{nt}|_{z_b} = \min \left(\alpha^2 \rho_i g (h - h_f) N, \beta^2 u_b^{1/m} \right) u_b^{-1} \mathbf{u}_t, \quad (7)$$

with where $\alpha^2 = 0.5$. N should be constructed by assuming a perfect hydrological connection with the ocean, so that

$$N = -\sigma_{nn} - \rho_{sw} g z_d \quad (8)$$

Hydrostatic models should approximate the normal stress σ_{nn} in the usual way, giving

$$N = \rho_i g (h - h_f), \quad (9)$$

where g is the acceleration of gravity, h is the ice thickness and

$$h_{f,f} = \max \left(0, -\frac{\rho_{sw}}{\rho_i} \frac{\rho_{sw}}{\rho_i} z_{b,b} \right) \quad (10)$$

is the flotation thickness given the bedrock elevation $z_{b,b}$ and the reference densities of ice and seawater, ρ_i and ρ_{sw} . Expressing the basal traction in this way ensures that it is continuous (though not differentiable) across the grounding line, but grows to ~ 10 – 100 kPa over the region ~ 1 km upstream (see Fig 2).

We obtain a formula for computing basal melt. The second modified law has the same limits as the first modified law (the power law for large effective pressure, and the Coulomb law near the grounding line where the effective pressure approaches zero) but transitions between these limits more smoothly:

$$\tau_{nt}|_{z_b} = \frac{\beta^2 u_b^{1/m} \alpha^2 N}{[\beta^{2m} u_b + (\alpha^2 N)^m]^{1/m}} \frac{u_t}{u_b}. \quad (11)$$

In this form, basal traction remains continuous everywhere and differentiable everywhere except across the grounding line.

We note that Eq. (8) is a zeroth-order hydrology model that assumes connectivity to the ocean throughout the domain and is likely only valid within a few tens of kilometers of the grounding line (Leguy et al., 2014). It is likely that simulations using more realistic topography would require a more sophisticated hydrology model to produce results consistent with observations inland of the grounding line.

We prescribe that the steady-state grounding line should cross the centerline of the trough at $x = 450 \pm 10$ km, ensuring that all models start from similar initial states. Participants should adjust the grounding line position by modifying first the values of A and, if necessary, the value of β^2 beginning with the suggested values given in Table 1. We have adopted this approach for model initialization to be more consistent with the methods used to initialize models for real-world problems: unknown parameters or fields are determined by search or inversion techniques so that initial conditions are consistent with observations. The precise method used to adjust A and/or β^2 and for finding the steady state is left up to the participant. Some participants will spin up their models for tens of thousands of years with different parameter values until the grounding line lies within the desired position. Others might construct a more formal optimization problem and solve it with variational methods.

A constant accumulation rate a , with the value given in Table 1, is applied over the entire ice surface. One of the three MISMP+ experiments uses a parameterization of basal

melting below the ice shelf, obtained by balancing the latent heat of melting with parameterized turbulent heat flux within the ocean (Jenkins et al., 2010), neglecting the heat flux into the ice:

$$m_{\underline{i}} = \frac{\rho_i c_w \Gamma_T}{\rho_{fw} L} \frac{\rho_i}{\rho_{fw}} m_w = \frac{\rho_i c_w \Gamma_T}{\rho_{fw} L} u_* \left(T_{\underline{w}w} - T_{\underline{f}f} \right), \quad (12)$$

5 where m_i is the basal melt rate of ice, m_w is the same melt rate expressed in water equivalent (w_{eq}), ρ_{fw} is the density of fresh water, c_w is the heat capacity of seawater, L is the latent heat of fusion, Γ_T is the heat-transfer coefficient, u_* is the ocean friction velocity and $T_* = (T_w - T_f)$, $T_* = (T_w - T_f)$ is the thermal driving, the difference between the ambient ocean water temperature T_w and the local freezing point T_f .

10 For the purposes of model intercomparison, we have developed an ad-hoc, simplified parameterization of basal melting based on results from the Parallel Ocean Program (POPv. 2x (POP2x)) using cavity shapes from a MISIP+ simulation. The parameterization prescribes melt rates as follows:

$$m_{\underline{i}} = \frac{\rho_i c_w \Gamma_T}{\rho_{fw} L} \frac{\rho_i c_w \Gamma_T}{\rho_{fw} L} u_* (H_{\underline{c}c}) T_*(z_{\underline{d}d}) \quad (13)$$

$$15 \quad u_*(H_{\underline{c}c}) = u_{*,0} \tanh \left(\frac{H_c}{H_{c0}} \frac{H_c}{H_{c0}} \right), \quad (14)$$

$$T_*(z_{\underline{d}d}) = \frac{T_{*,0}}{z_{ref}} \max \left(z_{\underline{d}0} - z_{\underline{0}d}, 0 \right), \quad (15)$$

$$H_{\underline{c}c} = z_{\underline{d}d} - z_{\underline{b}b}, \quad (16)$$

20 where $z_{\underline{d}d}$ is the elevation of the ice–ocean interface (ice draft), $z_{\underline{b}b}$ is the elevation of the bedrock topography (bathymetry), H_c is the water-column thickness, and $u_{*,0}$, H_{c0} , $T_{*,0}$ and z_{ref} are fitting constants.

The ~~POP-POP2x~~ results suggest that the friction velocity u_* increases linearly near the grounding line (for small H_c/H_c) but saturates to a nearly constant value when the ocean-cavity thickness exceeds a threshold thickness $H_{c0} = 75 H_{c0} = 75$ m. Galton-Fenzi (2009) also showed that melt rates tend to approach zero near the grounding line in a number of experiments, though he found that glacial meltwater fluxes can lead to increased melt rates immediately adjacent to the grounding line. Glacial meltwater fluxes are neglected here. In their idealized simulations studying the behavior of melt water impeded by a bathymetric ridge, De Rydt et al. (2014) saw a similar tapering of the melt rate near the grounding line. It should be noted that melt rates near grounding lines are not well constrained by observations and that ocean models may have particular difficulty in these regions. Therefore, the dependence upon water column thickness should be treated as an ad-hoc formulation for the purpose of a model intercomparison and not necessarily as a realistic representation of melting near grounding lines.

The ~~POP-POP2x~~ simulations used to calibrate the parameterization had a temperature profile that increased linearly with depth (similar to the profiles described in Sect. 3.1.3), leading to a thermal driving that also increased approximately linearly with depth. Thermal driving, and therefore melting, reached zero at a depth $z_0 = -100$ m $z_0 \sim -100$ m. Though the simulations showed some freezing above this depth, we assume our parameterization assumes for simplicity that no melting or freezing occurs at depths shallower than $z_0 \equiv -100$ m.

We simplify $m_i m_i$ by lumping various constants and coefficients from Eqs. (13)–(15) into a single coefficient Ω :

$$m_i = \Omega \tanh \left(\frac{H_c}{H_{c0}} \frac{H_c}{H_{c0}} \right) \max \left(z_0 - z_d, 0 \right). \quad (17)$$

The Fig 3 shows a schematic of the ice shelf, labeling the various depths and thicknesses involved in the melt parameterization, as well as the melt rate as a function of z_d and H_c is shown in Fig 3. Again, the parameter values are given in Table 1. The coefficient

Ω has been given a value of $0.2\text{yr}^{-1}0.2\text{a}^{-1}$, corresponding to a maximum ambient ocean temperature $\sim 1.0^\circ\text{C}$, which leads to a melt rate with a maximum value of $m_i \approx 75\text{m yr}^{-1}$ $m_i \approx 75\text{m a}^{-1}$ of ice near the grounding line of the BISICLES initial condition (see Fig. 2). We reiterate that the formulation given by Eq. (17) is an ad-hoc parameterization appropriate only for this intercomparison and not appropriate for other geometries, ocean ambient temperatures, etc. The melt parameterization is missing known physics such as dependence on the slope of the ice draft (Goldberg et al., 2012a) and superlinear dependence on ambient ocean temperature (Holland et al., 2008).

2.2 Experiments

MISMIP+ consists of three experiments with different melt rates. Each experiment is initialized by running the model with $m_i = 0$ with $m_i = 0$ (no melting), and should begin with a stable grounding line crossing the center of the channel on the retrograde slope around $x = 450 \pm 10\text{km}$. Stable in this case means that the ice sheet thickness and even the grounding line the grounding-line position is permitted to fluctuate, but any fluctuations should average to zero over time, and should be of low amplitude compared to the response to perturbations. Preliminary experiments indicate that, starting from a uniform thickness of 100 m, a stable state is found after around 20,000 a. One experiment (Ice0) is simply a control, where the melt rate is maintained at $m_i = 0$ $m_i = 0$ for 100 years, while the other two (Ice1 and Ice2) are intended to study the response to substantial ice shelf ablation.

Experiment Ice1 is divided into several parts, all beginning with Ice1r, where the melt rate given in Eq. (17) is applied from $t = 0$ to $t = 100\text{yr}$ $t = 100\text{a}$, and is expected to produce thinning of the ice shelf, a loss of buttressing, and grounding-line retreat. Ice1ra starts from the state computed at the end of the Ice1r simulation and runs at least until $t = 200\text{yr}$ $t = 200\text{a}$, and optionally until $t = 1000\text{yr}$ $t = 1000\text{a}$, with no melting, so that the ice shelf thickens, but buttressing is restored and the grounding line advances. Preliminary simulations have shown that the grounding-line position does not reach its initial steady state within even 1000 years. Finally, Ice1rr is optional and continues Ice1r, with the melt rate of Eq. (17), until

$t = 1000 \text{ yr}$, $t = 1000 \text{ a}$. Figure 2 shows example basal traction and melt rate fields calculated at several points during the Ice1r and Ice1ra experiments.

Experiment Ice2 is structured in the same way as Ice1, but a different melt rate is applied. The Ice1 melt rate adjusts to pursue the grounding line as it retreats, preventing the formation of a substantive ice shelf. In contrast, Ice2r prescribes a sub ice-shelf melt-rate of 100 m yr^{-1} , 100 m a^{-1} , where $x > 480 \text{ km}$ and no melt elsewhere from $t = 0$ to $t = 100 \text{ yr}$, $t = 100 \text{ a}$, resulting in substantial loss of ice concentrated away from the grounding line, as in a sequence of extensive calving events³. Preliminary calculations show that the grounding line retreats for more than 20 km but begins to stabilize as a thick ice shelf forms in its wake. Ice2ra takes the endpoint of the Ice2r experiment as its initial state, and evolves the ice sheet with no melting until $t = 200 \text{ yr}$, $t = 200 \text{ a}$ and optionally until $t = 1000 \text{ yr}$, $t = 1000 \text{ a}$, while Ice2rr is optional and continues Ice2r to $t = 1000 \text{ yr}$, $t = 1000 \text{ a}$.

As an example, Fig. 4 plots grounded area against time for all of the MISIP+ experiments carried out with the BISICLES ice sheet model BISICLES using SSA. We emphasize that the example results shown in this figure are *not* intended as a benchmark for other simulations, but simply to demonstrate generally what type of behavior might be expected in each experiment. Table 2 gives a brief summary of the MISIP+ experiments, as well as those from the other two MIPs.

Figure 5 shows the sensitivity of the BISICLES Ice1r results to various choices of basal traction, stress approximation, and values of A . Results are nearly insensitive to the differences between the basal-traction parameterizations of Tsai et al. (2015) and Schoof (2005), and also to differences between two stress approximations, SSA and SSA* (Schoof and Hindmarsh, 2010). However, the simulations with the basal traction of Weertman (1974) show a significant difference in both the initial grounded area and the rate of retreat compared with the other parameterizations. Furthermore, even when A is adjusted so that the initial grounding-line position (and therefore the grounded area) is in

³An alternative would be to have participants move the calving front upstream in Ice2r and allow it to advance in Ice2ra. We chose a melt-rate perturbation instead because it requires the same model capabilities as Ice1.

agreement with the other configurations, the rate of retreat remains significantly slower than for the other parameterizations.

2.3 Requested output

MISMIP+ requested output is divided into compulsory and optional parts. The compulsory components will be used to write an analysis paper, along the lines of the MISMIP3d paper (Pattyn et al., 2013). The optional data will be included with the compulsory data in an open access database.

Participants are required to supply point data at the grounding line, along the same lines as MISMIP3d, as well as integrated quantities such as volume above flotation, at set times throughout the experiments. Data should be stored in a single NetCDF 4 file for each experiment with the file-naming convention of `[expt]_[MODEL].nc`, where `[expt]` is an experiment name from Table 2 and `[MODEL]` is a unique identifier for the participant. For the core experiments, where $0 \leq t \leq 200$, data should be provided every 10 years starting from $t = 0$, while for the optional extensions, data should be provided every 100 years starting from $t = 200$. Since the length of the grounding line varies over time we expect that the number of point data required to describe it will vary over time in all models. It will be left to each participant to decide how to determine location of the grounding-line points (e.g. taking cell edges between grounded and floating regions or performing sub-grid-scale interpolation).

We ask participants to use the variable and dimension names given in bold and units given in square brackets as follows:

- **nPointGL**. An unlimited dimension – this is a netCDF4 feature that allows **nPointGL** to be decided as the data is written.
- **nTime**. A fixed dimension.
- **time**(nTime) [a]. The time in years since the beginning of the experiment.
- **iceVolume**(nTime) [m³], **iceVAF**(nTime) [m³], **groundedArea**(nTime) [m²]. The ice volume, volume above flotation, and the grounded area, integrated over the domain.

- **xGL**(nPointGL,nTime), **yGL**(nPointGL,nTime) [m]. The x and y coordinates of a given point on the grounding line.
- **iceThicknessGL**(nPointGL,nTime) [m]. Ice thickness at the grounding line.
- **uBaseGL**(nPointGL,nTime), **vBaseGL**(nPointGL,nTime) [m a^{-1}]. The x and y components of the basal velocity.
- **uSurfaceGL**(nPointGL,nTime), **vSurfaceGL**(nPointGL,nTime) [m a^{-1}]. The x and y components of the surface velocity.
- **uMeanGL**(nPointGL,nTime), **vMeanGL**(nPointGL,nTime) [m a^{-1}]. The x and y components of the vertical mean of the velocity.

Since the number of grounding line points $n(t)$ will vary over time, most of the slices **xGL**(:, t) will contain missing values, which should be filled with the default value `NC_FILL_FLOAT`. In Python, C and Fortran this can be achieved by writing data for each timestep in turn into the first $n(t)$ elements of the slice **xGL**(:, t). At the same time, the unlimited dimension **nPointGL** will be automatically adjusted by the netCDF library routines to the maximum value of $n(t)$. Two python programs are included in the Supplement: `write_example.py` creates a netcdf file given data in the MISMIP3d text file format, and `plot_example.py` reads example netcdf files, constructs a plot like Fig. 4, and takes advantage of numpy's masked array class to show the changing shape of the grounding line.

All submissions should include a brief model description, in a pdf file, which summarizes the stress approximation and parameters used, and evidence that simulations are adequately resolved. The model summary should be an enumerated list, indicating

1. Model: the name of the model (e.g. BISICLES), with a citation if available
2. Repository: a link to the repository where the model can be downloaded (if public) and specific tag, branch or revision (if available)
3. Englacial stresses: the stress approximation and coefficients (e.g. SSA, $A = 2.0 \times 10^{-17} \text{ Pa}^{-3} \text{ a}^{-1}$)

4. Basal traction: the choice of law and coefficients, e.g. $|\tau_b| = \beta^2 u_b^{1/3}$, $\beta^2 = 10^4 \text{ Pa m}^{-1/3} \text{ a}^{1/3}$
5. Space discretization: e.g. finite volume, adaptive non-uniform grid, square cells $0.25 \text{ km} < \Delta x < 4.0 \text{ km}$
6. Time discretization: e.g. Piecewise Parabolic Method, explicit, $\Delta t < \Delta x / (4|u|)$
7. Grounding line: any special treatment of the grounding line, e.g. one-sided differences of surface elevation
8. MISMIP3d name: the name of the model in MISMIP3d, with any relevant differences, e.g. DMA6 (different mesh resolution)

10 Evidence that the submissions are adequately resolved will vary from model to model. **Conventional** Typically, models should simply carry out a convergence study of experiment Ice1r and Ice1ra, showing that the grounding line shape and positions at the start and end of Ice1r and the volume-above-flotation curves throughout the experiments converge with mesh refinement and differ by a fraction at the finer resolutions. An example model
 15 description is included in the Supplement.

Optionally, participants can add further high-volume data to their NetCDF file. These consist of several fields on a uniform 1 km grid, and are the same fields requested in the coupled IceOcean experiments. They will not be used in the MISMIP+ analysis paper, but will be freely available once the analysis is published. The optional fields are:

- 20 – **nx,ny**. fixed dimensions, cell-centred points on an 800×80 grid of 1 km squares
- **x(nx)** and **y(ny)** [m] cell centers of the output grid as vectors. The grid spacing is 1 km.
- **iceThickness**(nTime,ny,nx) [m] ice thickness.
- **upperSurface**(nTime,ny,nx), **lowerSurface**(nTime,ny,nx) [m] upper and lower surface elevation.

- **basalMassBalance**(nTime,ny,nx) [m a^{-1}] of ice ~~;~~ (not water equivalent) basal mass balance (melt rate), positive for melting and negative for freezing.
- **groundedMask**(nTime,ny,nx), **floatingMask**(nTime,ny,nx) the fraction of grounded or floating ice in a given cell.
- 5 – **basalTractionMagnitude**(nTime,ny,nx), [Pa] the magnitude of the tangential basal traction field $\tau_{nt}|b|$ $\tau_{xt}|b|$.
- **uBase**(nTime,ny,nx), **vBase**(nTime,ny,nx) [m a^{-1}] x and y components of the basal velocity.
- **uSurface**(nTime,ny,nx), **vSurface**(nTime,ny,nx) [m a^{-1}] x and y components of the surface velocity.
- 10 – **uMean**(nTime,ny,nx), **vMean**(nTime,ny,nx) [m a^{-1}] x and y components of the vertical mean of the velocity.

3 ISOMIP+ design

The ISOMIP+ experiments have been designed to make a number of improvements on the original ISOMIP experiments. Whereas ISOMIP used highly idealized **geometry-topography** (the ocean column at the grounding line was 200 m thick, the ice draft sloped linearly with latitude and was invariant with longitude, and the bedrock was perfectly flat), ISOMIP+ makes use of relatively complex **geometry-topography** from MISMIP+ BISICLES simulations, including an ocean cavity that reaches zero thickness at the grounding line. Where ISOMIP uses a velocity-independent, two-equation formulation of the melt boundary conditions, ISOMIP+ uses the velocity-dependent three-equation formulation (e.g. Holland and Jenkins, 1999; Jenkins et al., 2010) more commonly used in realistic model configurations. ISOMIP specified ~ 10 km resolution, too coarse to resolve the 9 km Rossby radius

of deformation (Grosfeld et al., 1997), and large values of the horizontal viscosity and diffusivities, leading to a laminar flow that evolved toward steady state without eddies or other fluctuations. In contrast, ISOMIP+ runs will typically use smaller horizontal viscosity and diffusivities and higher resolution (~ 2 km), allowing for mesoscale eddies and unsteady flow.

5 A smaller computational domain makes the experiments computationally feasible despite the higher resolution. ISOMIP+ should provide more appropriate test cases than the original ISOMIP for realistic experiments, particularly for those focused on the Amundsen Sea region of WAIS.

ISOMIP+ prescribes ~~four experiments, Ocean1~~ five experiments, Ocean0 through Ocean4. ~~Ocean1 and Ocean2~~ Ocean0–2 have fixed topography while ~~Ocean3 and Ocean4~~ Ocean3–4 have prescribed, evolving ice topography. The experiments are summarized in Table 2.

3.1 Shared setup across the ~~four~~ five experiments

We request that ISOMIP+ participants perform each experiment once at a common resolution and with a common set of parameters (hereafter, the COM configuration), and once at a typical resolution and with typical parameters they would use for a realistic problem (hereafter, the TYP configuration). TYP allows participants to choose resolution, parameters and parameterizations typical to each model as it is most often used. We ask participants who do not feel they have time to perform both the COM and TYP experiments to prioritize the COM experiments.

The purpose of COM is to produce results that can be more easily intercompared. We would like to discover the consequences of certain modeling choices (e.g. the horizontal and vertical discretization), ~~in a configuration where keeping~~ as many aspects of the configuration as possible ~~are~~ common to all participating models. TYP will allow us to compare the results of models as they are configured for real problems and to better understand the diversity of results that different modeling choices produce. Given that there is currently no “right” answer to the ISOMIP+ experiments – there are no observations or exact mathemat-

ical solutions with which to compare – the spread in TYP model results ~~are~~ is expected to give us insight into how uncertainties reflected in parameter choices affect model solutions.

Parameters general to both COM and TYP runs are given in Table 3, while parameters specific to the COM runs are given in Table 4.

5 3.1.1 Domain and topography

The ISOMIP+ domain is a Cartesian box bounded by $320 \text{ km} \leq x \leq 800 \text{ km}$ and $0 \leq y \leq 80 \text{ km}$, overlapping with the right half of the MISMIIP+ domain. To aid in describing features within the domain, we define positive x as pointing north (the flow direction of most ~~antarctic~~ Antarctic ice shelves) and positive y as pointing west. These directions have no dynamic consequences. A region of open ocean extends beyond the edge of the MISMIIP+ calving front (which is not allowed to advance beyond $x_{\text{calve}} = 640 \text{ km}$) on the northern side of the domain. The southern boundary has been placed far enough south to accommodate the retreated ice-shelf ~~geometry~~ topography used in Ocean2, which is also the most retreated state in Ocean3 and Ocean4.

15 The Coriolis parameter requires latitude to be defined over the domain. We prescribe an ~~f -plane configuration~~ plane configuration (Gill, 1982, ch. 7; Pond and Pickard, 1983, ch. 6) at 75° S latitude, although models that do not support an f plane should vary latitude in the x direction with 75° S at the center of the domain (and ~~note this in their readme file~~ mention this in the description pdf that participants will submit with their results). Longitude plays no
20 role in the dynamics, and can be defined arbitrarily.

The bathymetry is the same as in Eq. (1). Because the ice-draft ~~geometry~~ topography is derived from ice-sheet model results, it cannot be described by an analytic function. Instead, both the ~~geometry used for Ocean1 and Ocean2 (see Figs. ?? and ??)~~ topography used for Ocean0–2 and the snapshots used to produce the dynamic ~~geometry for Ocean3 and Ocean4~~ topography for Ocean3–4 come from MISMIIP+ BISICLES results, and are available in NetCDF format for download ~~from the MISOMIP website ()~~. The ~~geometry~~ (Cornford and Asay-Davis, 2016). The topography data come from the BISICLES model (Cornford et al., 2013) in the SSA configuration. The ~~original BISICLES geometry~~

topography is provided on a uniform 1 km grid so that participants can process the data as they require. We prescribe a slightly coarser resolution, 2 km, for COM runs, since POP-POP2x simulations indicated that 1 km resolution would be too time consuming and resource-intensive for the purposes of a some participants in the MIP. For both COM and TYP runs, participants are expected to interpolate the ice-sheet topography to the ocean grid as part of whatever processing is required to make the data ocean-model friendly. To aid later analysis of the effect these modifications to the topography might have on the results, participants are asked to provide a description of their model specific modifications, e.g. smoothing_;, determining regions of land, open ocean and ice-shelf cavity_;, and expanding the water column to a minimum thickness₎. The calving criterion, described below, should also be applied during this processing step.

Some participating ocean models require a surface pressure rather than the ice draft as the upper boundary condition. These models are free to compute the ice thickness from the ice surface elevation and ice draft provided in the input geometry, and multiply these by $\rho_i g$ to get a pressure. Equivalently, the pressure can be derived from the ice draft as $p_{z_d} = -\rho_{sw} g z_d$. The elevation of the ice-ocean interface in the model will differ slightly from the prescribed z_d because of the dynamic pressure and variations in the ocean density, but the slight variation in topography across models is not expected to contribute significantly to differences between model results.

3.1.2 Calving

The MISIP+ experiments explicitly exclude a dynamic calving criterion, allowing the ice to become arbitrarily thin without calving. We felt that it was important that ISOMIP+ include the effects of a cliff-like calving front , so so that participating ocean models will be required to demonstrate their ability to handle advance and retreat of this jump in topography. We feel that this is important because ocean models will require this capability to handle real-world problems with dynamic calving fronts. Therefore, we prescribe a calving criterion on the MISIP+ geometry-topography used in ISOMIP+_;: Ice thinner than $H_{calve} = 100$ m (equivalent to an ice draft above ~ -90 m) is considered to have calved and

the ice draft is set to zero. This threshold was chosen to eliminate the thinnest ice on eastern and western flanks of the ice tongue while maintaining the tongue itself. A thicker threshold, more consistent with typical Antarctic ice shelves, would eliminate large portions of the ice shelf during retreat and make analysis of the evolving melt-rate field more challenging.

5 Ocean1 and Ocean2 have stationary [geometry_topography](#), so the calving criterion ~~need only be applied~~ needs to be applied only once when setting up the model domain. Ocean3 and Ocean4 have dynamic [geometry_topography](#) so it will be necessary to apply calving as the [geometry_topography](#) is interpolated in time. ~~Ice thinner than $H_{calve} = 100$ (equivalent to an ice draft above ~ -90) is considered to have calved and the ice draft is set to zero.~~

10 To accommodate models that wish to interpolate the MISMIP+ [geometry_topography](#) in time for Ocean3 and Ocean4 (see Sect. 3.2.1 and 3.2.1), we have not applied the calving criterion to the provided [geometry_topography](#). Calving must be applied as part of setting up the [geometry_topography](#). This prevents the cliff face at the calving front from ~~moving vertically pinching off vertically over the course of a year~~ (because of interpolation between
15 large thickness and zero thickness) instead of [advancing or retreating](#) horizontally in time. Models that do not support a sheer calving face or which update the ice topography at each time step will likely need to smooth the calving face over several horizontal grid cells and/or to relax to the new geometry gradually over time. In such cases, it is suggested that participants interpolate the geometry in time, then apply the calving criterion, and finally
20 apply whatever smoothing or relaxation is required. This way, the (smoothed) calving front is expected to move relatively continuously in the horizontal, rather than abruptly jumping to the new location each year as the ice between the old and new calving fronts thins to zero.

25 Calved ice is simply removed from the domain, and contributes no freshwater flux to the ocean. We feel this is justified partly because it keeps the problem as simple as possible and partly because an Antarctic iceberg would be transported out of the ISOMIP+ domain in a matter of months, meaning most meltwater would be deposited elsewhere in a real-world problem.

3.1.3 Forcing

There is no forcing at the surface of the open ocean (i.e. no atmospheric or sea-ice fluxes) in any of the experiments. Aside from melt fluxes under the ice shelf, the only forcing is via 3-D restoring within 10 km of the northern boundary. In the restoring region, potential temperature and salinity are restored to prescribed profiles with the following tendencies:

$$\left. \frac{\partial T}{\partial t} \right|_{\text{res}} = \dots - \gamma(x)[T - T_{\text{res}}(z)], \quad (18)$$

$$\left. \frac{\partial S}{\partial t} \right|_{\text{res}} = \dots - \gamma(x)[S - S_{\text{res}}(z)], \quad (19)$$

where $T_{\text{res}}(z)$ and $S_{\text{res}}(z)$ are the restoring profiles for potential temperature and salinity, respectively, γ and $\gamma(x)$ is the decay rate, ~~and where other contributions to the time evolution of T and S have been omitted for simplicity. The decay rate $\gamma(x)$ which~~ increases linearly from zero (no restoring) at ~~$x_{r0} = 790$~~ $x_{r0} = 790$ km to $\gamma_0 = 10 \text{ days}^{-1}$ at the northern boundary, ~~$x_{r1} = 800$~~ $x_{r1} = 800$ km:

$$\gamma(x) = \gamma_0 \max \left(0, \frac{x - x_{r0}}{x_{r1} - x_{r0}} \frac{x - x_{r0}}{x_{r1} - x_{r0}} \right). \quad (20)$$

~~For the initial ocean~~ The relatively fast restoring rate, corresponding to a restoring time scale of 0.1 days, was chosen following Goldberg et al. (2012a, b).

For the ocean initial conditions and boundary forcing, linear ~~depth~~ profiles for potential temperature and salinity as functions of depth are given by

$$T_{\text{res}}(z) = T_0 + (T_{\text{bot}} - T_0) \frac{-z}{B_{\text{max}}} \frac{z}{z_{b,\text{deep}}}, \quad (21)$$

$$S_{\text{res}}(z) = S_0 + (S_{\text{bot}} - T_0) \frac{-z}{B_{\text{max}}} \frac{z}{z_{b,\text{deep}}}, \quad (22)$$

where values at the surface (T_0 and S_0) and at the ocean floor (T_{bot} and S_{bot}) vary between the four correspond to either the COLD (Fig. 6 and Table 5) or WARM profiles (Fig. 6 and Table 6), depending on the experiment. The WARM profiles were chosen to produce strong thermal driving at depth but potential temperatures near freezing at the surface, qualitatively mimicking observations of deep, warm water observed in the Amundsen Sea region (Dutrieux et al., 2014). These relatively warm conditions, which result in large melt rates, are consistent with “warm” Antarctic ice shelves like those bordering the Amundsen and Bellingshausen Seas. The COLD profiles are consistent with ocean properties of “cold” Antarctic ice shelves like those bordering the Weddell and Ross Seas. The COLD potential temperature profile is constant at the surface freezing temperature throughout the water column and has a lower salinity, resulting in WARM and COLD density profiles that are nearly identical throughout the water column, thus reducing convective instabilities resulting from the transitions between COLD and WARM conditions that occur in Ocean1–2 as well as the MISOMIP1 IceOcean1–2 experiments.

3.1.4 Boundary and initial conditions

In the COM configuration, we request that participants use no-slip lateral boundary conditions at all walls including the northern wall adjacent to the restoring region and the calving front. We realize that free-slip or open boundary conditions may be more physically justifiable but no-slip boundary conditions are likely to be supported by the largest number of models. Also we prescribe no melting or drag from vertical ice faces (e.g. the calving front) both for simplicity and because many models do not support melting on vertical faces. Participants that use other boundary conditions should note this when they submit their results (see Sect. 3.3). The momentum boundary conditions at the ice-shelf base and seabed are quadratic drag with coefficients given in Table 4.

The ocean is initialized at rest with potential temperature and salinity profiles that are horizontally constant. The vertical functional forms of the initial profiles differ between the experiments, and are described below.

For TYP runs, no other model parameters or choices of model physics are prescribed. For COM runs, the recommended values for several relevant parameters are given in Table 4.

3.1.5 COM grid resolution

5 The nominal horizontal resolution for COM runs is 2 km. We leave it at the discretion of modelers with horizontally unstructured grids to determine what a characteristic resolution of 2 km means for their model.

Given the diversity of ocean-model vertical coordinates, it is not possible or useful to specify a vertical resolution that applies to all models. For this reason, we specify that all models should have 36 vertical layers, but we leave it at the modeler's discretion how the layers are distributed.

10 Many models will require a minimum ocean-column thickness. We recommend that models make the minimum ocean column as thin as can reasonably be achieved while retaining numerical stability and accuracy. For z level models, the minimum thickness is likely to be approximately two grid cells (~ 40 m if z levels are equally spaced). Models with other vertical coordinates may be less restricted, but ~~“digging” may still be required. We leave it up to each modeler to decide how the “digging” is distributed between the bathymetry and the ice draft. We recommend thickening the ocean column to the minimum thickness wherever the floating mask indicates that ocean is present, as opposed to removing ocean columns that are thinner than a minimum threshold~~some modification of the topography may be required to maintain a minimum ocean-column thickness. In locations where the ocean column is too thin, participants will need to decide for themselves whether it is more practical to modify the topography (ice draft, bathymetry or both) or to remove the column from the ocean (i.e. mark it as “land”).

25 We recommend that z level models use both partial top and bottom cells, if they are supported, for increased accuracy.

3.1.6 COM mixing parameterizations

Mixing is typically computed separately in the “horizontal” direction (i.e. within a model layer) and in the “vertical” direction (i.e. between model layers), regardless of which vertical coordinate is being used. To keep the experiments simple, we ask participants to perform “vertical” mixing with [harmonic diffusion and the constant vertical viscosities and diffusivities given in Table 4.](#) [However, enhanced vertical mixing near the ice-ocean interface may be appropriate for models with high vertical resolution near the ice-ocean interface, since the buoyant sub-ice-shelf plume likely induces enhanced turbulent mixing that entrains ambient fluid. Models using non-constant vertical mixing should document the mixing scheme along with their results.](#) Most models (e.g. those using the hydrostatic approximation) do not explicitly model convective instability. We prescribe a large vertical viscosity/diffusivity to be applied when the local stratification is unstable, with values given in the table. Participants whose models do not support this convective parameterization should note what other scheme was used to handle unstable stratification (e.g. convective adjustment or explicit modeling of convection).

“Horizontal” mixing should be parameterized with harmonic (“~~del2~~”) diffusion using a constant eddy viscosity/diffusivity. The values of the “horizontal” eddy viscosity and diffusivity have been chosen so to be small but (hopefully) sufficient to damp grid-scale numerical noise at the COM resolution. Participants may need to increase these values for numerical stability, in which case this should be noted with their results (see Sect. 3.3). The vertical eddy viscosity and diffusivity have the same values as in the original ISOMIP experiment. We note that, in many models, it may be that numerical diffusion is larger than the explicit mixing.

3.1.7 COM equation of state

We prescribe a linear equation of state (EOS) with ~~of~~ coefficients in Table 4:

$$\rho = \rho_{\text{ref}} [1 - \alpha_{\text{lin}} (T - T_{\text{ref}}) + \beta_{\text{lin}} (S - S_{\text{ref}})]. \quad (23)$$

For models that do not support a linear equation of state, we ask participants to note this and to describe the EOS they used in [their readme file](#) [the pdf describing their model](#). [Any model that requires \$\rho_{\text{ref}}\$ to be equal to \$\rho_{\text{sw}}\$ should use \$\rho_{\text{ref}}\$ for both values, and should note this difference along with their output.](#)

5 3.1.8 COM melt parameterization

The recommended melt-rate formulation is the three-equation formulation with constant nondimensional heat- and salt-transfer coefficients (Γ_T and $F_S \Gamma_S$). Following Jenkins et al. (2010), Eqs. (1), (3), (4) and (5), we have:

$$\rho_{\text{fw}} m_{\text{ww}} L = -\rho_{\text{sw}} c_{\text{ww}} u_* \Gamma_T \left(T_{\text{bz}_d} - T_{\text{ww}} \right), \quad (24)$$

$$10 \quad T_{\text{bz}_d} = \lambda_1 S_{\text{bz}_d} + \lambda_2 + \lambda_3 p_{\text{bz}_d}, \quad (25)$$

$$\rho_{\text{fw}} m_{\text{ww}} S_{\text{bz}_d} = -\rho_{\text{sw}} u_* \Gamma_S \left(S_{\text{bz}_d} - S_{\text{ww}} \right), \quad (26)$$

$$u_*^2 = C_{\text{D,top} \text{D,top}} \left(u_{\text{ww}}^2 + u_{\text{tidal}}^2 \right), \quad (27)$$

15 where m_{ww} is the melt rate expressed in water-equivalent (w_{eq}), u_* is the friction velocity, u_{w} , T_{w} and S_{w} are the far-field velocity, potential temperature and salinity in the ocean (see below) and T_{b} , S_{b} and p_{b} are the T_{z_d} , S_{z_d} and p_{z_d} are the potential temperature, salinity and pressure at, salinity and pressure at the interface, and u_{w} , T_{w} and S_{w} are the velocity magnitude, potential temperature and salinity some distance below the ice-shelf interface. The prescribed, as discussed below.

20 Because of differences in vertical resolution, vertical mixing and the method for computing u_{w} , T_{w} and S_{w} , appropriate values of the heat- and salt-transfer coefficients, Γ_T and Γ_S , are likely to vary significantly between models. In Sect. 3.2.1, we prescribe a procedure for tuning these coefficients to achieve a desired mean melt rate. With the

exception of Γ_T and Γ_S , we prescribe values for the coefficients ~~used in this formulation are given in Eqs. (24)–(27)~~ in Table 4.

The liquidous coefficients in Eq. (25) are based on values from Jenkins et al. (2010) but have been modified to compute the potential freezing point. This should save modelers the trouble of converting the boundary-layer potential temperature to in situ temperature before computing the thermal driving. Modelers will need to determine the best method for computing the pressure at the ice–ocean interface, $p_b p_{z_b}$, as we do not prescribe a method for doing so here. One commonly used method (Losch, 2008) computes $p_b p_{z_b}$ by integrating a reference density profile from sea level to the ice draft.

For simplicity, the ice is considered to be perfectly insulating. This means that modelers should not use the advection-diffusion scheme from Holland and Jenkins (1999) to determine the heat flux into the ice-shelf, as is common practice in ice-shelf cavity modeling. Top and bottom friction are computed with a quadratic drag law (surface stresses are proportional to the square of the local ocean flow speed) ~~with drag coefficients, taken using drag coefficients~~ from Hunter (2006), as given in the table. The root-mean-square “tidal” velocity, u_{tidal} , is used to parameterize the turbulent mixing that would be induced by tides if they were present and is used to prevent the friction velocity (and thus the melt rate) from going to zero when there is no motion under the ice shelf. The computation of top and bottom drag do not incorporate u_{tidal} .

~~Because vertical mixing is a strong function of the distance $z' = |z - z_b|$ from the ice–ocean interface, the heat and salt transfer coefficients, Γ_T and Γ_S , are also expected to vary with this distance (?Jenkins et al., 2010). Sophisticated parameterizations of vertical mixing are presumably required to adequately capture this variability, but such work lies outside the scope of this MIP. Theory suggests that most of the z' -dependence of Γ_S and (to a lesser extent) Γ_T occurs for $z' \lesssim 2\text{ m}$ (?). However, the theory holds that transfer coefficients are only fully independent of z' when the far-field T and S are sampled outside the turbulent boundary layer. We do not have a broadly accepted theory for how vertical viscosity and diffusivity should vary through the turbulent boundary layer. For simplicity, the GOM simulation prescribes constant vertical mixing coefficients (see~~

Sect. 3.1.6), meaning that vertical mixing is not likely to be represented accurately within the boundary layer. Indeed, preliminary results suggest that the melt rates will not converge with vertical resolution in the GOM configuration (with constant Γ_T and Γ_S) unless the thickness of the boundary layer is held fixed, independent of the resolution. We prescribe the boundary layer thickness to be 20. Participants should compute the [Methods for computing the “far-field” potential temperature, salinity and velocity](#) (T_w , S_w and u_w) either by averaging over the top 20 (similar to Losch, 2008) or by sampling T_w , S_w and u_w [differ across models. Some models sample these fields](#) at a fixed distance $z' = 10$ below the interface (following the approach of Kimura et al., 2013). The values for Γ_T and Γ_S given in Table 4 were calibrated using the Losch (2008) approach in simulations from the Parallel Ocean Program version 2 extended (POP2x). Transfer coefficients were calibrated so that the maximum melt rate in the first ISOMIP+ experiment (see Sect. 3.2.2) was ~ 80 , on the order of inferred melt rates near the grounding line of Pine Island Ice Shelf (?). Models that are not able to support a boundary layer of the prescribed 20 thickness will need to modify the drag coefficient C_D and/or the transfer coefficients Γ_T [below the ice draft](#) (e.g. Kimura et al., 2013) while others average the fields over a prescribed thickness (e.g. Losch, 2008). Participants are asked to describe how T_w , S_w and Γ_S [to arrive at a similar maximum melt rate, in which case this should be noted in the readme.](#) The ratio of Γ_T to Γ_S should remain a factor of ~ 35 [if \$u_w\$ are computed in the pdf included with their results.](#)

Some models will use virtual salt fluxes, while others will use volume fluxes (or perhaps mass fluxes) at the ice–ocean boundary. The freshwater, heat and salt fluxes for models using virtual salt fluxes should be computed following Jenkins et al. (2001) as:

$$F_{fw} = 0 \quad (28)$$

$$F_{HH} = -c_{ww} \left(\rho_{sw} u_* \Gamma_T + \rho_{fw} m_{ww} \right) \left(T_{fz_d} - T_{ww} \right), \quad (29)$$

$$F_{SS} = - \left(\rho_{sw} u_* \Gamma_S + \rho_{fw} m_{ww} \right) \left(S_{bz_d} - S_{ww} \right). \quad (30)$$

If volume fluxes are used instead, the same fluxes are given by:

$$F_{fw} = \rho_{fw} m_{ww} \quad (31)$$

$$F_H = -c_{ww} \left[\rho_{fw} m_{ww} T_{fzb} + \rho_{sw} u_* \Gamma_T \left(T_{fzd} - T_{ww} \right) \right], \quad (32)$$

$$F_{SS} = 0. \quad (33)$$

- 5 Though we do not require it, models may wish to ~~use the approach of Losch (2008) in which the melt fluxes are distributed proportionally to all cells in the boundary layer, rather than affecting only the top cell~~ distribute melt fluxes over several vertical grid cells, as in Losch (2008). This approach parameterizes additional vertical mixing within the boundary layer and may prevent noise and/or time-step restrictions in models with very thin cells
10 below the ice–ocean interface. This is an alternative approach to representing the enhanced turbulent mixing near the ice–ocean interface mentioned in Sect. 3.1.6.

Models using volume or mass fluxes will need a strategy for removing ~~freshwater mass~~ in the open ocean to compensate for the volume of melt water that enters the domain. Because of the small size of the domain, without such a strategy, sea level would likely
15 rise by hundreds of meters in simulations with large melt rates (Ocean1 and Ocean3). ~~We recommend imposing an~~ One possible approach is to impose an artificial evaporative flux in the ~~open ocean region ÷ restoring region ($x > 790$ km).~~ Corresponding salt and heat fluxes will be needed to prevent the top cells from becoming cooler and saltier as mass leaves the cell:

$$20 \quad F_{ee} = -\rho_{sw} \max \left\langle m_w \right\rangle \frac{A_{shelf}}{A_{res}}, \frac{0}{\tau_e} \quad (34)$$

$$\underline{F_{H,e}} = c_w T_0 F_e, \quad (35)$$

$$\underline{F_{S,e}} = S_0 F_e, \quad (36)$$

where $\tau_e = 30$ is the characteristic time of the evaporative forcing and η is the mean sea-surface height averaged in space over the open ocean and in time over one month ($\sim \tau_e$) to remove short-term variability. Participants who find that an alternative strategy is more appropriate for their model. $F_{e,r}$, $F_{H,e}$ and $F_{S,e}$ are the evaporative mass, heat and salt flux, respectively, A_{res} is the area of the restoring region, T_0 and S_0 are the prescribed temperature and salinity at the ocean surface in the restoring profile, and $\langle m_w \rangle$ is the melt rate averaged over the area of the ice shelf A_{shelf} and over a suitable period of time (perhaps one month). Participants are welcome to use alternative strategies. They are asked to document this in the readme file supplied with their results whichever approach (if any) they use for removing excess mass in their description pdf.

3.2 ISOMIP+ experiment 1 (Ocean1): cold-to-warm forcing with static ice-shelf geometry Experiments

Ocean1 and Ocean2-Ocean0-2 involve static ice-shelf geometry/topography, making them accessible to a wider range of ocean models. They are intended to represent the most advanced and most retreated states in the coupled ice sheet-ocean system to come later. These experiments are designed to test how changes in far-field ocean forcing result in changes in melt rates, which would drive ice-sheet dynamics in the coupled system. Preliminary simulations with POP2x suggest that, in each experiment, the system will experience an initial shock lasting a few days as the ocean water in contact with the ice shelf adjusts to the melting/freezing boundary conditions. Over several years, in Ocean0, strong melting begins immediately, and the system reaches a quasi-equilibrium within a few months. In Ocean1 and Ocean2, far-field changes in ocean properties will propagate from the far field take several years to propagate into the ice-shelf cavity, leading to a substantial increase (in Ocean1) or decrease (in Ocean2) in melting.

Ocean1 uses the Ocean3 and Ocean4 make use of dynamic ice topography that evolves over 100 years. Whereas preliminary results suggest that Ocean0-2 approach or have reached quasi-equilibria by the end of each experiment, Ocean3-4 do not reach steady state because of the evolving topography.

Figure 7 shows time-series of area-averaged melt rate for four of the five ISOMIP+ experiments from example POP2x simulations. Melt rates from Ocean0, not shown, are nearly indistinguishable from the first year of the Ocean3 experiment.

In the following sections, we present further results from these POP2x simulations. In each case, we show the evolution of a transect through the ocean temperature field through the center of the domain, which also indicates how the ice topography evolves (if at all) over time. We emphasize that we do *not* intend these results to be treated as a benchmark for other participants to try to match. Instead, the examples show that the simulations can be performed and that they achieve their intended purposes. They should give the participants a qualitative idea of what to expect. After all, the MIP is not to attempt to produce identical results with all models but rather to try to understand the differences that occur.

3.2.1 Ocean0: warm initial conditions and forcing with static ice-shelf topography

Ocean0 uses steady-state geometry shown in ice topography, as shown in the transects in Fig. ??, which comes 8, from the initial steady state of the MISMIP+ experiments Ice1 experiment (see Sect. 2.2) produced with BISICLES using the SSA and no melting. The experiment starts with cold conditions and a low melt rate, consistent with a “cold” Antarctic ice shelf like those bordering the Weddell and Ross Seas. The ocean is initialized with the GOLD WARM profiles in Fig. 6, making the deep ocean relatively cold and fresh. Far-field restoring to the WARM profiles (also shown in the figure) leads to warmer and saltier water at depth. The linear profiles of T and S are defined by Eqs. (21) and (22), respectively and parameters for the GOLD and WARM profiles are given in Tables 5 and 6, respectively. The WARM profiles was chosen to produce strong thermal driving at depth but potential temperatures near freezing at the surface, qualitatively mimicking observations of deep, warm water observed in the Amundsen Sea region (Dutrieux et al., 2014). The GOLD potential temperature profile is constant at the surface freezing temperature throughout the water column and a lower salinity designed to give a similar density as in the WARM profile throughout the water column (see and restored the same profile in the far field).

The combination of warm initial conditions and restoring is expected to lead the system to reach a quasi-equilibrium with strong melting over a few months to a year, based on preliminary results. The duration of the run should be the time needed to reach a quasi-equilibrium melt rate plus six months, so that time averages without trends may be taken over the final six months of the simulation. We expect the total run duration to be between one and two years.

Because Ocean0 is expected to reach a quasi-equilibrium within approximately one year, this experiment is well suited to parameter studies. In particular, we use this experiment to calibrate the values of the heat- and salt-transfer coefficients, Γ_T and Γ_S to achieve a target melt rate,

$$\langle m_w \rangle = 30 \pm 2 \text{ ma}^{-1}, \quad (37)$$

where the brackets indicate the average of m_w over the area where $z_b < -300\text{m}$ and over the final six months of the simulation. We focus on the melt rate over the deeper portion of the ice draft because we expect larger (therefore more dynamically relevant) melt rates in this region. Participants should use an optimization approach such as sampling or a continuation method to find a value of Γ_T such that $\langle m_w \rangle$ lies within the prescribed bounds. At each stage, the value of Γ_S should also be modified such that $\Gamma_S = \Gamma_T/35$ (McPhee et al., 2008; Jenkins et al., 2010). Fits to observations suggest that the thermal Stanton number is on the order of $St = \sqrt{C_{D,\text{top}}}\Gamma_T = 1.1 \times 10^{-3}$ (Jenkins et al., 2010), suggesting that $\Gamma_T = 2.2 \times 10^{-2}$ might be a good initial guess. Figure 9 shows an example of the tuning process applied in POP2x, plotting $\langle m_w \rangle$ for various values of Γ_T . The melt rate is $\sim 30 \text{ ma}^{-1}$ when $\Gamma_T \approx 0.11$ for this model. Figure 8 shows example Ocean0 results from POP2x with $\Gamma_T \approx 0.115$.

Models with high resolution near the ice–ocean interface may wish to deviate from the prescribed value of $C_{D,\text{top}}$ in addition to tuning Γ_T and Γ_S . For example, at high vertical resolution (higher than 0.1–1 m), the log law of the wall, in which C_D is a function of the log of the distance from the interface, is used in some models (Oey, 2006). Participants that

use a value or functional form for $C_{D,top}$ other than that given in Table 4 should document this with their submitted results.

3.2.2 Ocean1: cold initial conditions and warm forcing with static ice-shelf topography

Ocean1 uses the same topography and restoring as Ocean0 but is initialized to a colder, fresher profile (COLD from Fig. 6), thus reducing convective instabilities generated by the restoring, that is expected to result in low melt rates during the first several years of the simulation. Far-field restoring to the WARM profiles leads to warmer and saltier water in the far field at depth.

It is worth noting that this COLD-to-WARM scenario represents a transition between the two extremes of water masses observed on the Antarctic continental shelf, and is therefore a highly an unrealistic scenario designed purely to test the response of models to an extreme forcing.

The duration of the experiment is exactly 20 years (from the beginning of the date ~~1-January-0000~~ 1-Jan-0000 to the end of ~~31-December-0019~~ 31-Dec-0019), which preliminary results suggest is sufficient time to reach a quasi-steady state. Melt rates as well as the strengths of the barotropic and overturning circulations toward the end of the simulation are expected to be significantly larger than those within the first few years because of the warming.

3.3 ~~ISOMIP+ experiment 2 (Ocean2): warm-to-cold forcing with static ice-shelf geometry~~

Example results from a POP2x Ocean1 simulation, the top row of Fig. 10, show that warm water at depth gradually advects and mixes into the cavity during the first decade, becoming quasi-steady over the second decade. Melt rates from Fig. 7 are initially low, corresponding to a relatively weak overturning circulation. This weak circulation means that warm, deep water is pulled into the cavity only gradually over most of the first decade. As warmer

water reaches the back of the cavity, melt rates increase, driving stronger overturning and drawing more warm water. This positive feedback saturates over the course of several years once melt rates have increased by several orders of magnitude. The system remains in quasi-steady state for approximately the second half of the experiment.

3.2.1 Ocean2: warm initial conditions and cold forcing with static ice-shelf topography

In Ocean2, the ~~geometry-topography~~ is from the end of Ice1r (see Sect. 2.2) using BISICLES with the SSA. ~~The geometry is shown in~~ A temperature transect through the center of the domain can be seen in each panel of the bottom row of Fig. ??10. The ocean is initialized with the WARM profiles and restored to the COLD profiles in Fig. 6, with parameters given in Tables 5 and 6. Again, the experiment should run for 20 ~~, resulting in a quasi-steady state~~ years. As in Ocean1, ~~this is an unrealistic scenario designed purely to evaluate model consistency~~ the abrupt change between forcing profiles is unrealistically strong and is designed to test how the participating models respond to extreme changes.

3.3 ~~ISOMIP+ experiment 3 (Ocean3): warm forcing with retreating ice-shelf geometry~~

The bottom row of Fig. 10 and the green curve in Fig. 7 show example POP2x results from Ocean2. Initially, strong circulation driven by warm ocean temperatures and rapid melting pull in cold water from the far field. As this cold water reaches the back of the cavity within the first year, the melt rate begins to fall, decreasing by several orders of magnitude over the course of the simulation. The slower overturning during much of the simulation means that the timescale required to reach a quasi-steady state is longer for Ocean2 than for Ocean1 and equilibrium has not been reached after 20 years.

3.2.1 Ocean3: warm initial conditions and forcing with retreating ice-shelf topography

Ocean3 begins with the same geometry topography as Ocean1, but in this experiment the ice draft evolves over time according to a prescribed data set covering 100 years of ice retreat from Ice1r. ~~In this experiment, we prescribe both initialization and restoring to the WARM salinity and potential temperature profile in Fig. 6. Conceptually, this means we~~ Ocean3 is initialized and forced with the WARM profile. We expect strong melting to begin immediately as the sub-ice-shelf circulation spins up, consistent with the strong melt profile prescribed in conditions for Ice1r from which the geometry is taken used to generate the topography, and to persist for the duration of the experiment.

~~On the MISOMIP website, we provide ice geometry~~ The topography for Ocean3, available through Cornford and Asay-Davis (2016), includes snapshots of the ice draft and ice surface at yearly intervals on the original BISICLES-1 a 1-km grid. We expect that the frequency with which ocean models can update their geometry topography may vary considerably, from once per time step in some models to monthly or yearly in others. Modelers Participants wishing to update more frequently than yearly should interpolate the ice draft linearly between subsequent geometries to determine the geometry topography at intermediate times. As previously mentioned, we have not applied the calving criteria to the geometry topography provided because calving should be applied only after after interpolation in time and space. This means that models that update the geometry topography only every year and thus require no interpolation in time will need to apply the calving criteria themselves.

3.3 ISOMIP+ experiment 4 (Ocean4): cold forcing with advancing ice-shelf geometry

The red curve in Fig. 7 shows melt rates from Ocean3, and the top row of Fig. 11 shows a transect of monthly-averaged temperature as well as the evolving ice topography at four points in time. Mean melt rates remain strong throughout the simulation. As the ice draft steepens, melting becomes concentrated near the grounding line within the trough. As

[the cavity grows, melt fluxes remain strong but the mean melt rate decreases somewhat because of the increased area.](#)

3.2.1 [Ocean4: cold initial conditions and forcing with advancing ice-shelf topography](#)

5 Conceptually, Ocean4 is an extension of Ocean3. The ice-draft [geometry topography](#) from Ice1ra was produced by abruptly shutting off melting at year 100 and allowing the ice to re-advance for 100 [years](#) (see Sect. 2.2). Thus, Ocean4 begins with the final [geometry topography](#) from Ocean3 (which is also the same [geometry topography](#) as in Ocean2). This time, we prescribe both initialization and restoring to the COLD salinity and potential
10 temperature profile, which should lead to very low melt rates, consistent with the lack of melting in the MISMIP+ run that produced the ice [geometry topography](#). As in Ocean3, yearly topography data at 1 km resolution are provided [on the MISOMIP website through Cornford and Asay-Davis \(2016\)](#). Once again, participants will need to apply the calving criteria to these data.

15 [Example results from POP2x show that melt rates remain low for the duration of the simulation \(cyan curve in Fig. 7\) and that temperatures in the cavity evolve toward the freezing point over the first several decades, reaching a quasi-steady state after ~30 years. A transect through the temperature field in the bottom row of Fig. 11 also shows the evolving ice topography.](#)

20 3.3 Requested output

Participants are asked to supply a number of fields interpolated to a standard grid. NetCDF files with example output on the standard grid are [supplied on the MISOMIP website available for download \(see Sect. 5\)](#). Participants are asked to supply a single NetCDF4 file for each experiment with the file-naming convention of
25 `[expt]_COM_[MODEL].nc`, where `[expt]` is an experiment name from Table 2, COM or TYP indicates the type of run and `[MODEL]` is a unique identifier for the participant (e.g.

the name of the ocean model and/or the institute). We ask participants to provide all fields in 32-bit floating-point precision using the variable and dimension names given in bold and units given in square brackets as follows:

- **nx**, **ny**, **nz** and **nTime** dimensions.
- 5 – **x(nx)**, **y(ny)** and **z(nz)** [m] cell centers of the output grid as vectors. The origin of the horizontal grid should match MISMP+ so that the southeast corner of the grid is at $x = 320$ km and $y = 0$. The spacing between horizontal points is 2 km and between vertical points is 5 m.
- **time(nTime)** [s] from the start of the simulation as a vector running over the full duration of the simulation (20 years for Ocean1 and Ocean2, 100 years for Ocean3 and Ocean4). The time interval between entries is one month, using a standard 365 day calendar with no leap years.
- 10 – **meanMeltRate(nTime)** [m s^{-1}] w_{eq} , the melt rate, positive for melting and negative for freezing, averaged over the ice-shelf base.
- **totalMeltFlux(nTime)** [kg s^{-1}], the total mass flux of freshwater across the ice–ocean interface, positive for melting and negative for freezing.
- 15 – **totalOceanVolume(nTime)** [m^3], the total volume of the ocean.
- **meanTemperature(nTime)** [$^{\circ}\text{C}$], the potential temperature averaged over the ocean volume.
- 20 – **meanSalinity(nTime)** [PSU], the salinity averaged over the ocean volume.
- **iceDraft(nTime,ny,nx)** [m], the elevation of the ice–ocean interface (z_d). Dependence on **time** is only needed for Ocean3 and Ocean4.
- **bathymetry(nTime,ny,nx)** [m], the elevation of the bathymetry (z_b). Dependence on **time** is only needed for Ocean3 and Ocean4.

- **meltRate**(nTime,ny,nx) [m s^{-1}] w_{eq} , the melt rate, positive for melting and negative for freezing.
- **frictionVelocity**(nTime,ny,nx) [m s^{-1}], the friction velocity u_* used in melt calculations.
- **thermalDriving**(nTime,ny,nx) [$^{\circ}\text{C}$], the thermal driving used in the melt calculation. The thermal driving is the difference between the potential temperature in the boundary layer, $\overline{T_w}$, and the freezing potential temperature at the ice–ocean interface, $\overline{T_{zd}}$.
- **halineDriving**(nTime,ny,nx) [PSU], the haline driving used in the melt calculation. The haline driving is the difference between the salinity in the boundary layer, $\overline{S_w}$ and the salinity at the ice–ocean interface, $\overline{S_{zd}}$.
- **uBoundaryLayer**(nTime,ny,nx) and **vBoundaryLayer**(time, y, x) [m s^{-1}], the components of the velocity in the boundary layer that were used to compute u_* .
- **barotropicStreamfunction**(nTime,ny,nx) [$\text{m}^3 \text{s}^{-1}$], the barotropic streamfunction.
- **overturningStreamfunction**(nTime,nz,nx) [$\text{m}^3 \text{s}^{-1}$], the overturning streamfunction in x – z .
- **bottomTemperature**(nTime,ny,nx) [$^{\circ}\text{C}$] and **bottomSalinity**(nTime,ny,nx) [PSU], the potential temperature and salinity in the bottom-most cell in each ocean column.
- **temperatureXZ**(nTime,nz,nx) [$^{\circ}\text{C}$] and **salinityXZ**(nTime,nz,nx) [PSU], the potential temperature and salinity **slices transects** in x – z plane through the center of the domain, $y = 40$ km.
- **temperatureYZ**(nTime,nz,ny) [$^{\circ}\text{C}$] and **salinityYZ**(nTime,nz,ny) [PSU], the potential temperature and salinity **slices transects** in y – z plane outside the cavity $x = 520$ km.

Invalid values (e.g. field locations that lie within the ice shelf or bedrock) should be masked out using a fill value. In C and Fortran, this can be accomplished by assigning a value of

NC_FILL_FLOAT and setting the `FillValue` attribute of the NetCDF variable to this value. In Python, invalid data can be masked by using numpy masked arrays to assign to netCDF4 variables.

We ask participants to supply monthly mean values of all time-dependent quantities (except **iceDraft** and **bathymetry**, which should be snapshots), where the values in the **time** array indicate the beginning of the period being averaged. Participants who are unable to compute monthly mean values may supply snapshots instead but should indicate this with their submission.

We note that many functions are typically computed on staggered grids. For example, the barotropic streamfunction is typically computed at horizontal cell corners (vertices) and the overturning streamfunction is typically computed at cell corners on the vertical grid. Velocity components (**uBoundaryLayer** and **vBoundaryLayer**) are typically located at cell edges (on a C-grid) or cell corners (on a B-grid). Additionally, for most models, potential temperature and salinity fields will not have values exactly at $y = 40$ km as requested in **temperatureXZ** and **salinityXZ** (and similarly for the $y-z$ **slicestransects**). To aid in analysis and comparison of results, we ask all participants to interpolate these fields to the standard grid. The standard grid has a high vertical resolution ($\Delta z = 5$ m) in an attempt to accommodate models with a variety of vertical coordinates. Participants are welcome to provide plots of their results on their model's native grid in addition to supplying the output on the standard grid.

Participants are asked to provide the **iceDraft** and **bathymetry**, which are time-dependent for Ocean3 and Ocean4, to show how topography has been modified (interpolated in time, smoothed, the ocean column thickened, etc.).

Two python scripts for plotting the contents of a properly formatted results file are available in the Supplement (`plotMISOMIPOceanData.py` and `plotMISOMIPOceanMetrics.py`). Plots of the example POP2x simulation results produced with this script are available for download (see Sect. 5).

We ask participants to include a **“readme” file** (description of the result in a pdf file (using the same naming convention as the results, i.e. `[expt]_COM_[MODEL].readme.pdf`))

with their submission describing several specific properties of their model and its ISOMIP+ configuration. If appropriate, a single pdf can be used to describe Ocean1–4 results, as has been done in the example included in the Supplement. These include:

1. The Model: the name and version of the model used (as specifically as possible, including a citation if available).
2. A Repository: a link to the repository where the model can be downloaded (if public) and specific tag, branch or revision (if available).
3. Description–Vertical coordinate: description of the vertical coordinate of the model (z level, z^* , terrain, isopycnal, etc.).
4. Description–Horizontal mixing: description of how “horizontal” mixing was performed (harmonic, biharmonic, etc.; within model levels, along geopotentials, along isopycnals, etc.).
5. Description–Vertical mixing: description of how “vertical” mixing was performed (constant diffusivity, k-profile parameterization, etc.; harmonic, biharmonic, etc.).
6. Advection: description of the momentum- and tracer-advection schemes used (centered, third-order with limiter, etc.).
7. Description–EOS: description of the equation of state.
8. Description–Convection: description of the procedure for handling convection (explicitly modeled, parameterized using strong vertical mixing, etc.).
9. Description of how T_w , S_w and u_w Melt parameterization: description of how T_w , S_w and u_w in the melt parameterization are computed from T , S and u fields (e.g. averaging over the boundary layer, sampling at a fixed distance)
10. Description–Topography: description of procedure for interpolating, smoothing or otherwise modifying the ice draft and/or bedrock topography.

11. Maintaining sea level: description of strategy (if any) for maintaining sea level when volume or mass fluxes are used [e.g. use of Eq. (34)].
12. ~~For~~ Moving boundaries: for Ocean3 and Ocean4, a description of how the moving boundary is implemented (e.g. how T , S and u are computed in cells or ocean columns that were previously ice-filled and redistributed, if at all, when a cell or column is filled with ice)
13. ~~For~~ TYP parameters: for TYP results, details on resolution as well as melt and mixing parameterizations.
14. ~~For~~ TYP problem: for TYP results, a description of the types of problems the participant would typically apply the model to using this configuration (e.g. which region; over what time span; with what kind of initialization, forcing and boundary conditions)
15. ~~For~~ COM deviations: for COM results, details anywhere the model deviated from the COM resolution or the COM melt and mixing parameterizations.

3.4 Example results

~~We provide example results as evidence that the experiments are achievable; that Ocean1 and Ocean2 attain the qualitative goals of , respectively, greatly increasing and greatly reducing melting through changes in far-field restoring; and to illustrate the requested output. The example output is not intended to provide a benchmark for other model output.~~

~~Example results from Parallel Ocean Program version 2 extended (POP2x) simulations in GOM configuration are shown in Figs. ??-??. Figure ?? shows~~

16. COM parameters: for COM results, the values of Γ_T and Γ_S . Also, the value of $C_{D,top}$ if different from the prescribed value.

17. Γ_T figure: for COM Ocean0 results, a figure similar to Fig. 9 showing how the melt rate averaged over the ice-shelf area as a function of time for each experiment. The remaining figures show the requested output fields averaged over the last month of Ocean1 and Ocean3. Animations showing the time-evolution of these fields for all four experiments are available through the MISOMIP website. A version of all four experiments with slightly different parameter values has also been performed successfully with NEMO (the Nucleus for European Modelling of the Ocean) for $z_d < -300$ m varies with Γ_T .

We provide an example in the Supplement.

4 MISOMIP1 design

MISOMIP1 prescribes two coupled ice sheet-ocean experiments (IceOcean1–2, summarized in Table 2), each with two parts. We expect the MISOMIP1 experiment to play an analogous role in evaluating coupled ice sheet-ocean systems to that of the ISOMIP projects for standalone ocean models with ice-shelf cavities and the MISOMIP projects for ice-sheet models. We ask participants to first perform the MISOMIP+ and ISOMIP+ experiments, so that the behavior of each component on its own has been documented, before proceeding to MISOMIP1.

For both MISOMIP1 experiments, the bedrock topography is the same as for MISOMIP+ and ISOMIP+, as given by Eqs. (1)–(4). All ice-sheet parameters are, in general, ice-sheet parameters are the same as for MISOMIP+ except where noted below. To simplify the coupled problem, we prescribe a constant ice temperature as in MISOMIP+ and set the thermal conductivity of ice to zero (so that there is no sensible heat flux into ice at the ice–ocean interface). Thus, the only flux across the ice–ocean interface is of melt water. As in ISOMIP+, freshwater fluxes come only from melting. Calved ice disappears abruptly (or as abruptly as the ocean component can handle, since some ocean models will need a finite period of adjustment to prevent tsunamis) without producing a freshwater flux into the ocean.

4.1 MISOMIP1 experiment 1 (IceOcean1): retreat and re-advance without dynamic calving

IceOcean1 begins with the ice-sheet steady state that also served as the initial conditions for the MISOMIP+ Ice0, Ice1 and Ice2 experiments (see Sect. 2.2). Unlike in ISOMIP+, IceOcean1 does not include a dynamic calving criterion. Ice is allowed to become as thin as the ice sheet and ocean components permit (potentially zero thickness) without calving. As in MISOMIP+ and ISOMIP+, ice beyond $x = 640$ km is considered to have calved.

The experiment consists of two phases—a 100-year retreat phase, IceOcean1r, and a 100-year re-advance phase, IceOcean1ra. At the beginning of IceOcean1r, the ocean component is initialized with the steady-state ice topography from the ice-sheet component and the COLD salinity and temperature profiles from Fig. 6 and Table 5. The initial state should be cold enough to produce low melt rates ($\sim 0.2 \text{ m a}^{-1}$ in preliminary tests) that are approximately consistent with the ice sheet's initial state. For the 100-year duration of IceOcean1r, restoring to the WARM profile (see Fig. 6 and Table 6) is applied near the ocean's northern boundary. As in ISOMIP+ Ocean1, the warm water is expected to reach the ice-shelf cavity within the first decade, at which point it should induce strong melting and subsequent rapid ice retreat.

The re-advance phase, IceOcean1ra, begins where IceOcean1r ends but abruptly switches to the COLD restoring profile at the ocean's northern boundary. This should greatly reduce melting within a decade. The simulation evolves for another 100 years, during the first decade of which the ocean should cool and the melt rate should be greatly reduced, similarly to Ocean2. The reduced melting should allow ice to re-advance for the remaining 100 remainder of the simulation.

The blue curves in Fig. 12 shows the mean melt rate and the grounded area and from an IceOcean1 simulation using the POPSICLES model (coupled POP2x and BISICLES). The top row of Fig. 13 shows the evolution of the ice draft and ocean temperature over the course of the simulation. The mean melt rate is initially relatively small, increasing by several orders of magnitude over the first decade as warm water reaches the cavity and

initiating grounding-line retreat. Because of the ocean temperature profile, the melt rate is a strong function of the depth of the ice–ocean interface. As the ice shelf thins, melting becomes concentrated over a steep region within the channel near the grounding line. As the grounding line retreats, the area of the cavity increases (no calving occurs except beyond $x = 640$ of simulation km) while the total melt flux remains nearly constant, meaning that the mean melt rate gradually decreases. Between year 100 and about year 130, the melt rate decays by several orders of magnitude, reaching a nearly steady value for the remainder of the simulation as the ice shelf thickens and grounding line begin to re-advance.

4.2 MISOMIP1 experiment 2 (IceOcean2 ; (optional): retreat and re-advance with dynamic calving

Specifying calving ~~is~~ was a major ~~problem~~ challenge in the design of MISOMIP1. There was general agreement in the community that ice-sheet models have not been shown to behave reliably with dynamic calving, ~~nor is there any while there is a lack of~~ consensus about which calving parameterizations are appropriate or physically realistic. In Antarctica, calving events tend to be infrequent, producing large tabular icebergs, a process that is not well modeled by a continuous calving velocity or a simple calving criterion ~~such as that used on ISOMIP+ (see based on ice thickness (e.g. Sect. 3.1.2)).~~ Nevertheless, we felt that it was important for testing the robustness of the ice-sheet and ocean components in MISOMIP1 that there be an experiment with a dynamic, sheer cliff at the calving front. We include an optional coupled experiment, IceOcean2, that is identical to IceOcean1 except that it includes dynamic calving in the ice-sheet component. This experiment is designed test the ability of the ice-sheet component to apply dynamic calving, including detecting disconnected icebergs and the ability of the ocean component to handle abrupt changes in ice topography.

Whereas the MISOMIP+ experiments do not include a dynamic calving front, IceOcean2 prescribes the same simple calving criterion used in ISOMIP+: ice thinner than $H_{\text{calve}} = 100$ m (equivalent to an ice draft above ~ -90 m) ~~or beyond $x_{\text{calve}} = 640$~~ should be calved and the ice thickness set to zero. ~~The calving criterion~~ This thickness threshold

was chosen for consistency with ISOMIP+, and allows the ice shelf to become thinner than would typically be observed in Antarctica. We also maintain the fixed-front calving condition from MISMIP+ that ice beyond $x_{\text{calve}} = 640$ km is removed. The calving criteria should be enforced in the ice-sheet component.

5 Because the calving criterion will change the steady state of the ice sheet, IceOcean2 should begin with a new steady-state ice-sheet spinup initial condition, again without melting but with the calving criterion imposed. For models that are performing a spinup to steady state, we recommend starting with the IceOcean1 initial condition. This may also be an appropriate starting guess for those using continuation methods to find the initial steady state. As in MISMIP+, participants should modify the ice softness (A) and/or, if necessary, 10 the basal-traction coefficient (β^2) so that the steady state grounding line crosses the center of the trough at $x = 450 \pm 10$ km. Participants may wish to perform the Ice1 experiment with the calving criterion, but this is not required.

15 Mean melt rates and grounded area from an example POPSICLES IceOcean2 simulation are shown in the green curves in Fig. 12, and the evolution of the ice draft and ocean temperature are shown in the bottom row of Fig. 13. The beginning of the retreat phase of IceOcean2 proceeds similarly to IceOcean1, with small differences due to the smaller, thinner ice shelf in the steady state with the calving criterion. Starting at around year 30, dynamic calving removes significant portions of the ice shelf. Although the melt flux remains 20 relatively steady, the mean melt rate increases as the ice-shelf area decreases. Just after year 60, a large iceberg breaks off from the ice shelf, leading to an abrupt decrease in ice-shelf area and a corresponding increase in the mean melt rate. For the remainder of the retreat phase, the ice shelf exists only as a small remnant of its initial size close to the grounding line. The re-advance phase begins at year 100 when the far-field restoring is switched to the COLD profiles. As the ocean cools, the melt rate decreases by several 25 orders of magnitude. The ice-shelf area remains much smaller than in IceOcean1ra while melt fluxes are similar, meaning that the mean melt rate is nearly an order of magnitude higher.

4.3 Component resolutions and parameterizations

As in the ISOMIP+ experiments, we ask participants to perform the MISOMIP1 experiment once in a “common” (COM) configuration similar to that of ISOMIP+. For this configuration, the ocean component should have the same resolution and parameters as in the ISOMIP+ COM run. We do not prescribe the resolution of the ice-sheet component because the wider use of unstructured, dynamic and adaptive grids as well as higher-order elements in ice-sheet models compared with ocean models make it impractical to provide specifications that are appropriate for all models. Also, grounding-line dynamics in ice sheet models have been shown to converge with resolution (e.g. Durand et al., 2009; Cornford et al., 2013; Leguy et al., 2014), whereas the same has not been shown for melt rates in-produced by ocean models. ~~Since different ice stress approximations produce different results even at very high resolution (Pattyn et al., 2012, 2013), the evaluation will likely be most effective when comparing ice components using the same stress approximation. For this reason, we request that participants submit COM results using the shallow shelf approximation (SSA) if possible. COM results with other stress approximations are also welcome.~~

Whereas we prescribed a “typical” run for ISOMIP+ with resolution and parameters that the ocean model typically uses for Antarctic regional simulations, it is not obvious that this is appropriate for MISOMIP1 models. Coupled ice sheet-ocean models are not well enough established to have typical resolutions and parameters. Therefore, we invite participants to submit several sets of results with parameter choices at their discretion in addition to the COM run and ensure these are well documented in the readme filepdf describing the model and results.

The coupling interval for the model is left to each participant to decide. We recommend ~~based on experience with the POPSICLES (coupled POP2x and BISICLES) model that participants use a coupling interval of~~ that participants perform a relatively short test with strong melting (e.g. initializing and forcing the coupled model with WARM conditions) to demonstrate convergence of the results with decreasing coupling intervals. For example, in POPSICLES, we have found in several tests that the mean melt rate and volume above

flotation converge with coupling interval only when the coupling interval is six months or less if they are able, ~~as resultswith yearly coupling diverged significantly from those with more frequent couplings~~ shorter. In the example results, POPSICLES was coupled monthly. We ask participants who are able to do so to provide multiple sets of results using different coupling intervals.

4.4 Requested output

We request that participants supply separate NetCDF files for their ice-sheet and ocean MISOMIP1 results. This allows the results to be supplied on different grids and is expected to simplify comparing the final results. NetCDF files with example output on the standard grids for each component are ~~supplied on the MISOMIP website~~ (available (see Sect. 5)). Participants are asked to supply all fields in 32-bit floating-point precision, with the file-naming convention of `[expt]_COM_[component]_[MODEL_CONFIG].nc`, where `[expt]` is the experiment name from Table 2, `COM` indicates a verification run and is omitted for non-COM runs, `[component]` is either ice or ocean and `[MODEL_CONFIG]` is a unique identifier for the coupled-model configuration (e.g. the name of the model, the institute, ice stress approximation, etc.).

The requested ocean fields and the output grid are the same as in Sect. 3.3. The requested output from the ice-sheet component is the same as in MISOMIP+ (see Sect. 2.3) with the exception that `time` is sampled monthly, the 2-D fields are required, rather than optional, and any units involving time should be given in `s` rather than `a` for consistency with the ocean output. As in MISOMIP+, the 2-D ice-sheet fields should be interpolated from the ice-sheet model's native grid to the standard 1 km grid to simplify analysis.

4.5 Example results

The results should be accompanied by a pdf file giving details about the coupled model. In addition to the information requested in Sects. 2.3 and 3.3, this file should include a description of the coupling scheme and the length of the coupling interval.

Example results from POPSICLES (POP2x-BISICLES) simulations are shown in Fig. ???. An animated version of the first panel is available on the MISOMIP website. The figure shows the ice geometry as well as the basal melt rate and the ocean temperature at the end of POPSICLES IceOcean1r simulation. The ice draft has steepened near

5 Code and Data Availability

The BISICLES ice-sheet model (Cornford et al., 2013) was used to produce the example MISOMIP+ results and is the ice-sheet component of the POPSICLES model, which was used for the MISOMIP1 example results. The BISICLES source code is available via Subversion at <https://commons.lbl.gov/display/bisicles/BISICLES>. The example results were produced with svn revision r2975.

The source codes for the POP2x ocean model and the POPSICLES coupled model have not yet been made available to the public.

The Supplement for this article includes BISICLES Example results from all MISOMIP+ experiments as well as a python script demonstrating how these data are written (specifically how to handle variations over time in the number of points describing the grounding line where the majority of melting now occurs. The figure also shows the grounded ice area and mean melt rate as functions of time over IceOcean1. At present, we have not completed). Also included are pdf files describing the example results from all three MIPs to be used as templates for the participants. Finally, example python scripts are included for plotting the grounded area from MISOMIP+ results as in Fig. 4 and various fields from ISOMIP+ and MISOMIP1 ocean results (similar to Fig. 8).

The ice topography data required for ISOMIP+ are too large to be included in the Supplement and have been archived separately in NetCDF4 format (Cornford and Asay-Davis, 2016). These data come from a simulation of the IceOcean2 experiment, but example results produced with POPSICLES will be made available on the MISOMIP website as soon as they are completed Ice1r and Ice1ra using BISICLES (svn revision r2825) with SSA and the basal friction parameterization from Weertman (1974).

The MISOMIP website (<http://www.climate-cryosphere.org/activities/targeted/misomip>) includes links to both NetCDF files and movie files showing the evolution of the example BISICLES, POP2x and POPSICLES simulations. We firmly wish to avoid giving the sense that the example results should be treated as a benchmark for the MIPs, and for this reason we do not feel it is appropriate to submit the results on their own to a data repository. Revised versions of the example results will be included along with submissions from other participants in a data repository as part of the analysis of each MIP.

6 Conclusions

Here, we have described the experimental design for three interrelated model intercomparison projects (MIPs): the third Marine Ice Sheet MIP (MISMIP+), the second Ice Shelf-Ocean MIP (ISOMIP+) and the first Marine Ice Sheet-Ocean MIP (MISOMIP1). We expect that the results from each MIP will be published separately with all contributors as coauthors, following the tradition of the earlier MISMIPs.

We have demonstrated that all experiments are achievable with typical an example set of ice and ocean models (BISICLES, POP2x and POPSICLES), and that the results are consistent with the intended behavior behind the experimental design. The MISMIP+ experiments show significant grounding-line dynamics in response to forcing by basal melting (Ice1) and a large calving event (Ice2). One ISOMIP+ experiment, Ocean0, is designed to reach a quasi-steady state within one to two years, making it practical for parameter studies including calibrating the melt parameterization used in the remaining ISOMIP+ and MISOMIP1 experiments. Two ISOMIP+ experiments, Ocean1 and Ocean2, demonstrate that changes in far-field forcing can lead to basal melting being significantly enhanced or suppressed on decadal timescales. The remaining ISOMIP+ experiments, Ocean3 and Ocean4, provide a meaningful test of whether ocean models can handle dynamic ice-shelf geometry topography. The main MISOMIP1 experiment, IceOcean1, demonstrates that changes in far-field ocean conditions can induce significant grounding-line dynamics.

An optional experiment, IceOcean2, demonstrates that both the ice-sheet and ocean components can handle a dynamic calving front.

**The Supplement related to this article is available online at
doi:10.5194/gmdd-0-1-2016-supplement.**

5 *Acknowledgements.* This material is based upon work supported by the U.S. Department of Energy, Office of Science, Office of Biological and Environmental Research under Award Numbers DE-SC0011982 and DE-SC0013038. Support was provided through NYU Abu Dhabi grant G1204. Simulation results were produced using resources of the National Energy Research Scientific Computing Center, a DOE Office of Science User Facility supported by the Office of Science of the U.S.
10 Department of Energy under Contract No. DE-AC02-05CH11231. This work has received funding from the European Union Seventh Framework Programme (FP7/2007-2013) under grant agreement number 299035. Work at the Lawrence Berkeley National Laboratory was supported by the Director, Office of Science, Office of Advanced Scientific Computing Research, of the U.S. Department of Energy under Contract No. DE-AC02-05CH11231.

15 References

- Calov, R., Greve, R., Abe-Ouchi, A., Bueller, E., Huybrechts, P., Johnson, J. V., Pattyn, F., Polard, D., Ritz, C., Saito, F., and Tarasov, L.: Results from the Ice-Sheet Model Intercomparison Project-Heinrich Event Intercomparison (ISMIP HEINO), *J. Glaciol.*, 56, 371–383, doi:10.3189/002214310792447789, 2010.
- 20 Cornford, S. L. and Asay-Davis, X. S.: Ice-shelf surface, basal and bedrock topography data for the second Ice Shelf-Ocean Model Intercomparison Project (ISOMIP+), GFZ Data Services, doi:10.5880/PIK.2016.002, <http://doi.org/10.5880/PIK.2016.002>, 2016.
- Cornford, S. L., Martin, D. F., Graves, D. T., Ranken, D. F., Le Brocq, A. M., Gladstone, R. M., Payne, A. J., Ng, E. G., and Lipscomb, W. H.: Adaptive mesh, finite volume modeling of marine ice sheets,
25 *J. Comput. Phys.*, 232, 529–549, doi:10.1016/j.jcp.2012.08.037, 2013.
- De Rydt, J. and Gudmundsson, G. H.: Coupled ice shelf-ocean modeling and complex grounding line retreat from a seabed ridge, *J. Geophys. Res.*, in press, doi:10.1002/2015JF003791, 2016.

- De Rydt, J., Holland, P. R., Dutrieux, P., and Jenkins, A.: Geometric and oceanographic controls on melting beneath Pine Island Glacier, *J. Geophys. Res.: Oceans*, 119, 2420–2438, doi:10.1002/2013JC009513, 2014.
- 5 Determann, J., Thoma, M., Grosfeld, K., and Massmann, S.: Impact of ice-shelf basal melting on inland ice-sheet thickness: a model study, *Ann. Glaciol.*, 53, 129–135, doi:10.3189/2012AoG60A170, 2012.
- Drouet, A. S., Docquier, D., Durand, G., Hindmarsh, R., Pattyn, F., Gagliardini, O., and Zwinger, T.: Grounding line transient response in marine ice sheet models, *The Cryosphere*, 7, 395–406, doi:10.5194/tc-7-395-2013, 2013.
- 10 Durand, G., Gagliardini, O., de Fleurian, B., Zwinger, T., and Le Meur, E.: Marine ice sheet dynamics: Hysteresis and neutral equilibrium, *J. Geophys. Res.*, 114, F03 009, doi:10.1029/2008JF001170, 2009.
- Dutrieux, P., De Rydt, J., Jenkins, A., Holland, P. R., Ha, H. K., Lee, S. H., Steig, E. J., Ding, Q., Abrahamsen, E. P., and Schroder, M.: Strong Sensitivity of Pine Island Ice-Shelf Melting to Climatic Variability, *Science*, 3, 468–472, doi:10.1126/science.1244341, 2014.
- 15 Favier, L., Durand, G., Cornford, S. L., Gudmundsson, G. H., Gagliardini, O., Gillet-Chaulet, F., Zwinger, T., Payne, A. J., and Le Brocq, A. M.: Retreat of Pine Island Glacier controlled by marine ice-sheet instability, *Nature Clim. Change*, 5, 1–5, doi:10.1038/nclimate2094, 2014.
- Feldmann, J. and Levermann, A.: Interaction of marine ice-sheet instabilities in two drainage basins: simple scaling of geometry and transition time, *The Cryosphere*, 9, 631–645, doi:doi:10.5194/tc-9-631-2015, 2015.
- 20 Feldmann, J., Albrecht, T., Khroulev, C., Pattyn, F., and Levermann, A.: Resolution-dependent performance of grounding line motion in a shallow model compared with a full-Stokes model according to the MISIP3d intercomparison, *J. Glaciol.*, 60, 353–360, doi:10.3189/2014JoG13J093, 2014.
- 25 Gagliardini, O., Cohen, D., Råback, P., and Zwinger, T.: Finite-element modeling of subglacial cavities and related friction law, *J. Geophys. Res.*, 112, F02 027, doi:10.1029/2006JF000576, 2007.
- Galton-Fenzi, B. K.: Modeling Ice-shelf/Ocean Interactions, Ph.D. thesis, University of Tasmania, Hobart, Tasmania, Australia, 2009.
- Gill, A. E.: *Atmosphere-Ocean Dynamics (International Geophysics Series, Volume 30)*, Academic Press, San Diego, CA, 1982.
- 30 Gladish, C. V., Holland, D. M., Holland, P. R., and Price, S. F.: Ice-shelf basal channels in a coupled ice/ocean model, *J. Glaciol.*, 58, 1527–1544, doi:10.3189/2012JoG12J003, 2012.

- Gladstone, R. M., Payne, A. J., and Cornford, S. L.: Parameterising the grounding line in flow-line ice sheet models, *The Cryosphere*, 4, 605–619, doi:10.5194/tc-4-605-2010, 2010.
- Goldberg, D. N., Little, C. M., Sergienko, O. V., Gnanadesikan, A., Hallberg, R., and Oppenheimer, M.: Investigation of land ice-ocean interaction with a fully coupled ice-ocean model: 1. Model description and behavior, *J. Geophys. Res.*, 117, F02037, doi:10.1029/2011JF002246, 2012a.
- Goldberg, D. N., Little, C. M., Sergienko, O. V., Gnanadesikan, A., Hallberg, R., and Oppenheimer, M.: Investigation of land ice-ocean interaction with a fully coupled ice-ocean model: 2. Sensitivity to external forcings, *J. Geophys. Res.*, 117, F02038, doi:10.1029/2011JF002247, 2012b.
- Grosfeld, K. and Sandhäger, H.: The evolution of a coupled ice shelf–ocean system under different climate states, *Global Planet. Change*, 42, 107–132, doi:10.1016/j.gloplacha.2003.11.004, 2004.
- Grosfeld, K., Gerdes, R., and Determann, J.: Thermohaline circulation and interaction between ice shelf cavities and the adjacent open ocean, *J. Geophys. Res.*, 102, 15595–15610, doi:10.1029/97JC00891, 1997.
- Gudmundsson, G. H.: Ice-shelf buttressing and the stability of marine ice sheets, *The Cryosphere*, 7, 647–655, doi:10.5194/tc-7-647-2013, 2013.
- Gudmundsson, G. H., Krug, J., Durand, G., Favier, L., and Gagliardini, O.: The stability of grounding lines on retrograde slopes, *The Cryosphere*, 6, 1497–1505, doi:10.5194/tc-6-1497-2012, 2012.
- Holland, D. M. and Jenkins, A.: Modeling Thermodynamic Ice–Ocean Interactions at the Base of an Ice Shelf, *J. Phys. Oceanogr.*, 29, 1787–1800, doi:10.1175/1520-0485(1999)029<1787:MTIOIA>2.0.CO;2, 1999.
- Holland, D. M., Hunter, J., Grosfeld, K., Hellmer, H., Jenkins, A., Morales Maqueda, M. A., Hemer, M., Williams, M., Klinck, J. M., and Dinniman, M.: The Ice Shelf - Ocean Model Intercomparison Project (ISOMIP), *Eos Trans. AGU*, 84, Abstract C41A–05, Fall Meet. Suppl., 2003.
- Holland, P. R. and Feltham, D. L.: The Effects of Rotation and Ice Shelf Topography on Frazil-Laden Ice Shelf Water Plumes, *J. Phys. Oceanogr.*, 36, 2312–2327, doi:10.1175/JPO2970.1, 2006.
- Holland, P. R., Jenkins, A., and Holland, D. M.: The Response of Ice Shelf Basal Melting to Variations in Ocean Temperature, *J. Climate*, 21, 2558–2572, doi:10.1175/2007JCLI1909.1, 2008.
- Hunter, J. R.: ISOMIP Files, <http://staff.acecrc.org.au/~johunter/isomip/isomip.html>, (last accessed: June 30, 2015), 2003.
- Hunter, J. R.: Specification for test models of ice shelf cavities, Tech. Rep. June, Antarctic Climate & Ecosystems Cooperative Research Centre, http://staff.acecrc.org.au/~johunter/isomip/test_cavities.pdf, (last accessed: Nov. 7, 2015), 2006.

- Jenkins, A.: A One-Dimensional Model of Ice Shelf-Ocean Interaction, *J. Geophys. Res.*, 96, 20 671–20 677, doi:10.1029/91JC01842, 1991.
- Jenkins, A., Hellmer, H. H., and Holland, D. M.: The Role of Meltwater Advection in the Formulation of Conservative Boundary Conditions at an Ice–Ocean Interface, *J. Phys. Oceanogr.*, 31, 285–296, doi:10.1175/1520-0485(2001)031<0285:TROMAI>2.0.CO;2, 2001.
- Jenkins, A., Nicholls, K. W., and Corr, H. F. J.: Observation and Parameterization of Ablation at the Base of Ronne Ice Shelf, Antarctica, *J. Phys. Oceanogr.*, 40, 2298–2312, doi:10.1175/2010JPO4317.1, 2010.
- Joughin, I., Smith, B. E., and Medley, B.: Marine ice sheet collapse potentially under way for the Thwaites Glacier Basin, West Antarctica., *Science*, 344, 735–8, doi:10.1126/science.1249055, 2014.
- Kimura, S., Candy, A., Holland, P., Piggott, M., and Jenkins, A.: Adaptation of an unstructured-mesh, finite-element ocean model to the simulation of ocean circulation beneath ice shelves, *Ocean Model.*, 67, 39–51, doi:10.1016/j.ocemod.2013.03.004, 2013.
- Leguy, G. R., Asay-Davis, X. S., and Lipscomb, W. H.: Parameterization of basal friction near grounding lines in a one-dimensional ice sheet model, *The Cryosphere*, 8, 1239–1259, doi:10.5194/tc-8-1239-2014, 2014.
- Losch, M.: Modeling ice shelf cavities in a z coordinate ocean general circulation model, *J. Geophys. Res.*, 113, 1–15, doi:10.1029/2007JC004368, 2008.
- MacAyeal, D., Rommelaere, V., Huybrechts, P., Hulbe, C., Determann, J., , and Ritz, C.: An ice-shelf model test based on the Ross ice shelf, *Ann. Glaciol.*, 23, 46–51, 1996.
- McPhee, M. G., Morison, J. H., and Nilsen, F.: Revisiting heat and salt exchange at the ice-ocean interface: Ocean flux and modeling considerations, *J. Geophys. Res.*, 113, 1–10, doi:10.1029/2007JC004383, 2008.
- Oey, L.-Y.: An OGCM with movable land–sea boundaries, *Ocean Model.*, 13, 176–195, doi:10.1016/j.ocemod.2006.01.001, 2006.
- Pattyn, F., Perichon, L., Aschwanden, A., Breuer, B., de Smedt, B., Gagliardini, O., Gudmundsson, G. H., Hindmarsh, R. C. A., Hubbard, A., Johnson, J. V., Kleiner, T., Kononov, Y., Martin, C., Payne, A. J., Pollard, D., Price, S., Rückamp, M., Saito, F., Souček, O., Sugiyama, S., and Zwinger, T.: Benchmark experiments for higher-order and full-Stokes ice sheet models (ISMIP–HOM), *The Cryosphere*, 2, 95–108, doi:10.5194/tc-2-95-2008, 2008.
- Pattyn, F., Schoof, C., Perichon, L., Hindmarsh, R. C. A., Bueler, E., de Fleurian, B., Durand, G., Gagliardini, O., Gladstone, R., Goldberg, D., Gudmundsson, G. H., Huybrechts, P., Lee, V., Nick,

- F. M., Payne, A. J., Pollard, D., Rybak, O., Saito, F., and Vieli, A.: Results of the Marine Ice Sheet Model Intercomparison Project, *MISMIP, The Cryosphere*, 6, 573–588, doi:10.5194/tc-6-573-2012, 2012.
- 5 Pattyn, F., Perichon, L., Durand, G., Favier, L., Gagliardini, O., Hindmarsh, R. C. A., Zwinger, T., Albrecht, T., Cornford, S., Docquier, D., Fürst, J. J., Goldberg, D., Gudmundsson, G. H., Humbert, A., Hütten, M., Huybrechts, P., Jouvett, G., Kleiner, T., Larour, E., Martin, D., Morlighem, M., Payne, A. J., Pollard, D., Rückamp, M., Rybak, O., Seroussi, H., Thoma, M., and Wilkens, N.: Grounding-line migration in plan-view marine ice-sheet models: results of the ice2sea MISMIP3d intercomparison, *J. Glaciol.*, 59, 410–422, doi:10.3189/2013JoG12J129, 2013.
- 10 Payne, A., Huybrechts, P., Abe-Ouchi, A., Calov, R., Fastook, J. L., Greve, R., Marshall, S. J., Marsiat, I., Ritz, C., Tarasov, L., and Thomassen, M. P. A.: Results from the EISMINT model intercomparison: the effects of thermomechanical coupling, *J. Glaciol.*, 46, 227–238, doi:10.3189/172756500781832891, 2000.
- 15 Pond, S. and Pickard, G. L.: *Introductory Dynamical Oceanography*, Second Edition, Butterworth-Heinemann, Oxford, UK, 1983.
- Schoof, C.: The effect of cavitation on glacier sliding, *P. Roy. Soc. A–Math. Phys.*, 461, 609–627, doi:10.1098/rspa.2004.1350, 2005.
- Schoof, C.: Marine ice-sheet dynamics. Part 1. The case of rapid sliding, *J. Fluid Mech.*, 573, 27, doi:10.1017/S0022112006003570, 2007a.
- 20 Schoof, C.: Ice sheet grounding line dynamics: Steady states, stability, and hysteresis, *J. Geophys. Res.*, 112, 1–19, doi:10.1029/2006JF000664, 2007b.
- Schoof, C. and Hindmarsh, R. C. A.: Thin-Film Flows with Wall Slip: An Asymptotic Analysis of Higher Order Glacier Flow Models, *Q. J. Mech. Appl. Math.*, 63, 73–114, doi:10.1093/qjmath/hbp025, 2010.
- 25 Sergienko, O. V.: Basal channels on ice shelves, *J. Geophys. Res.: Earth*, 118, 1342–1355, doi:10.1002/jgrf.20105, 2013.
- Sergienko, O. V., Goldberg, D. N., and Little, C. M.: Alternative ice shelf equilibria determined by ocean environment, *J. Geophys. Res.: Earth*, 118, 970–981, doi:10.1002/jgrf.20054, 2013.
- 30 Seroussi, H., Morlighem, M., Larour, E., Rignot, E., and Khazendar, A.: Hydrostatic grounding line parameterization in ice sheet models, *The Cryosphere*, 8, 2075–2087, doi:10.5194/tc-8-2075-2014, 2014a.

- Seroussi, H., Morlighem, M., Rignot, E., Mouginot, J., Larour, E., Schodlok, M., and Khazendar, A.: Sensitivity of the dynamics of Pine Island Glacier, West Antarctica, to climate forcing for the next 50 years, *The Cryosphere*, 8, 1699–1710, doi:10.5194/tc-8-1699-2014, 2014b.
- 5 Thoma, M., Grosfeld, K., Mayer, C., and Pattyn, F.: Interaction between ice sheet dynamics and sub-glacial lake circulation: a coupled modelling approach, *The Cryosphere*, 4, 1–12, doi:10.5194/tc-4-1-2010, 2010.
- Tsai, V. C., Stewart, A. L., and Thompson, A. F.: Marine ice-sheet profiles and stability under Coulomb basal conditions, *J. Glaciol.*, 61, 205–215, doi:10.3189/2015JoG14J221, 2015.
- 10 Walker, R. T. and Holland, D. M.: A two-dimensional coupled model for ice shelf–ocean interaction, *Ocean Model.*, 17, 123–139, doi:10.1016/j.ocemod.2007.01.001, 2007.
- Walker, R. T., Dupont, T. K., Parizek, B. R., and Alley, R. B.: Effects of basal-melting distribution on the retreat of ice-shelf grounding lines, *Geophys. Res. Lett.*, 35, L17503, doi:10.1029/2008GL034947, 2008.
- 15 Walker, R. T., Dupont, T. K., Holland, D. M., Parizek, B. R., and Alley, R. B.: Initial effects of oceanic warming on a coupled ocean–ice shelf–ice stream system, *Earth Planet. Sc. Lett.*, 287, 483–487, doi:10.1016/j.epsl.2009.08.032, 2009.
- Walker, R. T., Holland, D. M., Parizek, B. R., Alley, R. B., Nowicki, S. M. J., and Jenkins, A.: Efficient flowline simulations of ice-shelf/ocean interactions: Sensitivity studies with a fully coupled model, *J. Phys. Oceanogr.*, p. 130722130458009, doi:10.1175/JPO-D-13-037.1, 2013.
- 20 Weertman, J.: Stability of the junction of an ice sheet and an ice shelf, *J. Glaciol.*, 13, 3–11, 1974.

Table 1. Parameters for the MISMIP+ experiments.

Parameter	Value	Description
L_x	640 km	Domain length (along ice flow)
L_y	80 km	Domain width (across ice flow)
B_0	-150.0 m	Bedrock topography at $x = 0$
B_2	-728.8 m	Second bedrock topography coefficient
B_4	343.91 m	Third bedrock topography coefficient
B_6	-50.57 m	Fourth bedrock topography coefficient
\bar{x}	300 km	Characteristic along-flow length scale of the bedrock
f_c	4.0 km	Characteristic width of the side walls of the channel
d_c	500 m	Depth of the trough compared with the side walls
w_c	24.0 km	Half-width of the trough
$B_{\max}^{z_{b,deep}}$	720-720 m	Maximum depth of the bedrock topography
x_{calve}	640 km	The location in x beyond which ice is removed
ρ_i	918 kg m ⁻³	Density of ice
ρ_{sw}	1028 kg m ⁻³	Density of seawater
Ω	-0.20.2 a ⁻¹	Melt-rate rate factor
z_0	-100 m	Depth above which the melt rate is zero
H_{c0}	75 m	Reference ocean cavity thickness
a	0.3 m a ⁻¹	Accumulation rate
A	6.338 × 10 ⁻²⁵ Pa ⁻³ s ⁻¹ = 2.0 × 10 ⁻¹⁷ Pa ⁻³ a ⁻¹	Glen's law coefficient
n	3	Glen's law exponent
m	3	Friction-law exponent
α^2	0.5	Coulomb law friction coefficient
β^2	3.160 × 10 ⁶ Pa m ^{-1/3} s ^{1/3} = 1.0 × 10 ⁴ Pa m ^{-1/3} a ^{1/3}	Power law friction coefficient
g	9.81 m s ⁻²	Acceleration of gravity
-	31 556 926 s a ⁻¹	Seconds per year (defined to have 365.2422 days)

Table 2. A list of the MISMIP+, ISOMIP+ and MISOMIP1 experiments.

MIP	Experiment	Description
MISMIP+	Ice0	100 <u>100-year</u> control simulation with no melting
MISMIP+	Ice1r	100 <u>100-year</u> run with melt-induced retreat
MISMIP+	Ice1ra	100 <u>100-year</u> (or optionally up to 900 <u>900-year</u>) simulation from end of Ice1r with no melting
MISMIP+	Ice1rr	Continue Ice1r for a further 900 <u>years</u> (optional)
MISMIP+	Ice2r	100 <u>100-year</u> “calving event” simulation
MISMIP+	Ice2ra	100 <u>100-year</u> (or optionally up to 900 <u>900-year</u>) simulation from end of Ice2r with no melting
MISMIP+	Ice2rr	Continue Ice2r for a further 900 <u>years</u> (optional)
ISOMIP+	<u>Ocean0</u>	<u>1-year run with static topography, WARM initial conditions and WARM forcing</u>
<u>ISOMIP+</u>	Ocean1	20 <u>20-year</u> run with static geometry <u>topography</u> , COLD initial conditions and WARM forcing
ISOMIP+	Ocean2	20 <u>20-year</u> run with static geometry <u>topography</u> , WARM initial conditions and COLD forcing
ISOMIP+	Ocean3	100 <u>100-year</u> run with dynamic geometry <u>topography</u> , WARM initial conditions and WARM forcing
ISOMIP+	Ocean4	100 <u>100-year</u> run with dynamic geometry <u>topography</u> , COLD initial conditions and COLD forcing
MISOMIP1	IceOcean1r	100 <u>100-year</u> coupled run with no dynamic calving, COLD initial conditions and WARM forcing
MISOMIP1	IceOcean1ra	100 <u>100-year</u> coupled run from end of IceOcean1r with no dynamic calving and COLD forcing
MISOMIP1	IceOcean2r	Optional: 100 <u>100-year</u> coupled run with dynamic calving, COLD initial conditions and WARM forcing
MISOMIP1	IceOcean2ra	Optional: 100 <u>100-year</u> coupled run from end of IceOcean2r with dynamic calving and COLD forcing

Table 3. Parameters shared between all ~~four~~^{five} ISOMIP+ experiments.

Parameter	Value	Description
x_0	<u>320 km</u>	<u>Southern boundary of the domain</u>
y_0	<u>0</u>	<u>Eastern boundary of the domain</u>
L_x	480 km	Domain length (<u>south to north</u> , along ice flow)
L_y	80 km	Domain width (<u>east to west</u> , across ice flow)
H_{calve}	100 m	The minimum <u>Minimum</u> thickness of ice, below which it is removed
θ_c θ_e	75° S	Latitude of the center of the domain
γ_0	10 days ⁻¹	The restoring <u>Restoring</u> decay rate at the northern boundary
x_{r0} x_{r0}	790 km	The southern <u>Southern</u> edge of the restoring region
x_{r1} x_{r1}	800 km	The northern <u>Northern</u> edge of the restoring region

Table 4. Parameters recommended for the common (COM) experiments.

Parameter	Value	Description
$\Delta x = \Delta y$	2 km	Horizontal resolution
c_w c_w	3974 J °C ⁻¹ kg ⁻¹	Specific heat capacity of seawater
L	3.34×10^5 J kg ⁻¹	Latent heat of fusion of ice
λ_1	-0.0573 °C PSU ⁻¹	Liquidus slope
λ_2	0.0832 °C	Liquidus intercept
λ_3	-7.53×10^{-8} °C Pa ⁻¹	Liquidus pressure coefficient
Γ_T	5.0×10^{-2} <u>model specific</u>	Nondimensional heat-transfer coefficient
F_S Γ_S	1.4×10^{-3} $\Gamma_T/35$	Nondimensional salt-transfer coefficient
$C_{D,top}$ $C_{D,top}$	2.5×10^{-3}	Top drag coefficient
$C_{D,bot}$ $C_{D,bot}$	2.5×10^{-3}	Bottom drag coefficient
u_{tidal}	0.01 m s ⁻¹	RMS velocity associated with tides
κ_i κ_i	0	Heat diffusivity into ice (perfectly insulating)
ν_{unstab}	0.1 m ² s ⁻¹	Convective vertical viscosity
κ_{unstab}	0.1 m ² s ⁻¹	Convective vertical diffusivity
ν_{stab}	1×10^{-3} m ² s ⁻¹	Stable vertical eddy viscosity
κ_{stab}	5×10^{-5} m ² s ⁻¹	Stable vertical eddy diffusivity
ν_H ν_H	6.0 m ² s ⁻¹	Horizontal eddy viscosity
κ_H κ_H	1.0 m ² s ⁻¹	Horizontal eddy diffusivity
ρ_{fw}	1000 kg m ⁻³	Density of fresh water
ρ_{sw}	1028 kg m ⁻³	Reference density of seawater
T_{ref}	-1 °C	reference <u>Reference</u> potential temperature for linear EOS
S_{ref}	34.2 PSU	reference <u>Reference</u> salinity for linear EOS
ρ_{ref}	1027.51 kg m ⁻³	in-situ <u>In-situ</u> density for linear EOS
α_{lin}	3.733×10^{-5} °C ⁻¹	thermal <u>Thermal</u> expansion coefficient for linear EOS
β_{lin}	7.843×10^{-4} PSU ⁻¹	salinity <u>Salinity</u> contraction coefficient for linear EOS

Table 5. Parameters for the COLD profiles.

Parameter	Value	Description
T_0	$-1.9\text{ }^\circ\text{C}$	Surface temperature
T_{bot}	$-1.9\text{ }^\circ\text{C}$	Temperature at the ocean floor
S_0	33.8 PSU	Surface salinity
S_{bot}	34.55 PSU	Salinity at the ocean floor

Table 6. Parameters for the WARM profiles.

Parameter	Value	Description
T_0	$-1.9\text{ }^\circ\text{C}$	Surface temperature
T_{bot}	$1.0\text{ }^\circ\text{C}$	Temperature at the ocean floor
S_0	33.8 PSU	Surface salinity
S_{bot}	34.7 PSU	Salinity at the ocean floor

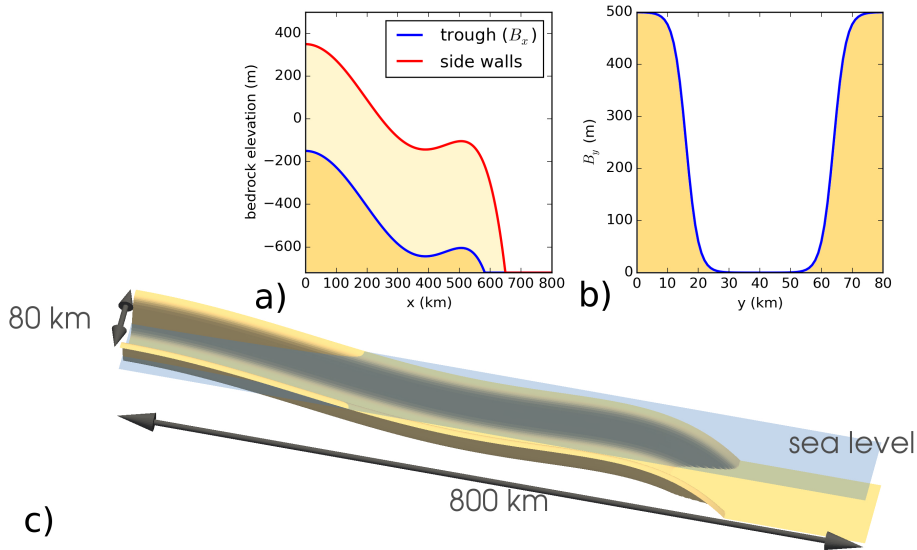


Figure 1. The bedrock topography for the three MIPs as defined by Eqs. (1)–(4). **(a)** $B_x(x)$, the variability of the bedrock ~~topography~~ topography in the x direction. The topography through the central trough is shown in blue and on the side walls is shown in red. **(b)** $B_y(y)$, the shape of the bedrock topography in the y ~~direction~~ direction relative to that at the center of the trough. Note that $B_y(y)$ is not a transect of the topography because $B_x(x)$ is never equal to zero. **(c)** The topography in 3-D at 1 km resolution. Sea level is shown in translucent blue.

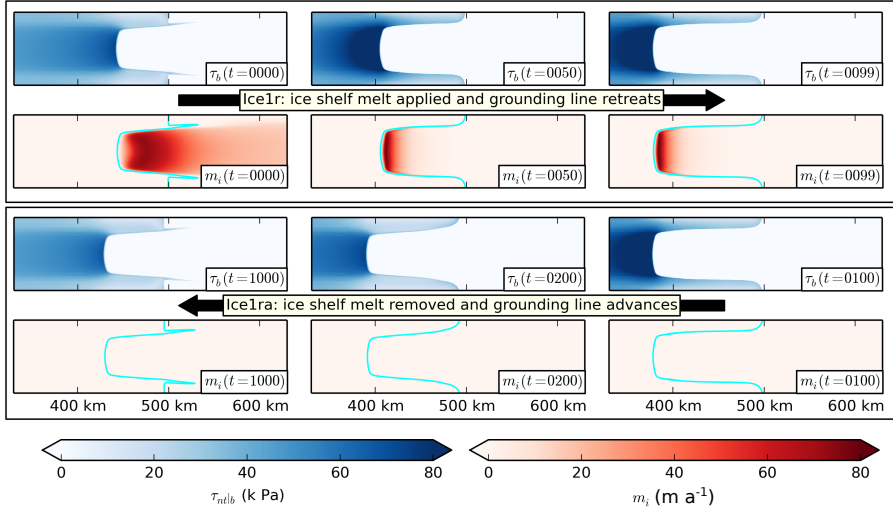


Figure 2. Evolution of the basal traction $\tau_{nt|_b}$ and ice shelf melt rate m_i fields during the Ice1r and Ice1ra experiments from a BISICLES run. Melt rates are applied when $0 < t < 100 \text{ yr}$ ($0 < t \leq 100 \text{ a}$), causing the ice shelf to thin and grounding line to **advance/retreat**. Once $t > 100 \text{ yr}$ ($t > 100 \text{ a}$), no melt is applied, the ice shelf thickens, and the grounding line advances. The choice of the Tsai et al. (2015) traction law ensures that $\tau_{nt|_b}$ is continuous across the grounding line but large $\sim 1 \text{ km}$ upstream. Similarly, the factor $\tanh(H_c/H_{c0})$ ensures that m_i is continuous across the grounding line but large $\sim 10 \text{ km}$ downstream.

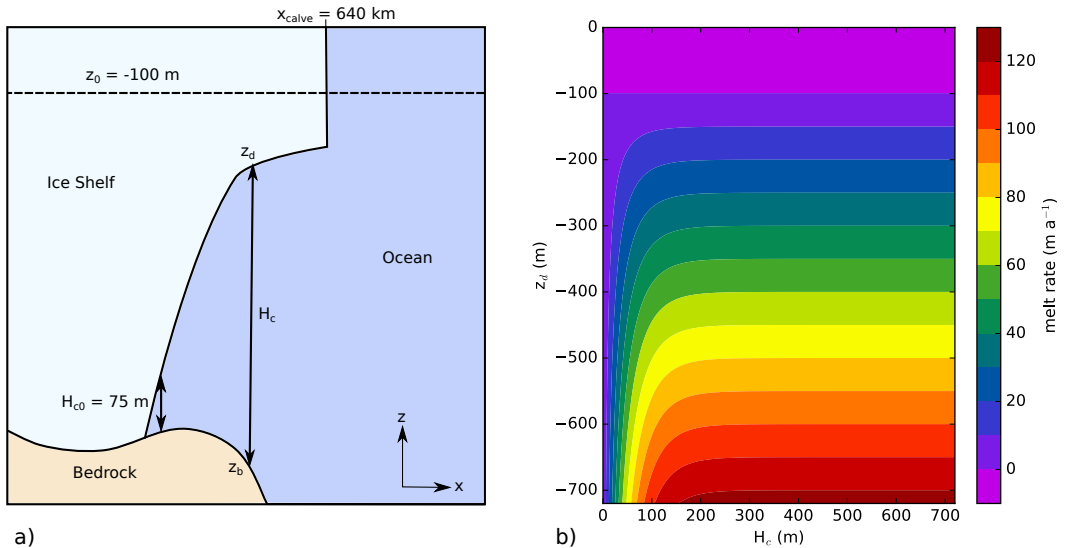


Figure 3. The melt parameterization given by Eq. (a) A schematic showing the ice draft ($+z_d$) as a function of the bedrock elevation (z_b), the cutoff depth (z_0) above which the melt rate is zero, the ocean column thickness (H_c) and the ice draft reference thickness H_{c0} . (b) The melt parameterization given by Eq. (a17). Melting increases linearly with decreasing z_d below $z_0 = -100$ m. The melt rate z_0 and is independent of H_c when H_c is larger than ~ 200 m, but falls to thick zero near the grounding line as H_c approaches zero the ocean column thins.

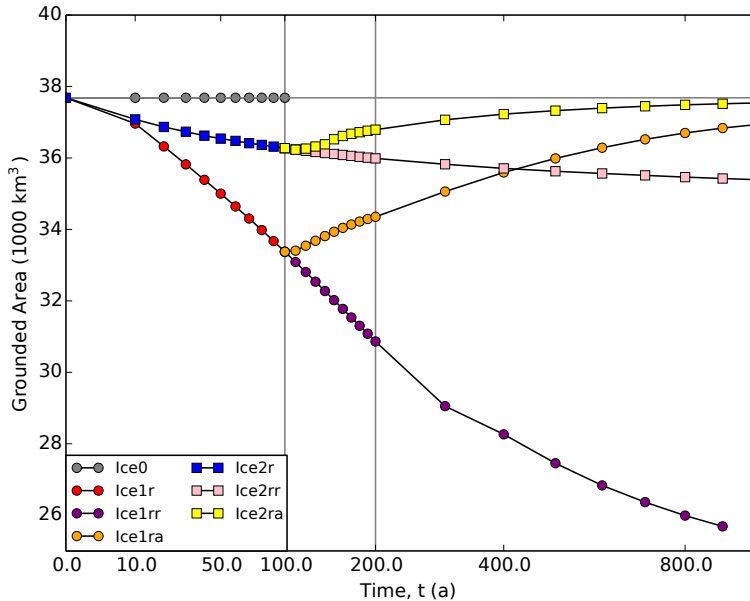


Figure 4. Grounded area plotted against time for the MISMIP+ experiments, computed using BISICLES with the SSA and the Tsai et al. (2015) basal traction. The Ice0, Ice1r and Ice2r experiments all start from steady-state, and apply either zero melt (Ice0) or melt rates derived from simple formulae (Ice1r and Ice2r) from $t = 0$ to $t = -100\text{yr}$ to $t = 100\text{a}$. Following on from Ice1r, the Ice1ra and Ice1rr experiments evolve the ice sheet until at least $t = 200\text{yr}$ to $t = 200\text{a}$ and optionally to $t = 1000\text{yr}$ to $t = 1000\text{a}$, with the melt rate set to zero in Ice1ra and derived from the same formula as Ice1r in Ice1rr. Ice2ra and Ice2rr follow on from Ice2r in a similar fashion.

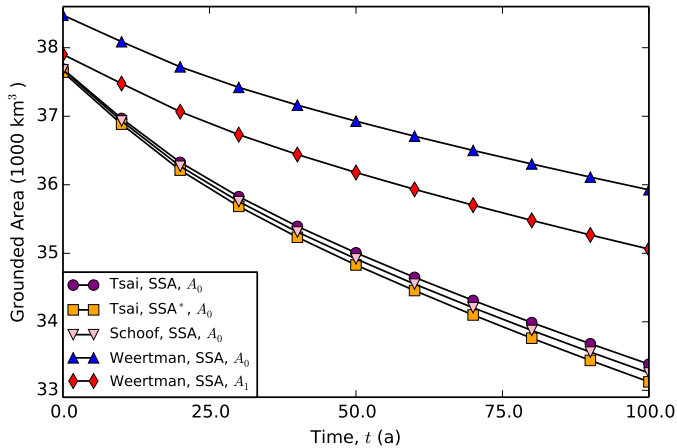


Figure 5. For Ocean1, the surface elevation (translucent blue), ice draft (white) and bathymetry (beige) cut down the center of the trough ($y=40$) for clearer visualization. The geometry is a steady-state profile from an SSA simulation in BISICLES without basal melting (Parameter sensitivity in the initial condition for MISIP+)Ice1r experiment. The blue walls indicates the bounds Tsai et al. (2015) and Schoof (2005) basal traction laws lead to similar initial states and rates of retreat, as do the ocean domain. This geometry is also SSA and SSA* stress approximations, given the starting state of Ocean3 same rate factor $A_0 = 2.0 \times 10^{-17} \text{ Pa}^{-3} \text{ a}^{-1}$. As On the other hand, the Weertman basal traction law results in Fig-a ?? except grounding line some way upstream given the geometry for Ocean2. The geometry is from -100 into same rate factor, a MISIP+ simulation using BISICLES with closer grounding line when the SSA. The geometry rate factor is also the final state of Ocean3 increased to $A_1 = 2.2 \times 10^{-17} \text{ Pa}^{-3} \text{ a}^{-1}$, and the initial state a far slower rate of Ocean4 retreat in either case.

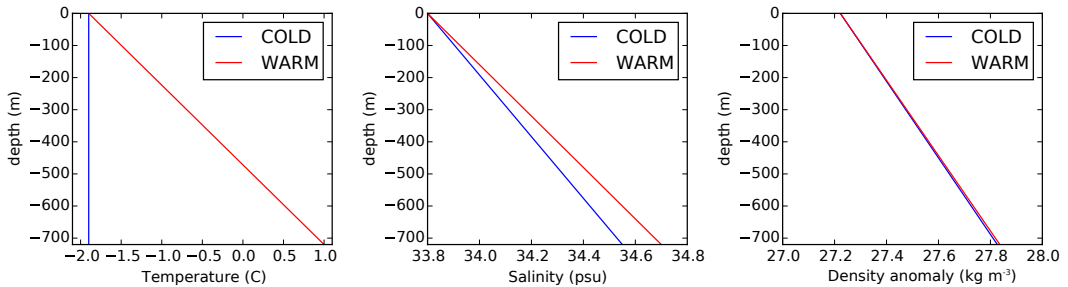


Figure 6. WARM and COLD temperature, salinity and density profiles used in all ~~four~~ **five** ISOMIP+ experiments. In Ocean1, the COLD profile specifies the initial condition and the WARM profile is used in the restoring, while in Ocean2 the profiles are switched. Ocean3 uses both WARM initial conditions and restoring whereas Ocean4 uses both COLD initial conditions and restoring. The WARM profiles were designed to qualitatively approximate observations in the Amundsen Sea Embayment near Pine Island Glacier (Dutrieux et al., 2014). The COLD profile is at the surface freezing temperature at all depths and has a salinity such that the densities of the WARM and COLD profiles are nearly identical.

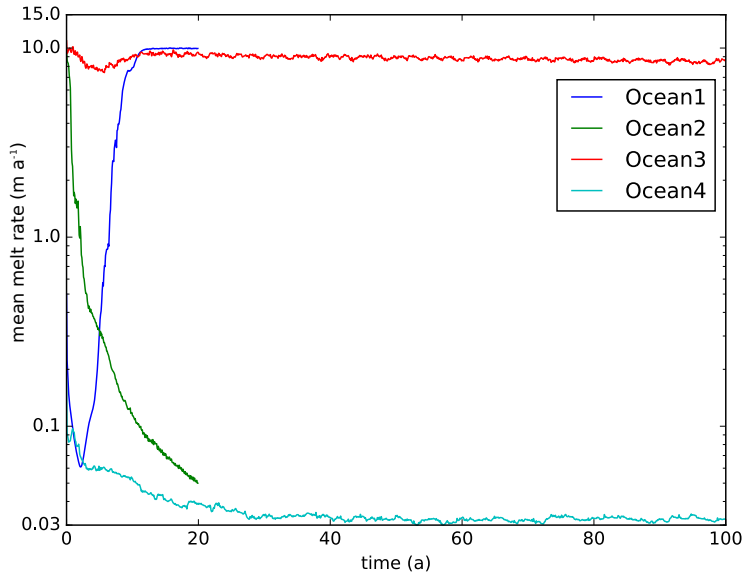


Figure 7. Example results from a POP2x simulation simulations showing the melt rate rates averaged over the shelf area as a function of time for the four ISOMIP+ experiments Ocean1–4. Melting increases by nearly two orders of magnitude in Ocean1, and decreases by about the same order in Ocean2, demonstrating that changes in far-field forcing can greatly increase or reduce melting. After a decade or two of initial adjustment, the melt rates in Ocean3 and Ocean4 remain relatively steady in time despite the changing geometry topography in those cases experiments, suggesting that the total cavity size has relatively little impact on total melting.

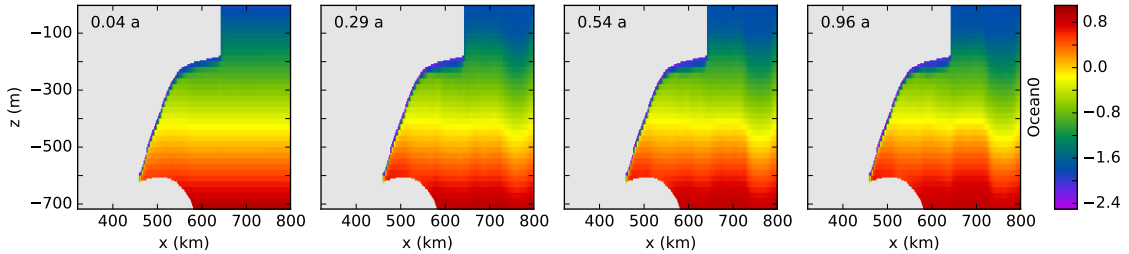


Figure 8. Example results from a POP2x-1-year Ocean0 simulation with the POP2x model using heat-transfer coefficient $\Gamma_T = 0.11$. Panels show the progression in time of Ocean0-averaged over transects of monthly-averaged ocean temperature through the last-month center of the experiment domain ($y = 40$ km). (a) The melt rate is proportional to initial conditions and far-field restoring at the product right-hand side of (b) the thermal driving across the sub-ice-shelf boundary layer and (c) domain both use the friction-velocity WARM profiles from Fig. 6. (d) The temperature ice draft does not evolve in the bottom-most cell, indicating that warm water has reached the ice-shelf base time. (e) The x -component of the boundary-layer velocity shows simulation reaches a quasi-steady state with relatively strong jet along the western boundary of the cavity. (f) The barotropic streamfunction shows two counter-rotating cells covering the open-ocean region and melting within a weaker clockwise circulation on the western flank of the ice-shelf cavity few months.

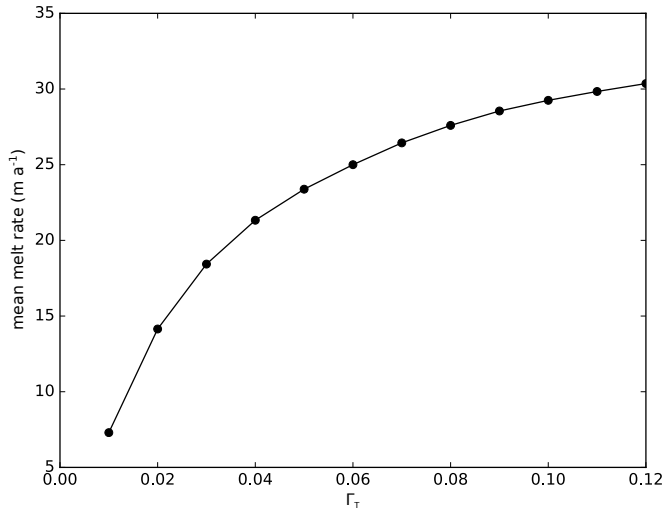


Figure 9. Further example results from the last month of a POP2x simulation series of Ocean1. (a) The overturning streamfunction shows inflow at depth and outflow at the surface within the cavity. A weaker overturning also occurs in the areas POP2x simulations of open ocean on Ocean0 showing the sides dependence of the ice tongue between $x = 500$ and 600 mean melt rate $\langle m_w \rangle$ averaged over locations below $z_d = -300$. (b, c) Slices of temperature and salinity in an $x-z$ plane through over the center final six months of the domain show cold, fresh melt water near simulation for various values of the ice-ocean interface turbulent heat-transfer coefficient Γ_T . (d, e) Slices of temperature and salinity in a $y-z$ planes looking south into Based on these results, the cavity show value $\Gamma_T \approx 0.11$, corresponding to a slightly thicker mean melt plume on the western (right) flank rate $m_w \approx 30 \text{ ma}^{-1}$, was used for subsequent ISOMIP+ and MISOMIP1 simulations.

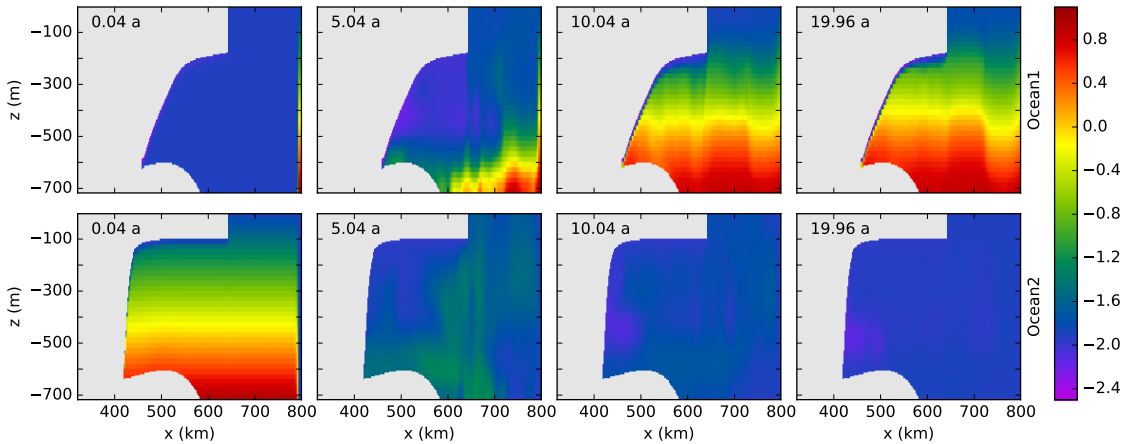


Figure 10. As- Example results from POP2x as in Fig. ?? 8 but averaged-over for Ocean1 (top) and Ocean2 (bottom) simulations each lasting 20 years. In both experiments, the last-month of Ocean3ice draft is held fixed in time. The ice-shelf has retreated Ocean1 is initialized with COLD profiles and calved significantly, leading restored to large melt WARM profiles. Melt rates concentrated near are initially low and the grounding line. The jet of melt water visible in (c, d) in Fig. ?? overturning strength is not as strong here initially relatively weak, presumably because of so that warm, deep water takes several years to reach the shallower ice draft over most back of the sub-ice-shelf cavity, at which point melting increases by several orders of magnitude, reaching a quasi-steady state for approximately the second half of the experiment. The barotropic circulation Ocean2 is strong-in initialized with WARM profiles and restored to COLD profiles, leading to a melt rate that decays by several orders of magnitude over the cavity-but weaker-in duration of the open ocean than-in-Ocean1 simulation. Ocean2 does not reach a quasi-steady state within its 20-year duration.

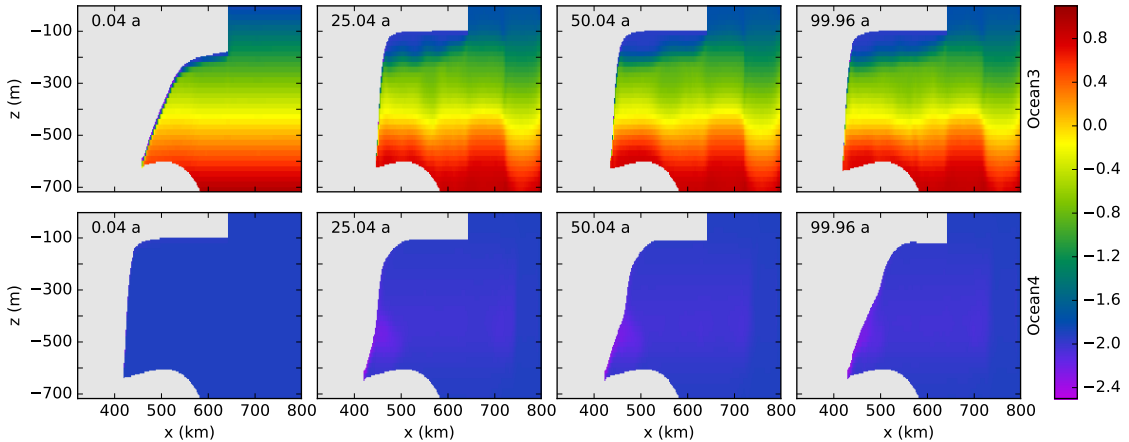


Figure 11. As- Example results from POP2x as in Fig. ??-8 but averaged over the last month of for Ocean3 (top) and Ocean4 (bottom) simulations each lasting 100 years. The overturning is somewhat weaker than in Ocean1. In these experiments, perhaps due to the weaker average ice draft evolves in time. Ocean3 prescribes WARM initial conditions and restoring, producing strong melting or throughout the relatively flat experiment, consistent with the retreating ice draft. The melt rate declines slightly over most the course of the cavity simulation as the retreats to shallower depths, associated with colder ocean temperatures. The melt plume appears Ocean4 is initialized and forced with COLD profiles, which lead to be significantly thicker than in Ocean1 relatively low melt rates, presumably as a result of fitting with the shallower advancing ice draft and cooler ambient topography. Melt water in much of cools the sub-shelf cavity, leading to several decades of decreasing melt rates followed by quasi-steady values for the remainder of the simulation.

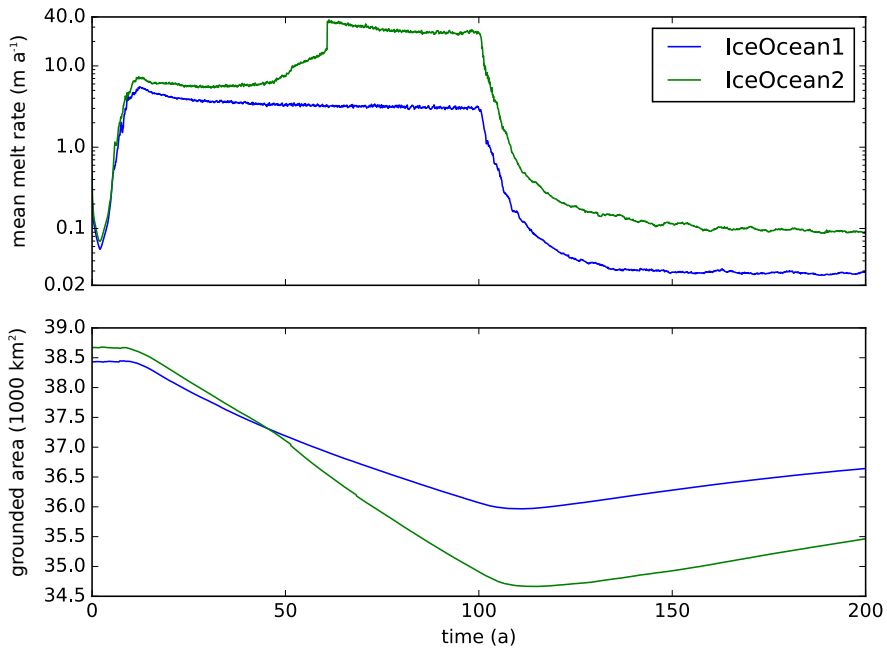


Figure 12. Results- Example results from a-POPSICLES simulation-simulations of IceOcean1 .-(a) The ice topography taken from 100 with the eastern 20 of the domain cut away to reveal the behavior within the trough. The basal melt rate is plotted on the ice draft (no dynamic calving) and IceOcean2 (thickness-based calving criterion) using SSA and the ocean temperature is plotted on sliding law from Weertman (1974) showing melt rates averaged over the bedrock topography shelf area (top panel) and the side-walls. The ice-shelf has retreated several tens grounded area as functions of kilometers and the ice draft has steepened significantly, leading to large time (bottom panel). Though melt rates concentrated near the grounding line are initially similar, as after about year 40 the dynamic calving in Ocean3.-(b) The grounded area IceOcean2 begins to remove substantial areas of the ice shelf (left axis notably when an iceberg is removed just after year 60) and, resulting in larger mean melt rate averaged over the ice-shelf base rates (right axis but similar total melt fluxes) for the 200 duration of the IceOcean1 that experiment. The change in IceOcean2 loses substantially more grounded area is less than IceOcean1 during retreat (the first 100 years), presumably due to a loss of buttressing from the ice shelf, which has nearly completely calved away. The grounding line re-advances at approximately the same rate in both experiments because the Ice1 advancing shelf is thick enough not to calve.

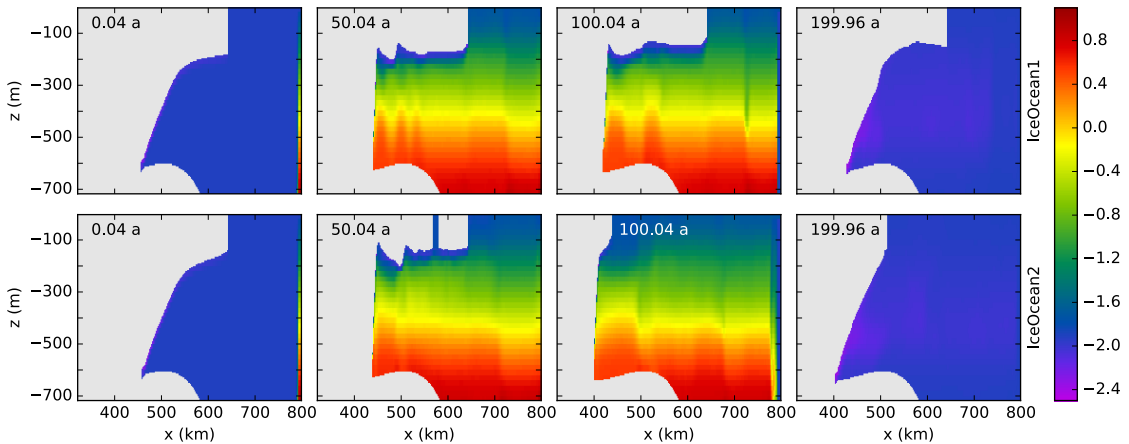


Figure 13. Example results from POPSICLES plotted as in Fig. 28 but for IceOcean1 (top) and IceOcean2 (bottom) simulations each lasting 200 years. As Both simulations begin with ice shelves that are in steady state without melting and with COLD ocean conditions. The WARM far-field restoring in Ocean1, the mean-ocean causes the melt rate increases significantly as warm water to increase by several orders of magnitude over the first reaches-decade and for the cavity-ice shelf to thin over the remainder of the retreat phase (100 years). As-in-Ocean3 In IceOcean2, dynamic calving significantly reduces the melting tails-off past year 10 as size of the ice shelf begins compared with IceOcean1. During the final 100 years, the switch to thinCOLD far-field restoring leads to cold ocean temperatures, leaving-less-area-exposed melt rates are reduced by several orders of magnitude, and the ice shelf begins to re-advance. One hundred years is not long enough for the warmer, deeper waters-ice shelf in either simulation to re-advance to its initial steady state.